On the origin of 1/f noise in epitaxial GaAs

ON THE ORIGIN OF 1/f NOISE IN EPITAXIAL GaAs

LIN REN

ON THE ORIGIN
OF 1/f NOISE IN EPITAXIAL GaAs

ON THE ORIGIN OF 1/f NOISE IN EPITAXIAL GaAs

PROEFSCHRIFT

ter verkrijging van de graad van doctor aan de Technische Universiteit Eindhoven, op gezag van de Rector Magnificus, prof. dr. J.H. van Lint, voor een commissie aangewezen door het College van Dekanen in het openbaar te verdedigen op maandag 17 mei 1993 om 16.00 uur

door

LIN REN

geboren te Xi'an, China

druk: wibro dissertatiedrukkerij, helmond.

DIT PROEFSCHRIFT IS GOEDGEKEURD DOOR DE PROMOTOREN:

Prof. dr. F.N. Hooge
Prof. dr. T.G.M. Kleinpenning

CIP-DATA KONINKLIJKE BIBLIOTHEEK, DEN HAAG

Ren, Lin

On the origin of 1/f noise in epitaxial GaAs / Lin Ren. - [S.l. : s.n.]. - Ill., fig., tab.
Thesis Eindhoven. - With ref. - With summary in Dutch.
ISBN 90-9006067-7
NUGI 812
Subject headings: 1/f noise / 3-5 semiconductors.

to Hong-guang and
our parents

The work described in this thesis is part of the research program of the "Stichting voor Fundamenteel Onderzoek der Materie (FOM)" with financial support from the "Nederlandse Organisatie voor Wetenschappelijk Onderzoek (NWO)".

Contents

Chapter 1

General Introduction

1.1 Electrical Noise

Electrical noise is a phenomenon widely encountered in various electronic systems, where the current or voltage is found not perfectly constant, but fluctuating around its average value. These time-dependent fluctuations are referred to as "noise". It is the noise that always sets lower limits to the accuracy of any measurement and to the signals that are processed electronically. It is impossible to avoid noise, but it is possible to minimize it. For that reason, studies of the physical origin of noise are important.

For a resistive device, the circuit used to measure voltage noise is somewhat identical to that used for resistance measurements, as illustrated in Fig. 1. The 4-probe arrangement together with a large series resistor, R_s, greatly

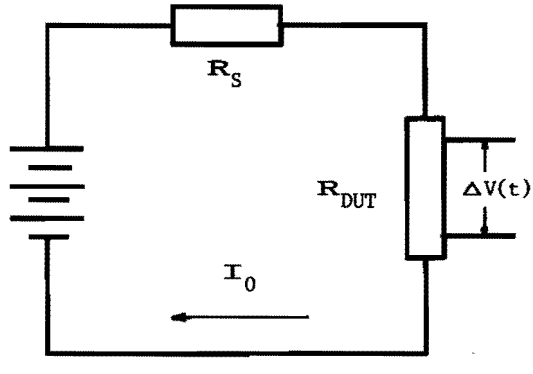

Fig. 1 4-Probe configuration for voltage noise measurement

suppresses the contact noise. The dry-cell batteries in series with a large wire-round resistor provide a constant, practically noiseless, current I_o through the circuit. The fluctuations, $\Delta R(t)$ in the resistance R of the device under test (DUT) lead to fluctuations in voltage, $\Delta V(t)$, across the sensor electrodes. The Ohmic law requires $\Delta V=I_o\Delta R$ and $<(\Delta V^2)> \propto I_o^2$.

The random fluctuations, $\Delta V(t)$, are then often characterized by their power spectral density (p.s.d), defined as time averages of the product of the Fourier transform of $\Delta V(t)$:

$$S_V(f) \sim \langle V(f)\, V^*(f) \rangle \qquad (1)$$

Where, V(f) is the Fourier transform of $\Delta V(t)$, f is the frequency. With the Wiener-Khinchin theorem [1], $S_v(f)$ can be written as

$$S_V(f) = 4\int_0^\infty C(t)\cos(2\pi f t)\, dt \qquad (2)$$

Here $C(t)=<\Delta V(t)\Delta V(0)>$, is the autocorrelation function of $\Delta V(t)$.

According to the physical origin, there are mainly five types of noise that are usually encountered.

(1) Thermal (or Johnson) Noise

This type of noise results from the Brownian (or thermal) motion of the charge carriers in the sample. Therefore it is always present and can not be reduced. The thermal noise can easily be characterized by its white spectrum ($<\sim 10^3$GHz) without a current dependence, where $S_v(f)$ can be written as:

$$S_V(f) = 4kTR \qquad (3)$$

with Boltzmann's constant k, temperature T and resistance R.

(2) Shot Noise

Shot noise is a Poisson-type of fluctuations in the electrical current. It is often found in a current of discrete charge carriers crossing a potential barrier or leaving a cathode. The physical origin of the shot noise is thermal fluctuations in the emission rate of the charge carriers. At frequencies small compared to the reciprocal of the transit time, the p.s.d of the shot noise is characterized also by a white spectrum but it is current dependent. The p.s.d is given by

$$S_I(f) = 2eI. \tag{4}$$

(3) Generation Recombination (G-R) Noise

This type of noise is a fluctuation in the number of the free charge carriers N as a result of trapping and detrapping of the free charge carriers at traps in semiconductors. The p.s.d of G-R noise is characterized by the Lorentzian spectrum:

$$S_N(f) = \langle(\Delta N^2)\rangle \frac{4\tau}{1 + (2\pi f\tau)^2}. \tag{5}$$

(4) Diffusion (or Transport) Noise

This type of noise is also a kind of number fluctuations arising from transport of charged particles in and out of a given volume under consideration. The p.s.d of diffusion noise is charaterized by the "universal 3/2 power law" [2], in which the high frequency asymptote is $S_v \propto f^{-3/2}$. In case of one dimensional diffusion, the spectrum shows two branches: $S_v \propto f^{-1/2}$ at low frequencies and $S_v \propto f^{-3/2}$ at high frequencies. The corner frequency, f_c, contains the information of the diffusion as it can be written as $f_c = D/(\pi L^2)$, with D is the diffusion coefficient and L the sample length.

(5) 1/f Noise

1/f Noise gets its name after its spectrum, where the p.s.d is inversely proportional to the frequency:

$$S_V(f) \propto \frac{1}{f^\gamma} \qquad (6)$$

with a spectral exponent γ nearly 1. Besides in electronic systems, 1/f fluctuations also appear in a diverse range of observations, like in music [3], in the level of the Nile river [4], in traffic flow on the high-way [5], in neuro-membranes [6], etc. No explanation exists for such a ubiquitous observations of 1/f fluctuations.

The physical origin of the first four types of noise are quite well understood. It is the 1/f noise that is the main subject of this thesis. Only electrical 1/f noise is considered here. In the following section, I shall try to give more details about the current understanding of 1/f noise in homogenous semiconductors and metals.

1.2 1/f Noise in Semiconductors and Metals

The history of electrical 1/f noise can be traced back to 1925 when Johnson discovered 1/f noise in a vacuum tube [7]. Since then the electrical 1/f noise has been subjected to discussion intensively [8-16]. But till now no agreement on its physical origin has been achieved. However, there is one basic feature which is agreed upon: 1/f noise results from resistance fluctuations at equilibrium, where the driving current or voltage only serves to observe it. This has been proved directly by Voss and Clarke [8] and later by Beck and Spruit [17] by their measurements of 1/f noise in the thermal noise. Furthermore, in most cases 1/f noise is believed to be stationary [9,11]. By accepting the equilibrium resistance fluctuations, the question that arises naturally is why a semiconductor or a metal exhibits a 1/f spectrum for its resistance fluctuations?

There are several ways to approach this problem. One

obvious way is to construct the 1/f noise spectrum by summation of a large number of relaxation processes since relaxation is one of the basic properties of materials. The arguments for constructing the 1/f spectrum are simple. For the relaxation process of a fluctuating quantity $\Delta X(t)$, the Langevin equation is usually given by

$$\frac{d\Delta X(t)}{dt} = -\frac{\Delta X(t)}{\tau} + H(t) \qquad (7)$$

Here, H(t) is the Langevin random source which has a white p.s.d and τ is the time constant of the relaxation. Making a Fourier transform of eq. (7), one obtains the Lorentzian spectrum of $\Delta X(t)$:

$$S_{\Delta X}(f) = \langle(\Delta X)^2\rangle \cdot \frac{4\tau}{1 + (2\pi f\tau)^2}. \qquad (8)$$

If there exists a distribution $g(\tau)$ of the relaxation times τ, in the range $\tau_1<\tau<\tau_2$, one will find

$$S_{\Delta X} = \langle(\Delta X)^2\rangle \cdot \int_{\tau_1}^{\tau_2} \frac{\tau g(\tau)}{1 + (2\pi f\tau)^2}\, d\tau. \qquad (9)$$

Eq. (9) will give a 1/f spectrum as

$$S_{\Delta X} = \frac{\langle(\Delta X)^2\rangle}{\ln(\tau_2/\tau_1)} \cdot \frac{1}{f}, \qquad for\ \ 1/(2\pi\tau_2) < f < 1/(2\pi\tau_1) \qquad (10)$$

if $g(\tau)$ is inversely proportional to τ, in particular

$$g(\tau)\, d\tau = \frac{1}{\tau \ln(\tau_2/\tau_1)}\, d\tau, \qquad for\ \ \tau_1 < \tau < \tau_2 \qquad (11)$$

In this way the problem is simply reduced to finding the right physical processes that have a distribution in the relaxation time τ inversely proportional to τ, as required for obtaining a 1/f spectrum. Obviously the main difficulties for this approach are lying in the long relaxation times required to construct the 1/f spectrum (recall that in some cases, 1/f noise can still be observed down to a frequency as low as 10^{-6}Hz [18-20]). Here I shall mention two such cases, where the

proposed distribution of relaxation times satisfies eq. (11).

(1) The McWhorter model [21]

The noise source in McWhorter model are the traps located in the oxide layer of a bulk semiconductor. The charge carriers penetrate into the oxide layer by tunnelling and then are trapped or released there. In this way, the total number of free charge carriers in the bulk semiconductor is modulated and fluctuates in time. The individual trapping event is therefore well characterized by a Lorentzian spectrum with a relaxation time τ being inversely proportional to the tunnelling probability. The probability varies exponentially with, -x, the trap distance to the interface. Therefore, τ can be written as

$$\tau = \tau_0 \exp(\beta x) \tag{12}$$

with β being the tunnelling parameter ($\sim 10^8 cm^{-1}$). Assuming a homogeneous distribution of the traps in the oxide layer, one obtains

$$g(\tau)\, d\tau = C dx = \frac{C}{\beta \tau} d\tau \tag{13}$$

If the relaxation time of traps at x=0, $\tau_0 \cong 10^{-12}$s (roughly the collision time), then a distribution of traps in a oxide layer with a thickness of 30Å will yield a 1/f spectrum down to about 0.1Hz.

(2) The Dutta-Dimon-Horn (DDH) Model [22]

Eberhard and Horn [23] measured the temperature dependence of the 1/f noise in metals like Cu, Ag, Au, Ni, Cr etc. Their results clearly showed that: (i) the p.s.d of the noise in these metals is not exactly 1/f, but $1/f^{\gamma}$ with a frequency exponent γ between 0.8 and 1.4 dependent on temperature; (ii) the noise intensity is strongly temperature dependent; (iii) there exists a relation between the temperature dependence of the noise intensity and the slope of the $1/f^{\gamma}$ spectra. Later,

Dutta *et al.* [22] developed a model to interpret the experimental observations. They assumed that there are some thermally activated processes in the metal, with relaxation times according to

$$\tau = \tau_0 \exp(E/kT) \qquad (14)$$

It was shown by Bernamont [24] that, when D(E) is the distribution of the activation energies E, D(E)=const will yield $g(\tau) \propto 1/\tau$, hence $S_V \propto 1/f$, with D(E) being the distribution of the activation energy E. However, when D(E)≠const but centred at E_0 with a width much larger than kT, then the intensity of the noise can be approximated by [22]

$$S_V \propto \frac{kT}{\omega} D(E_0) . \qquad (15)$$

Where $E_0 \equiv -kT\ln(\omega\tau_0)$ and $\omega = 2\pi f$ is the angular frequency. In particular, eq. (15) implies a relationship between the temperature dependence and the slope of $S_V(\omega,T)$ [22] as

$$\gamma(\omega,T) = 1 - \frac{1}{\ln(\omega\tau_0)}\left[\frac{\partial \ln S_V(\omega,T)}{\partial \ln T} - 1\right]. \qquad (16)$$

Dutta *et al.* [11] found that the noise data of Eberhard and Horn agree very well with eq. (16). The distribution of the activation energies was peaked at $E_p \approx 1$ eV with a width of about 0.2 eV. Both the peak energy and the width are reasonable values for defect motion in solids. The existence of such a distribution in the activation energy is, thus, simply a consequence of the microscopic inhomogeneity of the materials. If $\tau_0 = 10^{-12}$s is assumed, then an activation energy E of order 1 eV will yield a relaxation time τ of about 6×10^4s at room temperature according to eq. (14).

Since the review paper of Dutta and Horn was published much work has been done on various metals showing support for the model. This has made the DDH model quite popular for the

interpretation of 1/f noise in metals. A physical picture [14] underlying the DDH model is the changing of the scattering rate induced by the motion of scatters (atomic-scale defects) via quantum interference effects [25-27]. I shall consider this point somewhat later in this section.

Another way to approach the problem of the resistance fluctuations with a 1/f spectrum is Hooge's empirical relation. In order to compare the 1/f noise magnitude in different samples, a quantity is needed to normalize the 1/f noise power density in large systems. In 1969, Hooge [28] proposed that the relative noise power density, S_R/R^2, can be normalized to the total number of the free charge carriers N written as

$$\frac{S_R}{R^2} = \frac{\alpha}{fN}. \qquad (17)$$

Where f stands for the frequency, α is a constant of about 2×10^{-3} or as later suggested by Vandamme [29] an adjusting parameter (I shall come back to this point in the next section). The empirical relation as expressed by eq. (17) was found successful in describing 1/f noise in many semiconductors and metals [12]. The validity of using the number of the free charge carriers as the noise normalizing factor has also been proven many times: (i) in metals as $S_R/R^2 \propto 1/\Omega$ with Ω being the sample volume; (ii) in semiconductors [30-32] where the charge carrier number is changed by doping within a fixed sample volume; (iii) in an n-$Al_xGa_{1-x}As$ epitaxial layer [33] where the number of the charge carriers is changed by the Photo-excitation with both the sample volume and doping level being fixed. Furthermore, it has been shown by Hooge [34] that when the individual mobilities of a group of N charge carriers fluctuate independently then the number N will automatically appear as the noise normalizing factor.

There are two general mechanisms which can lead to resis-

tivity fluctuations in semiconductors and metals, namely fluctuations in the number of the charge carriers or fluctuations of their mobilities. In only a few cases, both number and mobility could fluctuate simultaneously, for example, in a p-i-n diode [35], or in the inversion layer of MOST's [36] where the trapping and detrapping of the charge carriers at the oxide traps also cause the scattering power to change via the charged-impurity scattering. As already pointed out by Weissman [37] that, for number fluctuations, it would require an unrealistic concentration of traps to account for the normal noise levels ($\alpha \sim 10^{-3}$) of 1/f noise in metals. For semiconductors, the McWhorter model is obviously a surface effect. Hence it is definitely excluded by the empirical relation [28]. For bulk semiconductors, the trapping and detrapping of the charge carriers at deep levels also can not account for the wide range of the 1/f noise, because Fermi statistics implies that only the traps within a few kT around the Fermi-level contribute significantly to the noise generation. Furthermore, such a Lorentzian contribution is extremely sensitive to temperature. Therefore, in a general sense, only mobility fluctuation mechanisms could be referred to the 1/f noise generation. The assumption of mobility fluctuations has already been proved by Kleinpenning [38-40] for Si and Ge following his studies of the 1/f noise in the thermal e.m.f. and Hall effect.

However, there are only a few models for mobility fluctuations. Neither of them could explain all the experimental observations. Here, I would like to mention three models: (i) quantum 1/f noise theory [16,41]; (ii) phonon fluctuation (PF) models [42,43]; (iii) quantum "local-interference" (LI) models [26,27].

The quantum 1/f theory attributes 1/f noise in semiconductors to a correction to the cross section of the scat-

tering process induced by the infrared divergence. So far this theory has not been currently accepted since it predicts too low α-values (10^{-9}-10^{-6}, depending on the scattering process [16]) to account for the experimentally found α-values [44].

The noise source, according to the phonon fluctuation (PF) models [42,43], is a 1/f fluctuation in the population of lattice modes. Such a 1/f fluctuation manifest itself in resistance fluctuations via the lattice phonon scattering. However, there are several points which the PF models can not explain. First of all, the PF models only deal with acoustic phonon scattering, obviously not applicable to III-V compound semiconductors. Secondly, the PF models assume a Lorentzian spectrum for each mode of phonons. Experimentally, instead of a Lorentzian, Musha *et al.* [45] observed a 1/f spectrum for the fluctuations in phonon number per mode and no correlations for the fluctuations in phonon number of different modes. Finally, as we shall point out in the Chapter 5 of this thesis, the current PF models do not predict a temperature dependence of α.

As discussed above, the 1/f noise in metals is often interpreted by the DDH model. In addition, the DDH model implies that defect motion is the 1/f noise source in metals. However, the question that arises is how can the defect motion induce fluctuations in the resistance? The quantum "local-interference" (LI) model has provided an answer to this question. Since the LI model is important for the understanding of the extrinsic noise source discovered in our proton-irradiated GaAs samples (Chapter 5 of this thesis), here I shall try to describe it in some detail and in a heuristic way. Consider two defects with a separation distance R. The essence of the "local-interference" effect is that the resistance is modulated when the two defects move so close to each other that within the coherent wavelength of electrons, the scattering

wavefunctions interfere. To put it more clearly, let us consider two point scattering centres. The contribution to the resistance of these two scattering centres is proportional to the net scattering rate Γ. Γ can be written as

$$\Gamma = \int S(\boldsymbol{k},\boldsymbol{k}')\,(1-\cos\theta)\,d\boldsymbol{k}' \qquad (18)$$

where $S(\boldsymbol{k},\boldsymbol{k}')$ is the probability for scattering from state $\boldsymbol{k}$ to $\boldsymbol{k}'$ and θ is the angle between $\boldsymbol{k}$ and $\boldsymbol{k}'$. By the familiar "Golden rule", we can write

$$S(\boldsymbol{k},\boldsymbol{k}') = \frac{2\pi}{\hbar}\,|M(\boldsymbol{k},\boldsymbol{k}')|^2\,\delta(\mathscr{E}_{\boldsymbol{k}}-\mathscr{E}_{\boldsymbol{k}'})\,, \qquad (19)$$

where $\delta(x-x')$ is the Dirac delta function, and M is a matrix element of

$$M(\boldsymbol{k},\boldsymbol{k}') = \int_{\Omega_K} \Psi^*_{\boldsymbol{k}'}(\boldsymbol{r})\,\Delta V \Psi_{\boldsymbol{k}}(\boldsymbol{r})\,d\boldsymbol{r}. \qquad (20)$$

The electron wavefunction, $\Psi_k(\mathbf{r})$, is given by a plane wavefunction of a free electron in case of metals or a Bloch wavefunction in case of semiconductors. In both cases, the matrix elements are

$$M(\boldsymbol{k},\boldsymbol{k}') \propto |V(\boldsymbol{k}'-\boldsymbol{k})| \qquad (21)$$

Here, $V(\boldsymbol{k}'-\boldsymbol{k})$ is simply the Fourier transform of the scattering potential ΔV regarding to a wave vector $\Delta\boldsymbol{K}=\boldsymbol{k}'-\boldsymbol{k}$. Then, the total scattering amplitude of the two point scattering centres will be

$$|V(\boldsymbol{k}',\boldsymbol{k})| = |V(\Delta\boldsymbol{K}) + V(\Delta\boldsymbol{K})\,e^{i\Delta\boldsymbol{K}\cdot\boldsymbol{R}}| = |V(\Delta\boldsymbol{K})|\,[1+\cos(\Delta\boldsymbol{K})\cdot\boldsymbol{R})]\,. \qquad (22)$$

Obviously, the term with the cosine function represents the interference. From eq. (22), it is clear that the interference term is only important when R is comparable to the wavelength of the scattered electrons. Detailed calculations of Hershfield [27] and Pelz *et al.* [26] show that the relative resis-

tance fluctuations in metals are, typically, about a few tenths for point scatterers.

Regarding the 1/f noise as induced by defect motion, one point that I would like to point out is that the assumption of independent fluctuations of the mobility would be no longer valid since after a reasonably long time interval all electrons will be scattered by one specific pair of the moving defects. Hence, to some extent, correlation of the fluctuations in the mobilities of the charge carrier is expected. In this sense, the relative noise power density in the empirical relation is expected to be normalized to the number of the moving defects instead to the number of free charge carriers. This point will not raise a serious problem for metals, but it will give a serious problem for semiconductors.

1.3 Scope of the Thesis

As discussed in the previous section, the approach by Hooge's empirical relation and hypothesis of the mobility fluctuations have experimentally been proved to be successful in describing the 1/f noise in homogeneous semiconductors. However, in both theoretical and experimental aspects, there still is a serious problem: α scatters in a wide range of 10^{-7}-10^{-2} [30,31]. It is this problem that has raised many criticisms [14,46] on Hooge's empirical relation, and hence obscured its physical meaning. To solve this problem, let us, at first, neglect some theoretical arguments [16], but concentrate on experimental facts. Several experimental studies have been done on silicon samples [30-31,47]. Besides the well known case of heavy impurity scattering reducing the 1/f noise [48], two trends were clearly observed: low α-values (10^{-7}-10^{-6}) are often observed in samples (i) of a small volume; (ii) with high perfection of the crystal lattice. Careful measurements of Clevers [31] on noise in Si samples with a volume down to $10^{-18}m^3$

showed that the small volume is not the decisive factor. Furthermore, there is good experimental evidence [47] suggesting that the α-values are determined by the perfection of the crystal lattice or in other words by the density of lattice defects. But, what is the physical mechanism behind it or how could α depend on the crystal quality, is still unknown or, more precisely, badly understood. Therefore, in this thesis I attempt to find an answer to the questions mentioned above.

The strategy to approach the problem of quality-dependent α-values is simple. We started with high-quality and well-defined semiconductors with different doping levels. Here we could rely on the epitaxial layers of n-GaAs grown at the Physics Department of Eindhoven University of Technology, by molecular beam epitaxy (MBE). Noise measurements were performed in order to check the validity of Hooge's empirical relation and the assumption of mobility fluctuations. Special attention has been paid to the temperature dependence of the 1/f noise. Then, the crystal lattice of epitaxial GaAs was gradually damaged by means of electron and proton irradiation. The changes in the noise were investigated of these damaged samples.

The contents of this thesis are outlined as follows:

- chapter 2 contains two papers published in Physica B, in which are presented the experimental results of 1/f noise and its temperature dependence in epitaxial n-GaAs, with the thickness and the dope concentration as parameters.
- chapter 3 presents a study of 1/f noise in Hall-voltage of MBE-grown n-GaAs, which has been published in Physica B.
- chapter 4 contains two papers. One is published in Journal of Applied Physics, in which a study of low-frequency noise in electron-irradiated n-GaAs epitaxial layers is presented. Here we observed also g-r noise. For the interpretation we needed a simple formalism, which is presented in the second

paper submitted to Physica B.

- chapter 5 is a paper submitted to Journal of Applied Physics, in which we report our investigations of 1/f noise in proton-irradiated n-GaAs epitaxial layers.
- chapter 6 is a paper submitted to Physica B, in which a study of 1/f noise in an $Al_xGa_{1-x}As/GaAs$ heterostructure with a two-dimensional gas, is presented.
- chapter 7 presents the conclusions of the thesis. Some suggestions for future work are also given in this chapter.

The author has presented parts of chapter 2 at the 11th International Conference on Noise in Physical Systems held at Kyoto (1991). The text of the Proceedings, see [49], is not included in this thesis.

REFERENCES

[1] N.G. van Kampen, *Stochastic Processes in Physics and Chemistry*, North Holland, Amsterdam, 1981, p. 61.

[2] K.M. van Vliet and J.R. Fassett, In *Fluctuation Phenomena in Solids* (Edited by R.E. Burgess), Chapter 7, Academic Press, New York (1965).

[3] R.F. Voss and J. Clarke, J. Acoust. Soc. Am., 63, 258-263(1978).

[4] M.Gardner, *Scientific American*, 238(4), 16-32(1978).

[5] T. Musha and H. Higuchi, in *Proceedings of the Symposium on 1/f Fluctuations* (Inst. Elect. Engineers, Tokyo, Japan)p. 187(1977).

[6] *Proceedings of the International Conference on Noise in Physical Systems and 1/f Fluctuations* (Edited by T. Musha, S. Soto and M. Yamamoto, Ohmsa, Tokyo), section 17-20 (1991).

[7] J.B. Johnson, Phys. Rev. 26, 71(1925).

[8] R.F. Voss and J. Clarke, Phys. Rev. B 13, 556(1976).

[9] A. Van der Ziel, Adv. Electron. Electron Phys. 49, 225

(1979).

[10] D.A. Bell, J. Phys. C: Solid State Phys. **13**, 4425(1980).

[11] P. Dutta and P.M. Horn, Rev. Mod. Phys. **53**, 497(1981).

[12] F.N. Hooge, T.G.M. Kleinpenning and L.K.J. Vandamme, Rep. Prog. Phys. **44**, 479(1981).

[13] Sh.M. Kogan, Usp. Fiz. Nauk **145**, 285(1985).

[14] M.B. Weissman, Rev. Mod. Phys. **60**, 537(1988).

[15] A. Van der Ziel, Proc. IEEE **76**, 233(1988).

[16] C. M. Van Vliet, Solid-St. Electron. **34**, 1(1991).

[17] H.G.E. Beck and W.P. Spruit, J. Appl. Phys. **49**, 3384 (1978).

[18] I.R.M. Mansour, R.J. Hawkins and G.G. Bloodworth, Radio and Elec. Eng. **35**, 212(1968).

[19] M.A. Caloyanides, J. Appl. Phys. **45**, 307(1974).

[20] T.G.M. Kleinpenning and A.H. de Kuijper, J. Appl. Phys. **63**, 43(1988).

[21] A.L. McWhorter, *Ph.D. dissertation*, Massachussetts Institute of Technology, Cambridge, Massachussettes (1955).

[22] P. Dutta, P. Dimon and P.M. Horn, Phys. Rev. Lett. **43**, 646(1979).

[23] J.W. Eberhard and P.M. Horn, Phys. Rev. B **18**, 6681(1978).

[24] J. Bernamont, Ann. Phys. (Leipzig) **7**, 71(1937).

[25] S. Feng, P.A. Lee and A.D. Stone, Phys. Rev. Lett. **56**, 1960(1986).

[26] J. Pelz and J. Clarke, Phys. Rev. B **36**, 4479(1987).

[27] S. Hershfield, Phys. Rev. B **37**, 8557(1988).

[28] F.N. Hooge, Phys. Lett **29A**, 139(1969).

[29] L.K.J. Vandamme, in *Noise in Physical Systems and 1/f Noise*, edited by M. Savelli, G. Lecoy, and J.P. Nougier (North-Holland, Amsterdam), p.183(1983).

[30] J. Bisschop, *Ph. D. dissertation*, Eindhoven University of Technology, Eindhoven(1983).

[31] R. Clevers, *Ph. D. dissertation*, Eindhoven University of Technology, Eindhoven(1988).

[32] *Chapter 2 of this thesis.*

[33] F. Hofman and R.J.J. Zijlstra, Solid-St. Comm. **72**, 1163 (1989).

[34] F.N. Hooge, Physica B **114**, 391(1982).

[35] R.J. Fronen, *Ph. D. dissertation*, Chapter 3, Eindhoven University of Technology, Eindhoven(1990).

[36] K.K. Hung, P.K. Ko, C. Hu and Y.C. Cheng, IEEE Trans. Electron Dev. **37**, 654(1990).

[37] M.B. Weissman, in *Proceedings of the Sixth International Conference on Noise in Physical Systems*, edited by P.H.E. Meijer, R.H. Mountain and R.J. Soulen (Dept. of Commerce, NBS Special Publication **619**, Washington D.C.), 133(1981).

[38] T.G.M. Kleinpenning, Physica **77**, 78(1974).

[39] H.M.J. Vaes and T.G.M. Kleinpenning, J. Appl. Phys. **48**, 5131(1977).

[40] T.G.M. Kleinpenning, J. Appl. Phys. **51**, 3438(1980).

[41] P.H. Handel, Phys. Rev. Lett. **34**,1492(1975).

[42] R.P. Jindal and A. Van der Ziel, J. Appl. Phys. 52, 2884(1981).

[43] B. Dierickx and E. Simoen, IEEE Trans. Electron Dev. **38**, 1913(1991).

[44] F.N. Hooge, in *Proceedings of 11th Int. Conf. on Noise in Physical Systems*, edited by T. Musha, S. Sato and M. Yamamoto, Ohmsa, Tokyo, 7(1991).

[45] T. Musha, G. Borbely and M. Shoji, Phys. Rev. Lett. **64**, 2394(1990).

[46] R.D. Black, M.B. Weissman and P.J. Restle, J. Appl. Phys. **53**, 6280(1982).

[47] L.K.J. Vandamme and S. Oosterhoff, J. Appl. Phys. **59**, 3169(1986).

[48] F.N. Hooge and L.K.J. Vandamme, Phys. Lett. **A 66**, 315 (1978).

[49] L. Ren, in *Proceedings of 11th Int. Conf. on Noise in Physical Systems*, edited by T. Musha, S. Sato and M. Yamamoto, Ohmsa, Tokyo, 45(1991).

Chapter 2

1/f Noise in Epitaxial n-GaAs

Part I.

1/f noise at room temperature in n-type GaAs grown by molecular beam epitaxy

L. Ren and M.R. Leys

Department of Electrical Engineering & Department of Physics, Eindhoven University of Technology, Eindhoven, The Netherlands

Received 4 December 1990
Revised 8 February 1991

The $1/f$ noise in n-GaAs epitaxial layers grown by molecular beam epitaxy was investigated at room temperature for various doping concentrations. The measured $1/f$ noise is a bulk effect. The noise parameter α between 10^{-4} and 10^{-3} was found to be dependent on the doping concentration.

1. Introduction

Epitaxial grown techniques are now being used more and more widely for the fabrication of GaAs devices. Low-frequency noise in the epitaxial GaAs devices was often observed to have a frequency dependence f^{-1}, the so-called $1/f$ noise [1–5]. A parameter α, defined by Hooge's empirical relation [6] for this special type of noise, is commonly used to compare the $1/f$ noise level in different samples. In epitaxial GaAs MESFETs the α-values were found to be about 10^{-4} [1, 2, 5]. An α-value of about 7.1×10^{-4} was determined for an AlGaAs/GaAs heterostructure [3]. For determining the $1/f$ noise parameter α simple homogeneous layers are preferable to complicated devices.

There are not many reports on $1/f$ noise in homogeneous n-GaAs epitaxial layers. However, in addition to $1/f$ noise, generation–recombination noise and possibly diffusion noise were also present in such homogeneous GaAs epitaxial layers and the noise spectra were found to be dependent on the contact materials [7] and surface treatment [8]. It should be noted that the noise levels reported for these epitaxial layers were relatively high with a modified noise parameter α greater than 10^{-2} (defined by the relation $S_v = \alpha' V^2 / f^{\beta} N$ with $\beta \neq 1$, see eq. (2) of ref. [7]), so that further investigation is needed.

Here we report noise measurements on homogeneous Si-doped n-GaAs epitaxial layers grown by molecular beam epitaxy. The $1/f$ noise in such layers was systematically studied as functions of contact materials, the thickness of the epitaxial layers and the carrier concentration.

2. Experimental

Epitaxial layers of GaAs were grown in a Varian MOW 3″ MBE system. Semi-insulating undoped GaAs (0 0 1) wafers were used as substrates. The growth temperature was 630°C, the growth rate was 1 μm/h with a measured arsenic beam flux $P_{As_4} = 9.0 \times 10^{-6}$ Torr. Silicon was used as n-type dopant. Four epitaxial layers with different doping levels were grown as: 2.5NE14, $N_d \cong 2.5 \times 10^{14}$ cm^{-3}, and 10 μm thick; 1NE15, $N_d \cong 1.0 \times 10^{15}$ cm^{-3}, 11 μm thick; 1NE16, $N_d \cong 1.0 \times 10^{16}$ cm^{-3} cm^{-3}, 3.2 μm thick; 1NE17, $N_d \cong 1.0 \times 10^{17}$ cm^{-3}, 4 μm thick.

We used a bridge-shaped Hall bar structure to avoid contact noise and achieve a homogeneous electrical field distribution in the samples. The Hall bar structures were fabricated by conven-

tional photolithography, lift-off and etching. The dimensions are shown in fig. 1. Two kinds of metallization were used to make the Ohmic contact: (1) tin balls were placed on the contact areas and annealed in a N_2/H_2 mixture at 400°C for 1 min; (2) a mixture of Au/Ge (88/12%) was evaporated onto the contact areas to a thickness of 52 nm followed by a 12 nm thick layer of Ni and finally a 26 nm thick layer of pure gold, after which the samples were annealed in a N_2/H_2 mixture at 450°C for 30 s. The current–voltage characteristics of the contacts, irrespective of the metallization processes, were completely linear in the applied bias range.

The noise measurements were performed in a Faraday cage at room temperature. A DC bias current was supplied by batteries with a metal-film series resistor whose resistance was at least 20 times larger than that of the samples. The current flows through contacts 1 and 2. The spectral noise intensity S was determined from the equivalent noise voltage generator in series with the measuring probes. The voltage fluctuations, here called longitudinal noise, were measured parallel to the current flowing on the side contacts 3 and 5. The voltage noise, here called transverse noise was also measured perpendicular to the current flowing on the contacts 4 and 7. The calculated ratio $S_{47}/S_{35} \cong 0.11$ [9] was used check the contact noise. The voltage fluctuations were amplified by an ultra-low-noise preamplifier, EG&G 5004. The output was fed into a dynamic spectrum analyser with a frequency range of from 1.6 Hz to 20 kHz, Brüel & Kjaer type 2131, which was connected to a microcomputer. The current-independent noise was also measured and subtracted from the noise measured with a current flowing. The pure excess noise was plotted by the computer.

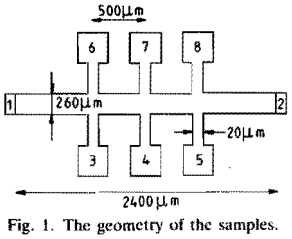

Fig. 1. The geometry of the samples.

3. Results and discussions

Most of the noise spectra we measured had a good $1/f$ shape with the frequency exponents between 0.9 and 1.1 in the frequency range considered. This holds both for the samples with the Sn and AuGeNi contacts. The $1/f$ noise levels increase proportionally with the square of the terminal voltage, indicating a resistivity fluctuation mechanism. Figure 2 shows some experimentally observed noise spectra from the four-probe measurements on the samples with

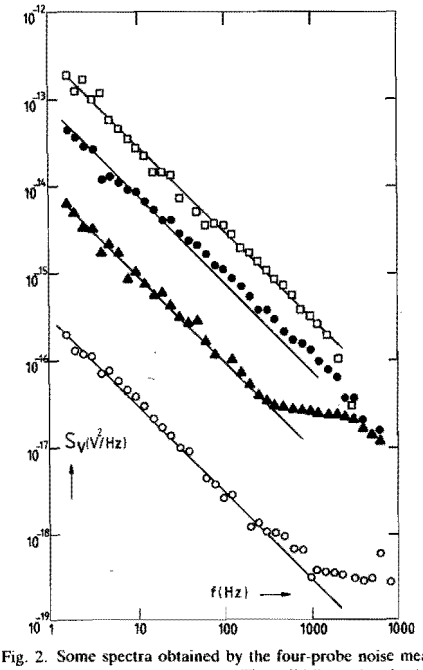

Fig. 2. Some spectra obtained by the four-probe noise measurements at room temperature. The solid lines give the $1/f$ noise levels (□: 2.5NE14, $E = 6.1$ V/cm; ●: 1NE15, $E = 11.6$ V/cm; ▲: 1NE16, $E = 10.7$ V/cm; ○: 1NE17, $E = 11.5$ V/cm).

Sn contacts. We observe that, like Tacano et al. [7], despite the higher contact resistance of Sn the $1/f$ noise levels in the samples with Sn contacts were about 2–3 times lower than that of the samples with AuGeNi contacts for all the doping levels. This could hardly be attributed to the scattering of the experimental data since we have observed rather good reproducibility in the noise measurements on various samples made from one and the same wafer.

In order to study the influence of the surface and the interface on $1/f$ noise we used samples with different thicknesses. The thicknesses of an epitaxial layer were obtained by wet etching on one and the same wafer of 1NE15. The thickness of 11 μm for the 1NE15 epitaxial layer prior to etching was accurately determined by the growth rate of MBE. The thicknesses after etching were measured by mechanical probing. The experimental values for this thickness, called metallurgical thickness t_m, Hall mobility μ_H and the noise parameter α of 1NE15 are presented in table 1. The values were obtained on the Sn contact samples. In view of depletion regions near the surface and near the semiconductor-substrate interface [10], the effective thickness t_{eff} of the conducting layer is less than the metallurgical thickness t_m. The values of t_{eff} can be found from the Hall effect measurements by plotting the sheet carrier concentration n_{sheet} versus t_m the metallurgical thickness, where the relation $n_{sheet} = nt_{eff} = n(t_m - t_0)$ holds. By extrapolation we found $t_0 \cong 2.5$ μm, the thickness of the depletion layers. The values of t_{eff} are also presented in table 1. The value $t_0 \cong 2.5$ μm is in good agreement with Chandra's calculation [10] for an n-GaAs epitaxial layer with a doping concentration of about 10^{15} cm^{-3}. The Hall mobilities measured on these three samples were almost the same, which implies a good homogeneous doping. The noise spectra of the thinnest sample 1NE15-c was spoiled by some not well understood low-frequency bulges, so that only an upper limit of α was obtained. In contrast to Tacano et al. [7] we found that the $1/f$ noise dominates at the low-frequency range, and our α-values were all of the same order and no significant thickness dependence was observed (see table 1). It is therefore concluded that the $1/f$ noise measured in our samples is bulk noise.

It seems that the low-frequency noise measured by Tacano et al. was a different type of noise, considering that their modified α'-values depended on the thickness and their α'-values were relatively high ($1 \geqq \alpha' \geqq 10^{-2}$). It should be pointed out that the interpretation by Tacano et al. of their noise spectra (see fig. 1 of ref. [7]) as $1/f$ noise superimposed on the generation-recombination noise is unlikely, since such a superposition would give a low-frequency part of the spectra that is flatter than f^{-1} due to the plateau of the Lorentzian spectra of the generation–recombination noise. Using their published data, a rough estimation of the upper limit of the $1/f$ noise level indicates that α of their 0.4 μm thick sample would be smaller than 8×10^{-4}, assuming that the $1/f$ noise was dominated by another type of noise of unknown nature.

Figure 3 shows the mobilities and the α-values as a function of the carrier concentration. The data points of α were obtained on the differently doped samples with Sn contacts. The carrier concentration n and the mobility μ were determined from Hall-effect and resistivity mea-

Table 1
Experimental results at $T = 295$ K for t_m, t_c, μ_H and α.

	1NE15-a	1NE15-b	1NE15-c
Metallurgical thickness t_m (μm)	11	7.8	4.7
Effective thickness t_{eff} (μm)	8.6	5.1	2.2
Mobility μ_H (cm^2/Vs)	7350	7410	7460
α	$(4.7 \pm 0.8) \times 10^{-4}$	$(5 \pm 1) \times 10^{-4}$	$\leqslant 6 \times 10^{-4}$

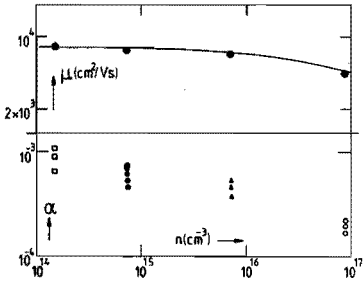

Fig. 3. Mobility μ and α versus carrier concentration n at room temperature (for symbols see fig. 2). Solid line: theoretical prediction after Rode [11].

surements under the assumption that the Hall factor equals 1. The solid curve is a theoretical prediction for n-GaAs taken from ref. [11]. Both the mobilities and the α-values decrease with increase of the doping concentration.

Hooge and Vandamme [12] experimentally showed that the ionized impurity scattering does not contribute to the generation of $1/f$ noise in Ge. Following their approach, we assume that Matthiessen's rule holds, hence

$$\frac{1}{\mu_{exp}} = \frac{1}{\mu_{imp}} + \frac{1}{\mu_0}, \qquad (1)$$

where μ_{exp} is the experimentally obtained mobility, μ_{imp} the mobility determined by the ionized impurity scattering and μ_0 the mobility due to the other scattering mechanism. Then eq. (2) can be derived on the assumption that the ionized impurity scattering does not produce $1/f$ noise, that is

$$\alpha_{exp} = \left(\frac{\mu_{exp}}{\mu_0}\right)^2 \cdot \alpha_0, \qquad (2)$$

in which α_0 is a noise parameter due to the other scattering mechanisms. The magnitude of α_0 could depend on the crystal lattice quality [13] and is assumed to be the same in our epitaxial layers with different doping. In fig. 4 we replotted our α-values against the experimental

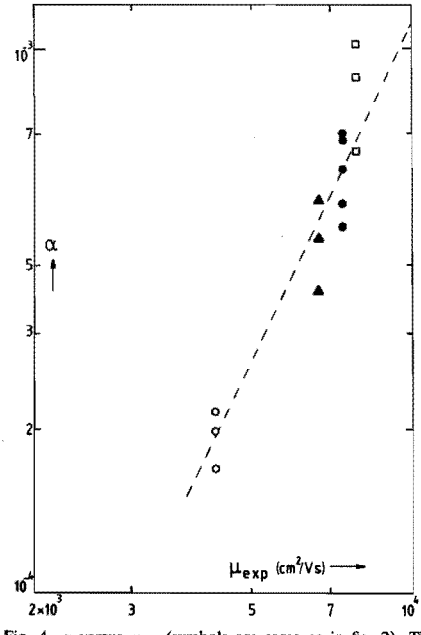

Fig. 4. α versus μ_{exp} (symbols are same as in fig. 2). The dashed line represents a μ_{exp}^2 dependence.

mobility μ_{exp}. The α-values decrease more or less as the square of μ_{exp} as predicted by eq. (2). We are aware of the theoretical objections that have been put forward against eq. (2) [14, 15]. We cannot refute them but establish here that eq. (2) correctly describes the variation of the $1/f$ noise with the experimental mobility. An α-value of 1.9×10^{-4} for our samples with doping of about 1×10^{17} cm^{-3}, is in good agreement with the value of about 10^{-4} often found for MBE-grown channel layers with a doping concentration of about $(2\text{–}3) \times 10^{17}$ cm^{-3} in epitaxial GaAs MESFETs [2, 5]. If we take 8500 cm^2/Vs as the highest value found for pure n-GaAS [11] for μ_0, we find $\alpha_0 \cong 7.6 \times 10^{-4}$ for our epitaxial GaAs material, which is in quite good agreement with a value of 7.1×10^{-4} determined at a AlGaAs/GaAs heterostructure [3] where

the ionized impurity scattering can be neglected due to the spatial separation between the mobile charge carriers and their parent donors.

4. Conclusion

$1/f$ noise in n-GaAs epitaxial layers grown by MBE were investigated. We observed that samples with nonalloyed Sn contacts showed less $1/f$ noise compared to the samples with alloyed Au-GeNi contacts. The $1/f$ noise we measured was bulk noise without a significant dependence on thickness. The dependence of α-values on doping can be interpreted by the noise reduction factor $(\mu/\mu_0)^2$ proposed by Hooge and Vandamme [12]. The α-values between 10^{-4} and 10^{-3} for our MBE-grown epitaxial layers are in agreement with α-values found in GaAs epitaxial devices.

Acknowledgements

The authors would like to thank Professor Dr. F.N. Hooge for his encouraging interest in this work. We also thank R. Windgassen for performing part of measurements and W. v.d. Eijnden, S. Couwenberg, W.C. v.d. Vleuten and P.A.M. Nouwens for their technical assistance.

This work is part of the research program of the "Stichting voor Fundamenteel Onderzoek der Materie (FOM)", which is financially supported by the "Nederlandse organisatie voor wetenschappelijk onderzoek (NWO)".

References

[1] K.H. Duh and A. van der Ziel, IEEE Trans. Electron. Dev. 32 (1985) 662.
[2] S. Hashiguchi, N. Aoki and H. Ohkubo, Solid State Electron. 29 (1986) 745.
[3] M. Tacano, Y. Sugiyama and H. Soga, Solid State Electron. 32 (1989) 49.
[4] S. Hashiguchi and H. Irie, in: 10th Int. Conf. on Noise in Physical Systems, Budapest (1989), ed. A. Ambrozy (Akadamiai Kiado, Budapest, 1990) p. 507.
[5] J.M. Peransin, P. Vignaud, D. Rigaud and L.K.J. Vandamme, IEEE Trans. Electron. Dev. 37 (1990) 2250.
[6] F.N. Hooge, Phys. Lett. A29 (1969) 139.
[7] M. Tacano, Y. Sugiyama, T. Taguchi and H. Soga, Solid State Electron. 31 (1988) 1215.
[8] A. Ambrozy, P. Gottwald and B. Szentpali, in: 10th Int. Conf. on Noise in Physical Systems, Budapest (1989), ed. A. Ambrozy (Akademiai Kiado, Budapest, 1990) p. 445.
[9] L.K.J. Vandamme and W.M.C. van Bokhoven, Appl. Phys. 14 (1977) 205.
[10] A. Chandra, C.E.C. Wood, D.W. Woodard and L.F. Eastman, Solid State. Electron. 22 (1979) 645.
[11] D.L. Rode, Semiconductors and Semimetals, Vol. 10 (Academic, New York, 1973).
[12] F.N. Hooge and L.K.J. Vandamme, Phys. Lett. A66 (1978) 642.
[13] F.N. Hooge, Physica B 162 (1990) 344.
[14] M.B. Weissman, Physica B 100 (1980) 157.
[15] T.G.M. Kleinpenning, Physica B 103 (1981) 345.

Part II.

Physica B 176 (1992) 209–212
North-Holland

PHYSICA B

Temperature dependence of $1/f$ noise in epitaxial n-type GaAs

L. Ren and F.N. Hooge

Department of Electrical Engineering, Eindhoven University of Technology, Eindhoven, The Netherlands

Received 27 July 1991

The $1/f$ noise of n-type epitaxial GaAs was measured between 77 and 300 K. The $1/f$ noise turns out to be a fluctuation in the lattice scattering. At low temperatures $\alpha_{\text{latt}} \cong 7 \times 10^{-5}$. At high temperatures the noise generation is thermally activated with an activation energy of about 0.13 eV.

1. Introduction

About half a year ago we published a paper on the $1/f$ noise in n-type epitaxial GaAs at room temperature [1]. The present paper deals with the temperature dependence of the noise in the same samples. We will, therefore, use the same symbols in the text and figures as in the first paper. The preparation of the samples is described in full detail in ref. [1].

We measured the noise between 1 Hz and 10 kHz. At all temperatures we found pure $1/f$ spectra, without any systematic deviation in the exponent -1.0.

We determine a value of α according to

$$\frac{S_R}{R^2} = \frac{\alpha_{\text{exp}}}{fN}, \tag{1}$$

where N is the total number of the free charge carriers in the sample [2]. The value of α, experimentally found without any further interpretation, we call α_{exp}.

2. Experimental part

The samples were made from three epitaxial layers 1NE15 with $n \cong 0.7 \times 10^{15}$ cm^{-3}, thickness 11 μm; 1NE16 with $n \cong 0.8 \times 10^{16}$ cm^{-3}, thickness 3.2 μm; 1NE17 with $n \cong 0.8 \times 10^{17}$ cm^{-3}, thickness 4 μm. The concentrations of the free charge carriers were almost temperature independent. Either Sn or AuGeNi alloy was used to make Ohmic contacts, which showed perfect Ohmic behaviour in the temperature range from 77 to 300 K. In some samples with AuGeNi contacts we found generation–recombination noise. Samples with Sn contacts never showed GR noise.

The samples were mounted in a cryostat cooled by liquid nitrogen. The temperature was measured by a copper-constantan thermocouple on the sample holder close to sample. The resistance of the sample R as a function of the temperature, and the Nyquist noise level $4kTR$ were also measured to check the actual sample temperature. We made sure that the contact noise could be neglected compared to the noise in the epitaxial layer.

The Hall effect and resistivity were measured at all temperatures where the noise was measured. Under all circumstances we used for the Hall factor $r_H = 1$.

The results of the noise measurements will be presented as plots of $\log \alpha$ versus $1000/T$, because we found α-values proportional to $\exp(-E/kT)$. The different scattering mechanisms play an important part in the interpretation of the temperature dependence of α. Therefore, we start with a plot of the different mobility contributions. In order to facilitate the com-

parison of α with μ we have plotted log μ versus $1000/T$, instead of the usual double-log plots suggested by $\mu \propto T^{\gamma}$. Our values of μ are in agreement with the well-known values for n-GaAs epitaxial layers reported by Wolf and Stillman [3]. Our values which will be used in determining the contributions of the different scattering mechanisms are presented in fig. 1. These results will be used in the analysis of the temperature dependence of the noise. The formulas and parameters for the calculation of the temperature dependence of the three relevant lattice mobilities, which are shown in fig. 1(a), were taken from ref. [4].

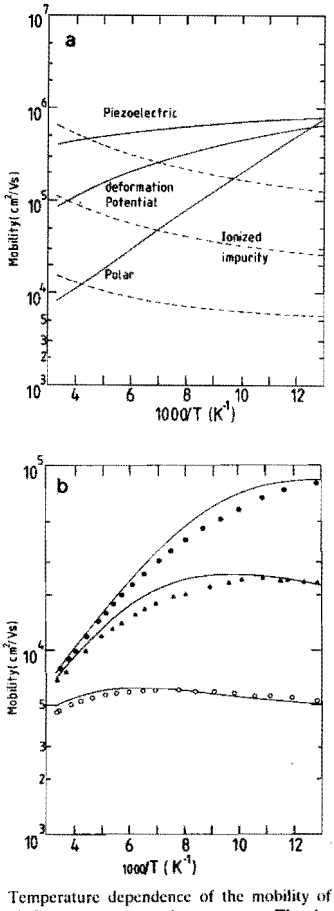

Fig. 1. Temperature dependence of the mobility of n-type GaAs. (a) the separate scattering processes. The three lines for the impurity scattering are for the concentrations 10^{15}, 10^{16} and 10^{17} cm^{-3}. (b) the combined processes and the experimental values (● = 1NE15; ▲ = 1NE16; ○ = 1NE17).

Figure 2 shows α_{exp} versus $1000/T$. Such a temperature dependence of α – steep at high temperatures, flat at low temperatures – agrees with a model proposed by Luo [5]. His model is a surface model, from which follows that α, as defined and measured by us, would depend on sample thickness. This, however, turns out not to be the case in our samples [4].

The general trend is the same as with Si and Ge [6–10]. At lower temperatures we find a constant low value of α. At higher temperatures there is an exponential dependence that is described by the activation energies 0.14 ± 0.02, 0.15 ± 0.02, and 0.20 ± 0.03 eV (If we would describe α by $\alpha \propto T^{\gamma}$ we can reasonably well approximate the experimental curves with $\gamma \cong 7$, $\gamma \cong 8$ and $\gamma \cong 10$). The three values found for the activation energy do not have a physical meaning because the slope is strongly influenced

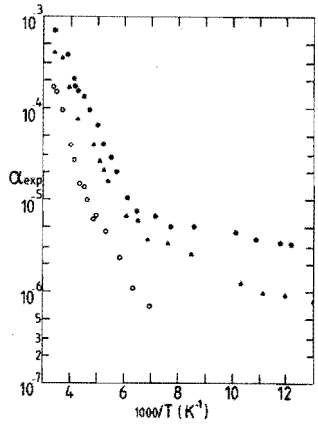

Fig. 2. Temperature dependence of α_{exp} (for symbols see fig. 1).

by the contribution of the impurity scattering. This contribution is different in the three samples and is temperature dependent.

3. Discussion of the experimental results

Matthiessen's rule gives, as usual, a satisfactory approximation for treating mixtures of scattering mechanisms. For the mobility we have

$$\mu_{\rm exp}^{-1} = \mu_{\rm imp}^{-1} + \mu_{\rm pol}^{-1} + \mu_{\rm def}^{-1} + \mu_{\rm pie}^{-1}, \qquad (2)$$

where the subscripts stand for exp: experimentally found average value, imp: scattering by charge impurities, pol: scattering by polar optical phonons, def: scattering by acoustic phonon deformation potential and, pie: scattering by acoustic phonon piezoelectric potential. Taking the three components from lattice vibrations together we use

$$\mu_{\rm latt}^{-1} = \mu_{\rm pol}^{-1} + \mu_{\rm def}^{-1} + \mu_{\rm pie}^{-1}. \qquad (3)$$

If we assume no or very little noise in the impurity scattering we find from eq. (2) the simple expression

$$\alpha_{\rm exp} = \left[\frac{\mu_{\rm exp}}{\mu_{\rm latt}}\right]^2 \cdot \alpha_{\rm latt}. \qquad (4)$$

$\alpha_{\rm latt}$ can be presented in more detail as

$$\alpha_{\rm latt} = \mu_{\rm latt}^2 \cdot \left[\frac{\alpha_{\rm pol}}{\mu_{\rm pol}^2} + \frac{\alpha_{\rm def}}{\mu_{\rm def}^2} + \frac{\alpha_{\rm pie}}{\mu_{\rm pie}^2}\right], \qquad (5)$$

where the three αs could have different values and different temperature dependences.

We first tried relation (4) at two fixed temperatures, $T = 78$ K and $T = 295$ K, where we were certain that the sample temperature was constant during the noise measurement. The results are presented in fig. 3. Each point represents the average of the measurements on one sample. Different samples give different points. The α-values at 78 K of the sample 1NE17 could not be included in fig. 3 because the $1/f$ noise produced at an acceptable power dissipation could not be detected above the thermal noise of the sample and the $1/f$ noise of the preamplifier. From this it follows that α must be below 10^{-7}. Instead we include a GaAs sample grown by metal organic chemical vapour deposition (MOCVD). The electrical properties of this MOCVD sample agree with the MBE samples.

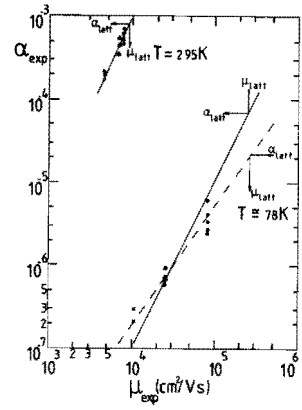

Fig. 3. α versus $\mu_{\rm exp}$ at two fixed temperatures $T \cong 295$ K and $T \cong 78$ K (symbols are same as in fig. 1, and × = MOCVD n-GaAs with $n \cong 4 \times 10^{16}$ cm^{-3}). The full lines represent $\mu_{\rm exp}^2$ dependences. The broken line is the best fit to the experimental data.

If we use eq. (4) the full line at $T = 295$ K in fig. 3 gives $\alpha_{\rm latt} = 8 \times 10^{-4}$ at $\mu_{\rm latt} = 8500$ cm^2/Vs. The full line at 78 K gives $\alpha_{\rm latt} = 7 \times 10^{-5}$ at $\mu_{\rm latt} = 2.5 \times 10^5$ cm^2/Vs. If we use the experimental data at 78 K (without bothering about Matthiessen's rule) we can draw a line that fits the experimental points better. This is the broken line shown in fig. 3 with α proportional to $\mu_{\rm exp}^{1.5}$. This line gives at $\mu_{\rm latt} = 2.5 \times 10^5$ cm^2/Vs an α-value $\alpha_{\rm latt} = 2 \times 10^{-5}$. The deviation from the simple equation (4) implies that either the use of Matthiessen's rule is inaccurate or the impurity scattering is not completely free of $1/f$ noise. If the latter case is true the real value of $\alpha_{\rm latt}$ could be even lower than 2×10^{-5}.

We then applied eq. (4) to the temperature range between $T = 77$ and 295 K. Figure 4 shows that at higher temperatures ($1000/T \leq 7$) we obtain one single line for $\alpha_{\rm latt}$ from the three curves

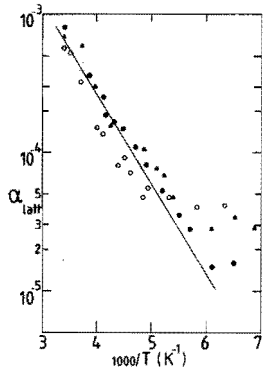

Fig. 4. Temperature dependence of α_{latt} (symbols are same as in fig. 1).

for α_{exp}. An activation energy of about 0.13 eV was determined from the slope of the line. For the lower temperature range ($7 \leq 1000/T \leq 13$) a simple application of Matthiessen's rule leads to a value of α_{latt} that is nearly constant. It is possible that α_{latt} slightly increases with $1/T$, certainly for high doping. That could mean that it is not correct to take the three scattering mechanisms together and express their effects as one single value of μ_{latt} and of α_{latt}. The least one could do is to write μ_{latt}^{-1} as three terms, like eq. (3), and to try to find three different α-values in eq. (5) with possibly different temperature dependences of α_{pol}, α_{def} and α_{pie}. However, such detailed noise calculations make no sense if they remain based on Matthiessen's rule, with scattering times averaged over all states in the conduction band. Figure 1 clearly shows that we do not have a situation at lower temperatures where one lattice scattering mechanism prevails, therefore application of Matthiessen's rule is not warranted. Hence we did not attempt any further analysis of α_{latt} at low temperatures. We end up with α_{latt} without any further refinement as

$$\alpha_{latt} = 0.1 \exp\left[\frac{-0.13\,\text{eV}}{kT}\right] + 7 \times 10^{-5}. \qquad (6)$$

These two terms could mean that we have here two types of $1/f$ noise. In any case the two noise mechanisms lead both to mobility fluctuations since both show a systematic dependence of α_{exp} on μ_{exp}.

In a recent paper Van Vliet [11] concluded that low α-values, of the order 10^{-5} to 10^{-6} could be explained by Handel's quantum $1/f$ noise theory [12] in case of umklapp and intervalley scattering that can be expected for low effective masses. The low-temperature $1/f$ noise in our samples could be Handel's type of noise, especially if we use the lower value for α_{latt}. At higher temperatures we then have a different, yet unexplained, noise mechanism.

Acknowledgements

The authors wish to thank Dr. M.R. Leys, W.C. v.d. Vleuten and P.A.M. Nouwens for the preparation of the MBE-grown GaAs samples. We express our gratitude to Professor dr. J. Gilling of the Catholic University of Nijmegen for kindly putting the MOCVD-grown samples at our disposal.

This work is part of the research program of the "Stichting voor Fundamenteel Onderzoek der Materie (FOM)", which is financially supported by the "Nederlandse Organisatie voor Wetenschappelijk Onderzoek (NWO)".

References

[1] L. Ren and M.R. Leys, Physica B 172 (1991) 319.
[2] F.N. Hooge, T.G.M. Kleinpenning and L.K.J. Vandamme, Rep. Prog. Phys. 44 (1981) 479.
[3] G.E. Stillman and C.M. Wolfe, Thin Solid Films 31 (1976) 69.
[4] D.C. Look, Electrical Characterization of GaAs materials and devices (Wiley, New York 1989) Ch. 1, Sec. 3.
[5] J. Luo, W.F. Love and S.C. Miller, J. Appl. Phys. 60 (1986) 3196.
[6] J. Bisschop, Ph.D. Thesis, Eindhoven University of Technology (1983).
[7] J. Bisschop and J.L. Cuijpers, Physica B 123 (1983) 6.
[8] R.H.M. Clevers, Ph.D. Thesis, Eindhoven University of Technology (1988).
[9] R.H.M. Clevers, Physica B 154 (1989) 214.
[10] R.H.M. Clevers, J. Appl. Phys. 62 (1987) 1877.
[11] C.M. van Vliet, Solid State Electron. 36 (1991) 1.
[12] P.H. Handel, Phys. Rev. Lett. 34 (1975) 1492.

Chapter 3

1/f-Noise in the Hall voltage of epitaxial n-GaAs

L. Ren[a] and J.S. Liberis[b]

[a]*Department of Electrical Engineering, Eindhoven University of Technology, The Netherlands*
[b]*Lithuanian Academy of Sciences, Semiconductor Physics Institute, Vilnius, Lithuania*

Received 13 August 1992

The effects of magnetic induction on 1/*f*-noise in n-GaAs are investigated both at room temperature and at liquid-nitrogen temperature. A numerical calculation for such effects in n-GaAs is given, based on optical-phonon scattering. By comparing the experimental data with the theoretical predictions for mobility fluctuations and for number fluctuations, we conclude that 1/*f*-noise in n-GaAs epitaxial layers is caused by mobility fluctuations.

1. Introduction

The magnetic effects on 1/*f*-noise have served as one of the means to distinguish between mobility fluctuations and number fluctuations in semiconductors [1,2]. By measuring 1/*f* noise in the Hall effect, it was concluded that 1/*f*-noise in n-Ge is caused by mobility fluctuations. Van de Voorde and Love [4] performed an experimental study of the magnetic effects on 1/*f*-noise in n-InSb at low temperature about 80 K. Their experimental results were found to agree with mobility fluctuations, though they did not explicitly claim so. However, the opposite conclusion, namely number fluctuations, was drawn from experiments on 1/*f*-noise in magnetoresistance by Song and Min et al. [5,6], where a special MESFET structure and high-quality n-GaAs grown by molecular-bean epitaxy (MBE) were used to avoid surface effects. We cannot explain the results of Song and Min, which contradict our previous work [7,8] and most studies on 1/*f*-noise in semiconductors. In our studies [7,8] we measured 1/*f*-noise in the conductance ($B = 0$) of similarly MBE-grown n-GaAs layers. The contributions from the lattice phonon scattering and impurity scattering to the overall mobility were changed both by doping and by temperature. The results did not suggest that 1/*f*-noise in our epitaxial n-GaAs has some special origin but it appears to be the normal bulk-type noise caused by mobility fluctuations. In order to give further support for the mobility-fluctuation hypothesis, we performed measurements of 1/*f*-noise in the Hall voltage of MBE-grown n-GaAs since with n-GaAs it is easy to obtain (μB)-values much larger than unity, which is impossible with Ge samples.

Correspondence to: L. Ren, Department of Electrical Engineering, Eindhoven University of Technology, P.O. Box 513, 5600 MB Eindhoven, The Netherlands.

2. Magnetic influence on the 1/*f*-noise in the Hall voltage in n-GaAs

When, in a semiconductor, a magnetic field B is directed (in the z-direction) at right angles to an applied electric field E (in the x-direction), a Hall voltage (in the y-direction) is generated perpendicular to both the current flow and the magnetic field. The transport of charge-carriers can generally be considered to be two-dimensional. For an n-type nondegenerate homogeneously doped semiconductor, the current density J in the (x,y)-plane can be described by

$$\boldsymbol{J} = \begin{pmatrix} A(B) & -D(B) \\ D(B) & A(B) \end{pmatrix} \cdot \boldsymbol{E} \tag{1a}$$

and

$$\nabla \cdot \boldsymbol{J} = 0 . \tag{1b}$$

The matrix elements $A(B)$ and $D(B)$ are given by ref. [9] as

$$A(B) = \int_0^\infty \frac{\sigma(\varepsilon)}{1 + \mu^2(\varepsilon)B^2} \, \mathrm{d}\varepsilon , \tag{2a}$$

$$D(B) = \int_0^\infty \frac{\sigma(\varepsilon)\mu(\varepsilon)B}{1 + \mu^2(\varepsilon)B^2} \, \mathrm{d}\varepsilon \tag{2b}$$

and

$$\sigma(\varepsilon) = q\mu(\varepsilon)\left(\frac{2\varepsilon}{3kT}\right) n(\varepsilon) , \tag{2c}$$

where $\sigma(\varepsilon)$, $\mu(\varepsilon)$ and $n(\varepsilon)$ are the conductivity, the mobility and the carrier density, all of which depend on the energy ε of the carriers.

On the basis of the theory developed by Kleinpenning [10], calculating noise in arbitrary four-probe conductors, Vaes and Kleinpenning [1] calculated the effect of a magnetic field on $1/f$-noise in the Hall voltage for an n-type nondegenerate semiconductor with a parabolic conduction band. Two different $1/f$-noise sources, (i) mobility fluctuations and (ii) number fluctuations, were taken into account. For each noise source, the empirical relation for $1/f$-noise [11] as defined by

$$\frac{S_R}{R^2} = \frac{\alpha}{fN} \tag{3}$$

was used, where S_R is the noise power density of the fluctuations in the resistance R, α the $1/f$-noise parameter, f the frequency and N the total number of charge-carriers. Energetical and spatial uncorrelatedness was assumed for the mobility fluctuations in the sublevel of the conduction band. Meanwhile, the number fluctuations were assumed to be energy-independent and spatially uncorrelated. They then found two different expressions for the ratio γ for mobility fluctuations and for number fluctuations. γ is the ratio of the $1/f$-noise power density with an applied magnetic field B to the $1/f$-noise power density without magnetic field, as defined by

$$\gamma = \frac{S_V(f, B)/V^2(B)}{S_V(f, 0)/V^2(0)} \tag{4}$$

where S_V is the Hall-voltage noise power density, V the applied voltage and f the frequency. γ_μ of the mobility fluctuations is given [2][1] by

$$\gamma_\mu = \frac{A^2(0)}{A^2(B)}\left[1 + \frac{D^2(B)}{A^2(B)}\right] \times \int_0^\infty \frac{\sigma^2(\varepsilon)/n(\varepsilon)}{[1 + \mu^2(\varepsilon)B^2]^2} \, \mathrm{d}\varepsilon \Big/ \int_0^\infty \frac{\sigma^2(\varepsilon)}{n(\varepsilon)} \, \mathrm{d}\varepsilon . \tag{5}$$

γ_N of the number fluctuations is given [2] by

$$\gamma_N = \left[1 + \frac{D^2(B)}{A^2(B)}\right]^2 . \tag{6}$$

Both expressions contain the essential integrals of the related momentum relaxation-time $\tau(\varepsilon)$ and its higher-order moments over all the energy levels in the conduction band. The integrals can only be evaluated analytically either at very low magnetic induction ($\mu_H B \ll 1$) or at very high magnetic induction ($\mu_H B \gg 1$). For the middle range of the magnetic induction, these integrals have to be evaluated numerically. An important feature which can be deduced from eqs. (5) and (6) is that at very high magnetic induction ($\mu_H B \gg 1$)

$$A(B) \propto \mu_H^{-1} B^{-2} , \tag{7a}$$

$$D(B) \propto B^{-1} , \tag{7b}$$

$$\int_0^\infty \frac{\sigma^2(\varepsilon)/n(\varepsilon)}{[1 + \mu^2(\varepsilon)B^2]^2} \, \mathrm{d}\varepsilon \Big/ \int_0^\infty \frac{\sigma^2(\varepsilon)}{n(\varepsilon)} \, \mathrm{d}\varepsilon \propto (\mu_H B)^{-4} . \tag{7c}$$

[1] There is an error in eq. (7.31) of ref. [2]. The term $[1 + D(B)/A(B)]^2$ on the right-hand side of eq. (7.31) should be $[1 + D^2(B)/A^2(B)]$.

At $\mu_H B \gg 1$, therefore,

$$\gamma_\mu \propto (\mu_H B)^2 \tag{8}$$

and

$$\gamma_N \propto (\mu_H B)^4 , \tag{9}$$

provided the integrals of $\tau(\varepsilon)$ and its higher-order moments are convergent, which is generally true. However, the relation between relaxation time τ and energy ε has to be known for the evaluation of γ.

For the acoustic-phonon scattering, τ is proportional to $\varepsilon^{-1/2}$ [12]. For the polar optical-phonon scattering, which is the dominant scattering mechanism in n-GaAs, there is no simple definition of τ_{op} owing to a rather large energy exchange (comparable with kT) between the charge-carriers and the optical phonons. However, for averaging over the energies, an effective relaxation time can be defined after solving the Boltzmann transport equation either numerically or by a variation method. For a high-electron-energy region, τ_{op} can be well approximated by $\tau_{op} \propto \varepsilon^{1/2}$ [12,13]. At low electron energies comparable with the energy $\hbar\omega_{op}$ needed to absorb or emit one optical phonon, τ_{op} can be considered as energy-independent [13,14]. τ_{op} could therefore be given by

$$\tau_{op} = \begin{cases} h + \tau_0(\varepsilon/kT)^{1/2} , & \varepsilon \leqslant \hbar\omega_{op} , \\ \tau_0(\varepsilon/kT)^{1/2} , & \varepsilon > \hbar\omega_{op} . \end{cases} \tag{10}$$

Figure 1 shows the schematic diagram of such an approximated τ_{op} versus the electron energy ε. The height h of the rectangular part of τ_{op} is used as an adjusting parameter in order to fit the mobility data. For pure GaAs, if we take the highest value of 8500 $cm^2/V s$ at 300 K for the electron mobility and the characteristic temperature $\theta \simeq 420$ K for the polar optical phonon scattering, then we find the height $h \simeq 4.2\tau_0$ (where τ_0 is the prefactor of the $\varepsilon^{1/2}$-branch of τ_{op}) and the Hall factor $\gamma_H = \langle\tau^2\rangle/\langle\tau\rangle^2 \simeq 1.35$, which is in reasonably good agreement with $\gamma_H \simeq 1.20$ as calculated by a variation method [14,15]. With the parameters determined above of τ_{op}, numerical calculations of eqs. (5) and (6) were made for γ_μ and for γ_N. The results are shown by the dashed and solid lines in figs. 2 and 3.

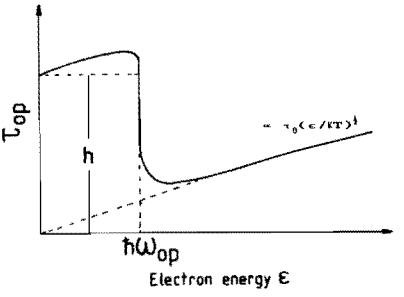

Fig. 1. Schematic diagram for the effective relaxation time τ_{op} versus electron energy ε for the polar optical-phonon scattering [14]. The broken curve shows the approximation.

3. Experimental results and discussion

The samples used in this study were the same as those we use in previous measurements [7,8]. All samples were prepared from the lightly-doped n-GaAs epitaxial layers of 1 NE15 [7] grown by MBE. The thickness of 1 NE 15 is 11 μm and the doping concentration about 1×10^{15} cm^{-3}. The mobility of the samples was found to be about 7450 $cm^2/V s$ at 295 K and about 81 000 $cm^2/V s$ at 78 K. The geometry of the samples is a Hall bar with six-sided contacts (see the inset of fig. 2). The voltage noise spectra across the Hall probes were measured at both $T \simeq 295$ K and $T \simeq 78$ K with and without a magnetic field which was applied perpendicularly to the current flow. All the voltage-noise spectra were found to be of the $1/f$-type in the frequency range from 1 Hz to 1 kHz. The dependence of the noise-spectrum power density on the applied electric field was found to be quadratic both with and without magnetic field. The $1/f$-noise parameter α, as defined in eq. (3), was found to be about 8×10^{-4} at $T \simeq 295$ K and about 3×10^{-6} at $T \simeq 78$ K.

Figure 2 shows the ratio γ at $T \simeq 295$ K as a function of $(\mu_H B)^2 \cdot \gamma$ is obtained from eq. (4)

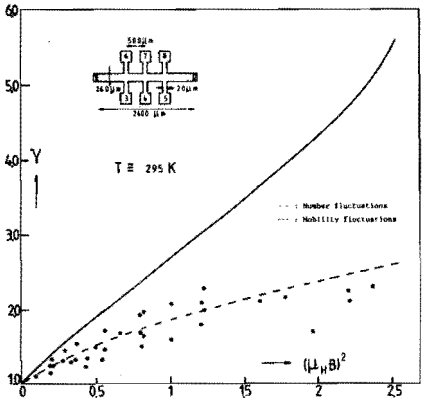

Fig. 2. The ratio γ between $1/f$-noise power densities with and without magnetic induction $(\mu_{\rm H}B)^2$ at a constant applied voltage and at $T \simeq 295$ K. The inset shows the pattern of the samples. The broken curve represents the calculated results assuming mobility fluctuations and the solid curve for number fluctuations.

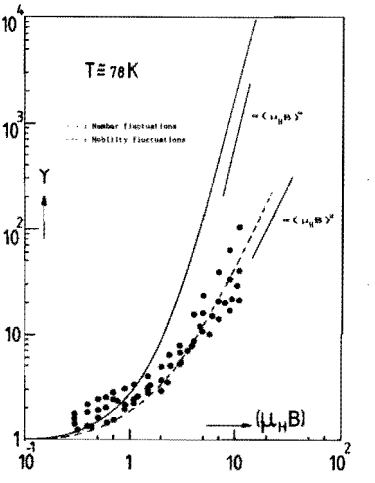

Fig. 3. Ratio γ at a constant applied voltage and at $T \simeq 78$ K as a function of $(\mu_{\rm H}B)$. Broken curve: prediction for mobility fluctuations. Solid curve: prediction for number fluctuations.

using the measured spectral power densities. Each data point represents one measured value from one out of four samples. The theoretical ratios of γ_μ and γ_N for the mobility fluctuations and the number fluctuations are also shown in fig. 2 as dashed line and solid line, respectively. The mobility fluctuation model agrees very well with the experimental data at $T \simeq 295$ K.

In fig. 3 we present the experimental data at $T \simeq 78$ K as γ versus the product $(\mu_{\rm H}B)$. In the same figure, the calculated predictions for the mobility fluctuations and for the number fluctuations are presented as dashed line and solid line, respectively. It should be added that, owing to the small $1/f$-noise parameter α at $T \simeq 78$ K, only a small amount of $1/f$-noise could be excited. The $1/f$-noise was about one order of magnitude above the thermal noise at admissible power dissipation. The data at low magnetic induction are therefore not very accurate. However, the data are in quite good agreement with the mobility fluctuation model. Here, it may be not correct to compare the experimental results with a theoretical calculation based on polar optical-phonon scattering only, because the ionized impurity scattering and the acoustic-phonon scattering also become important in our samples at $T \simeq 78$ K. However, this does not influence the conclusion at all since, at high magnetic induction ($\mu_{\rm H}B \gg 1$), the ratio γ_μ is expected to increase with $(\mu_{\rm H}B)^2$ and the ratio γ_N with $(\mu_{\rm H}B)^4$, as has been shown in the previous section. The trend of the experimental data in fig. 3 is clearly seen to be more likely to follow a quadratic dependence on the magnetic induction $(\mu_{\rm H}B)$. We have done a similar numerical calculation for a combination of optical-phonon scattering and impurity scattering using Matthiessen's rule. The results do not differ much until the impurity scattering contributes 50% of the total scattering. The introduction of impurity scattering mainly influences the value of γ at lower magnetic inductions. Actually, at very high magnetic field, the quadratic dependence of γ_μ on $(\mu_{\rm H}B)$ and the fourth-power dependence of γ_N on $(\mu_{\rm H}B)$ are not dependent on a definite scattering mechanism. It only requires τ to be energy-dependent.

4. Conclusions

We measured $1/f$-noise in the Hall voltage of MBE-grown n-GaAs at $T \simeq 295$ K and $T \simeq 78$ K. The experimental data presented in this paper clearly show that the $1/f$-noise in epitaxial n-GaAs originated from mobility fluctuations.

Acknowledgements

The authors thank Prof. Dr. F.N. Hooge for discussions and Dr. M.R. Leijs for providing the samples. This work is part of the research programme of the 'Stichting voor Fundamenteel Onderzoek der Materie' (FOM), which is financially supported by the 'Nederlandse Organisatie voor Wetenschappelijk Onderzoek' (NWO).

References

[1] H.M.J. Vaes and T.G.M. Kleinpenning, J. Appl. Phys. 48 (1977) 5131.
[2] F.N. Hooge, T.G.M. Kleinpenning and L.K.J. Vandamme, Rep. Prog. Phys. 44 (1981) 479.
[3] T.G.M. Kleinpenning, J. Appl. Phys. 51 (1980) 3438.
[4] P. van de Voorde and W.F. Love, Phys. Rev. B 24 (1981) 4781.
[5] J.H. Song and H.S. Min, J. Appl. Phys. 58 (1985) 4221.
[6] J.H. Song, A.N. Birbas, A. van der Ziel and A.D. van Rheenen, J. Appl. Phys. 64 (1988) 727.
[7] L. Ren and M.R. Leys, Physica B 172 (1991) 319.
[8] L. Ren and F.N. Hooge, Physica B 176 (1992) 209.
[9] R.A. Smith, Semiconductors (Cambridge U.P., London, 1964).
[10] T.G.M. Kleinpenning, J. Appl. Phys. 48 (1977) 2946.
[11] F.N. Hooge, Phys. Lett. A 29 (1969) 139.
[12] J. Bardeen and W. Shockley, Phys. Rev. 80 (1950) 72.
[13] H. Ehrenreich, J. Appl. Phys. 32 (1961) 2155.
[14] S. Datta, in: Quantum Phenomena, Modular Series on Solid State Devices, Vol. 8 (Purdue University, W. Lafayette, IN 1989).
[15] G.E. Stillman, C.M. Wolfe and J.O. Dimmock, J. Phys. Chem. Sol. 31 (1970) 1199.

Chapter 4

Low-frequency Noise in Electron Irradiated n-GaAs Epitaxial Layers

Abstract

This chapter contains two papers. One deals with the low-frequency noise in MBE-grown n-GaAs between 77 and 300 K. The other one deals with the problem of generation-recombination noise of two trapping centres.

Part I.

Low-frequency noise in electron irradiated *n*-GaAs epitaxial layers

L. Ren
Department of Electrical Engineering, Eindhoven University of Technology, 5600 MB Eindhoven, The Netherlands

P. Baucour
Centre d'Electronique de Montpellier, Université des Sciences et Techniques du Languedoc, 34060 Montpellier Cedex, France

F. N. Hooge
Department of Electrical Engineering, Eindhoven University of Technology, 5600 MB Eindhoven, The Netherlands

L. H. Luthjens
Interfaculty Reactor Institute, Delft University of Technology, 2629 JB Delft, The Netherlands

M. R. Leijs
Department of Physics, Eindhoven University of Technology, 5600 MB Eindhoven, The Netherlands

(Received 5 August 1992; accepted for publication 4 November 1992)

We report on the results of measurements of temperature dependent Hall-effect and low-frequency noise of molecular-beam-epitaxy-grown *n*-GaAs layers irradiated by 3 MeV electrons. The results of Hall-effect measurements agree with the literature for the electron traps *E*1 and *E*2. Besides $1/f$ noise, an additional generation-recombination (g-r) noise is observed. We attribute the observed g-r noise to an unknown deep level induced by the electron irradiation, which is about 0.18 eV below the conduction band. Its capture cross section is extremely small and thermally activated. The irradiation does not cause a significant change in the $1/f$ noise parameter α at high temperatures. Possible roles of the defect motion $1/f$ noise sources are discussed.

I. INTRODUCTION

Much attention[1-8] has been given to the possible relation between $1/f$ noise and lattice defects in semiconductors and metals. It has been suggested that the $1/f$ noise in metals is induced by changes in scattering due to the motion of defects.[2-7] The noise generation is thermally activated and well interpreted by the Dutta–Dimon–Horn model.[1] Similar evidence was also obtained in semiconductors,[8] where the $1/f$ noise was greatly reduced by annealing the damage caused by high-energy ion implantation. Although there is evidence in favor of the importance of point defects,[3,6] the relative importance of different types of defects and their interactions is still unclear. In this article we present the results of Hall-effect and noise measurements on electron-irradiated *n*-GaAs layers grown by molecular beam epitaxy (MBE). In contrast to high-energy ion implantation, the defects created by high-energy electron irradiation are mainly simple intrinsic point defects,[9,10] which provide a test for the importance of point defects for the $1/f$ noise in semiconductors.

II. PREPARATION OF THE SAMPLES

The samples investigated in this article were cleaved from one single wafer. The GaAs epitaxial layer was grown on a 2 in. semi-insulating GaAs substrate of orientation (001) using MBE. The epitaxial layer, with a thickness of 3.2 μm, was doped to a level of $1. \times 10^{16}$ cm^{-3} using silicon as an *n*-type dopant. The temperature during growth was 630 °C and the growth rate was equal to 1 μm/h. Hall bar structures with six side contacts were prepared using conventional photolithography and etching procedures. The width of the Hall bars was 260 μm. The length of the bars was 2400 μm, similar to the samples described previously.[11,12] Ohmic contacts to the epitaxial layer were formed by placing small tin balls on the contact areas and annealing in a N_2/H_2 mixture at 400 °C for 1 min on a strip heater.

The epitaxial samples were irradiated with 3 MeV electrons using the Van de Graaff electron accelerator of the Interfaculty Reactor Institute of the Delft University of Technology.[13] The accelerator was operated in the continuous beam mode at an electron beam current of 10 μA measured on the watercooled aluminum irradiation table at 15 cm below the exit window. The table can be positioned by remote control over a span of 80 cm. In our experiments the current was set and measured in a position at a certain distance from the target area to prevent stray electrons from having any effects. Samples were positioned at the opposite end of the table in the 1×1 cm^2 target area vertically below the beam tube and attached with MgO-filled silicone heat conduction paste (Schaffner). Timing of the irradiation was determined by switching of the electron beam from a deflected position to the target, using the timing unit of the accelerator.

The exact position of the target area and the dose density distribution were determined using densitometry of a glass plate colored by the beam irradiation, and more accurately, with Radiachromic nylon thin film dosimetry (Far West Technology Inc: Box # 403, Reader FWT-92 # 3179) based on N.I.S.T. calibration and checked against

 0021-8979/93/050001-07$06.00

TABLE I. Irradiation time, dose, and expected defect concentrations.

Sample	Irradiation time (s)	Electron dose (in 10^{15} cm^{-2})	Expected defect concentration (in 10^{15} cm^{-3})
b	0	0.0	0
$r1$	40	0.2	1
$r3$	120	0.6	3
$r10$	400	2.0	10
$r30$	1200	6.0	30

Fricke ferrous sulphate dosimetry using the IRI ^{60}Co gamma source.

It was found that the dose density distribution in the target area on the table could be represented by a Gaussian distribution with a standard deviation of 1.54 cm. The value for the current density in the irradiation target area, at a total beam current of 10 μA, is taken as the value obtained from a direct current measurement and a surface dose measurement as 7.5×10^{-7} A cm^{-2} or 4.7×10^{12} electrons cm^{-2}s^{-1}, with an estimated error of $\pm4\%$. The temperature of the samples during irradiation did not exceed 35 °C as measured by a thermocouple during test irradiations.

The samples are thin enough (3.2 μm) to guarantee a uniform production of defects. We studied five groups of samples irradiated with different doses. The measurements were performed on several samples from each group. The notation is as follows: b means before irradiation, r means an irradiated sample, the number after r indicates the defect production, for example, $r1$ means that we expect a defect concentration of roughly 1×10^{15} cm^{-3} in that sample. All concentrations are in 10^{15} cm^{-3}. Table I gives the sample code, irradiation time, dose, and the expected defect concentration. The expected defect concentrations are based on an assumed production rate $\tau\sim5$ cm^{-1}.[14] The radiation mainly produced acceptors. As the irradiation dose increased, the n-type samples became more compensated. The resistance of $r30$ was very high and we could not make ohmic contacts. The samples must have become p type, as follows from the extrapolation of the data in Table II.

III. EXPERIMENTAL RESULTS AND DISCUSSION

A. Temperature dependence of the Hall effect

The Hall effect was measured between 77 and 300 K with a current of 10 μA and a magnetic field of 0.5 T. Because our samples were rather thin (3.2 μm) a correction for the depletion layers at the surface and the interface has to be taken into account when determining the carrier concentration in the neutral bulk.[15,16] The real free-charge carrier concentration $n(T)$ is related to the carrier concentration found from the Hall-effect, $n_H(T)$, by

$$n(T)=n_H(T)\left(r_H\frac{t}{t_{\rm eff}(T)}\right), \tag{1}$$

where

$$t_{\rm eff}(T)=t-t_s-t_i, \tag{2}$$

t is the thickness of the sample, t_s and t_i are the thicknesses of the depletion regions at the surface and at the interface, respectively, r_H is the Hall factor, and T is the temperature.

We had already made such calculations before for n-GaAs at room temperature[11] using the method of Chandra *et al.*[15] In those calculations we used 0.6 and 0.75 V for the surface pinning potential and the interface pinning potential. Good agreement between calculated and observed thicknesses was found. Therefore we use the same values here for the pinning potentials. The Hall factor was taken as $r_H=1$ at all temperatures. Figure 1 shows $n(T)$ vs $1000/T$. The Hall-effect curves were fitted according to the charge-balance equation developed by Look.[14] We found that the curves for the irradiated samples could be fitted well by assuming that two single-charged centers are created at $\Delta E_1\cong0.02$ eV and at $\Delta E_2\cong0.155$ eV below the conduction band. Both degeneracy factors are taken as $B=4$. The concentrations are $C_1\cong4.5\times10^{15}$ cm^{-3} and $C_2\cong4.7\times10^{15}$ cm^{-3} in the sample $r10$. This gives introduction rates of 2.3 and 2.4 cm^{-1}. Considering the obtained defect production rates, it is almost certain that the two centers are just the well known electron traps $E1$ with $\Delta E_1\cong0.045$ eV and $E2$ with $\Delta E_2\cong0.15$ eV induced by electron irradiation.[9] The difference in the energy level of the identified center $E1$ could be due to a large error in the correction of the temperature dependent Hall-effect curves

TABLE II. Electron traps obtained from our present work and from literature.

	After Pons, Bourgoin,[a] and Look[b]				From this work				
						Concentration in 10^{15} cm^{-3}			
	ΔE	Electron cross section σ_n in Å^2	Type	Introduct. rate (τ cm^{-1})	ΔE	$r1$	$r3$	$r10$	Introduct. rate (τ cm^{-1})
E_1	0.045	22	Acc.	1.5	0.02	0.45	1.35	4.5	2.3
E_2	0.15	1200	Donor	1.5	0.15	0.47	1.4	4.7	2.4
E_3	0.30	62	Acc.	0.4	deep	~0.08	~0.25	~0.8	0.4

[a]See Ref. 9.
[b]See Ref. 14.

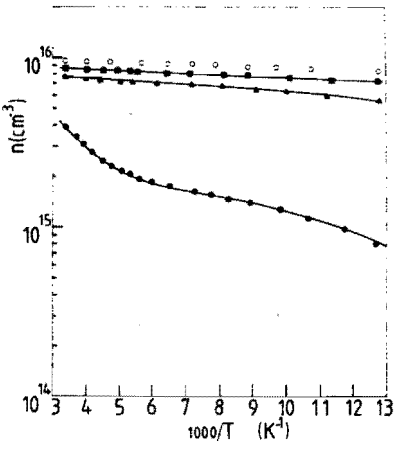

FIG. 1. Carrier concentration as a function of inverse temperature for various doses. The solid curves are theoretical fits with $E1$, $E2$, and $E3$ and the other deep acceptors A_x. (○) = b: before irradiation, (■) = $r1$: a dose of 0.2×10^{15} e^{-1}/cm^2. (▲) = $r3$: a dose of 0.6×10^{15} e^{-1}/cm^2. (●) = $r10$: a dose of 2×10^{15} e^{-1}/cm^2.

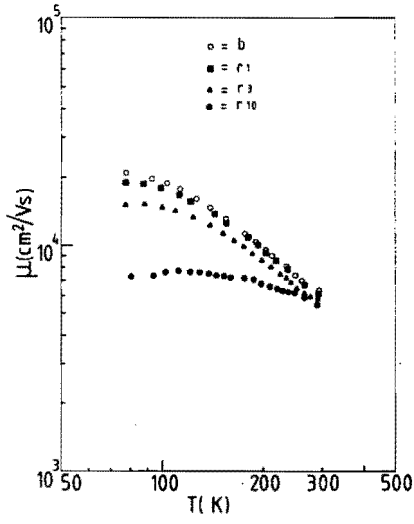

FIG. 2. Mobility vs temperature (symbols the same as in Fig. 1).

to the depletion region thickness at the lower temperatures, considering that at 77 K more than 80% of the electrons were depleted. Following the literature,[9] another commonly identified center $E3$ with the energy level $\Delta E_3 \cong 0.30$ eV and an introduction rate of about 0.4 cm^{-1} was also taken into account in the fitting procedure. Apart from $E1$, $E2$, and $E3$, there is a constant contribution of a fourth term that has to be taken into account in the charge-balance equation. That must be an acceptor A_x, low in the band gap.

The production of defects in GaAs has been studied before.[9,14] Our results fit well in this generally accepted picture. The difference with Look's samples is that ours are not so close to compensation. Therefore we do not find a steep slope in the low temperature part of the $n(T)$ curve. Table II shows the results from literature and from our present work.

The donor or acceptor character is suggested by the value of σ_n. Neutral centers have capture-cross sections corresponding to their geometric cross section, which equals several Å^2.

Figure 2 shows the mobility versus temperature. We used the empirical Stillman–Wolfe relation[17] and found the donor densities $D_b \cong 15\times10^{15}$ cm^{-3} and the acceptor densities $A_b \cong 5.5\times10^{15}$ cm^{-3} for the samples before irradiation. For the samples after irradiation we used the Brooks–Herring relation[18] to estimate the total concentration of charged defects from the mobility at 77 K where impurity scattering prevails. That concentration is about $(D_b + A_b) + 14\times10^{15}$ cm^{-3}.

The cross sections reported in the literature suggested that $E1$ is an acceptor and $E2$ is a donor. From the Hall-effect alone Look could not decide on the donor-acceptor character and neither can we. However, there are four situations regarding the donor-acceptor characters of $E1$ and $E2$, where the concentration of extra acceptors A_x are different. The results are given in Table III. The values are obtained under two assumptions: (i) $E3$ is an acceptor; (ii) the mobility at 77 K is dominated by the charged impurity scattering.

A_x from μ at 77 K is consistently 4×10^{15} cm^{-3} too high, which could mean that the assumption of $E1$ and $E2$ being single-charged centers is not appropriate. Nevertheless, it does not create a serious problem. The best estimation for A_x is from $n(T)$, the values derived from μ confirm the general trend. The only case where we do not need any A_x is where both $E1$ and $E2$ are acceptors.

The conclusion is for $r10$:

$C_1 = 4.5\times10^{15}$ cm^{-3},

$C_2 = 4.7$,

$C_3 = 0.8$,

$A_x \cong 10$ if DD for $E1$ and $E2$,

$A_x \cong 5$ if DA or AD for $E1$ and $E2$,

$A_x \cong 0$ if AA for $E1$ and $E2$.

TABLE III. Concentration of extra acceptors A_x in 10^{15} cm^{-3} for sample $r10$.

E_1	D	D	A	A
E_2	D	A	D	A
A_x from $n(T)$:	10	5.0	5.0	~0
A_x from μ at 77 K:	~14	~9.3	~9.5	~4

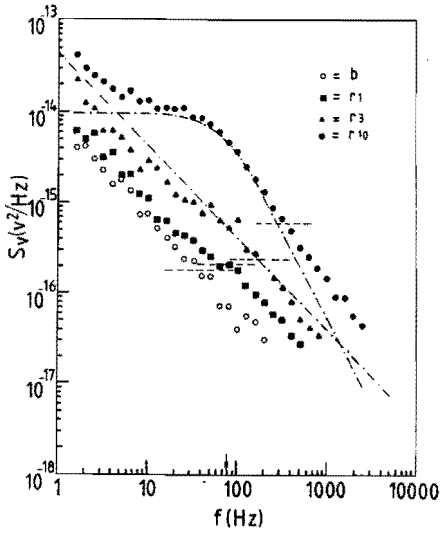

FIG. 3. Typical noise spectra measured at $T \cong 300$ K and $E = 6$ V/cm for the samples with different doses. The thermal noise of $4kTR$ is subtracted and its level is given by the dashed horizontal lines. The $1/f$ and the g-r components for fitting are also shown as the dashed-dot curves.

The total defect production is then $(C1+C2+C3+A_x) \cong 20$ or 15 or 15 or 10×10^{15} cm^{-3} with $\tau \cong 11$ or 8.5 or 8.5 or 5 cm^{-1}. If we conclude from the values of the capture cross section that $E1=A$ and $E2=D$ we obtain $\tau \cong 8.5$ cm^{-1}, in agreement with the reported value $\tau \sim 7$ cm^{-1} for 1 MeV electrons.[9]

In conclusion we cannot definitely decide on the donor-acceptor character of $E1$ and $E2$, but we feel sure of the concentrations C_1 and C_2 in our samples. These concentrations will be used in the analysis of the noise.

B. Noise measurements

Low-frequency voltage noise was measured on samples with different irradiation doses. The noise was measured as a function of temperature between 77 and 300 K in the frequency range from 1.6 Hz to 20 kHz. Figure 3 shows a number of voltage noise spectra measured at room temperature. Before irradiation, pure $1/f$ noise was observed. After irradiation an additional generation-recombination (or g-r) noise with a Lorenzian spectrum was present. The total spectrum can be described by

$$S_V = \frac{\alpha V^2}{fN} + \frac{S_V(0)}{1+(2\pi f\tau)^2} + 4kTR, \tag{3}$$

where α is the $1/f$ noise parameter,[19] f is the frequency, V is the applied voltage, N is the total number of free electrons in the sample subvolume involved in the noise process, τ is the noise relaxation time, T is the sample temperature, R is the resistance of the samples, and k is the Boltzmann constant. $S_v(0)$ is the so-called low-frequency plateau value, to be calculated below.

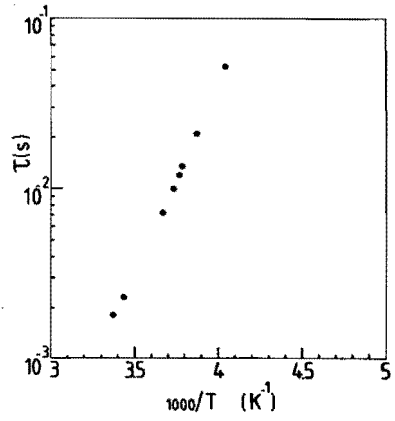

FIG. 4. The noise relaxation-time as a function of inverse temperature for sample r10.

1. Generation-recombination noise

The g-r noise was found to vary as with square of the applied voltage, which was expected as a consequence of resistivity fluctuations. It was also observed that the normalized low-frequency plateau values $S_v(0)/V^2$ of the g-r noise increased with the dose of the electron irradiation, which indicates that the g-r noise was associated with the defects induced by the irradiation. The ratio between the longitudinal and transversal noise measurements for the g-r noise was found to be the same as for the $1/f$ noise,[11] which indicates that the g-r noise source is also homogeneously distributed along the conducting channel. We used a computer fit of Eq. (3) to obtain the low-frequency plateau values and the noise relaxation time τ. Figures 4 and 5 show the temperature dependence of τ and of $S_v(0)/V^2$ obtained from samples of $r10$ with an electron dose of 2.0×10^{15} cm^{-2}.

The number fluctuations of the g-r noise cause fluctuations in the number of ionized impurities. This will influence the mobility via impurity scattering. However, that effect can be neglected since in our case lattice scattering prevails. This assumption leads to

$$\frac{S_V(0)}{V^2} = \frac{S_N(0)}{N^2}, \tag{4}$$

and

$$S_N(0) = 4\langle(\Delta X)^2\rangle\tau, \tag{5}$$

where $\langle(\Delta X)^2\rangle$ is the variance of number fluctuations in the center related to the observed g-r spectrum.

We observed only one Lorenzian in the frequency range from 1 Hz to 10 kHz. However, more g-r processes could be present with $1/\tau$ values outside our frequency

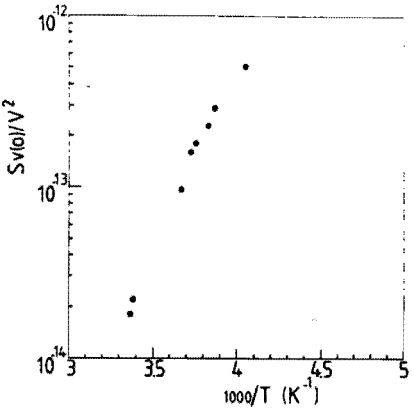

FIG. 5. The low-frequency plateau values as a function of inverse temperature for sample r10.

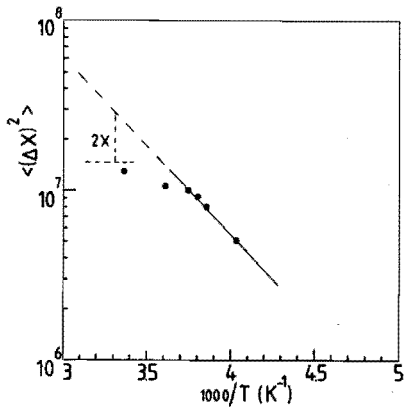

FIG. 6. Variance $\langle(\Delta X)^2\rangle$ as a function of inverse temperature for sample r10.

range. If there is only one trap then $\langle(\Delta X)^2\rangle$ is the variance of the number of trapped electrons. In another publication,[20] using a thermodynamic approach, we have shown that in the case of two traps $\langle(\Delta X)^2\rangle$ of the observed Lorenzian still corresponds to the variance of the electrons trapped by the X center if the conditions $N \gg x$ and $N \gg y$ are fulfilled. x and y are defined by

$$\frac{1}{x}=\frac{1}{X_n}+\frac{1}{X_p}, \quad \frac{1}{y}=\frac{1}{Y_n}+\frac{1}{Y_p}, \tag{6}$$

where X_p or Y_p is the number of empty traps X or Y, and X_n or Y_n is the number of occupied traps X or Y. This means that x is the smaller one of X_n and X_p. This condition is fulfilled with our samples in the temperature range 300 K $\geq T \geq$ 200 K if we assume $X = E1$ at about 0.045 eV below the condition band and $Y = E2$ at about 0.15 eV below the conduction band. Similar conditions for decomposition of two g-r spectra were derived by Van Rheenen *et al.*,[21] which are sufficient but not necessary.[20] The values of $\langle(\Delta X)^2\rangle$, determined from the low-frequency plateau are plotted as a function of inverse temperature in Fig. 6. From this figure we can easily obtain a first estimate of the position of the g-r center. According to a simple model[22] the complete figure consists of two exponential branches with $+E_x/kT$ and $-E_x/kT$. There is a maximum at the temperature at which the Fermi level crosses the center. We find the maximum at about $1000/T = 3.3\ K^{-1}$ where the estimated $\langle(\Delta X)^2\rangle$ value is a factor 2 lower than the extrapolated branch with E_x/kT. The slope gives $E_x = 0.14$ eV. At $T = 300$ K the Fermi level is 0.12 eV below the conduction band, as follows from Fig. 1 and

$$E_F = E_C - kT \ln\left(\frac{N_C}{N}\right), \tag{7}$$

where N_c is the density of state in the conduction band. From Fig. 6 therefore, it follows that the g-r center is at about 0.13 eV below the conduction band.

Considering the known electron traps created by electron irradiation,[9] $E2$ would be a probable candidate for the observed g-r noise. By applying the modified Copeland method developed by Van Rheenen *et al.*,[22] we found that the concentration and energy level of the trap were about $0.14 \times 10^{15}\ cm^{-3}$ and $E_c - 0.18$ eV. The capture cross section σ of the trap can be determined from the noise relaxation time τ. The full expression for the noise relaxation-time τ for one center is described[22] by

$$\frac{1}{\tau}=\beta\left[N\left(1+\frac{X_p}{X_n}\right)+X_p\right], \tag{8}$$

where β is the capture coefficient associated with the recombination process. The capture coefficient β can be written as

$$\beta = \sigma v_{\text{th}}/\text{volume}, \tag{9}$$

where σ is the capture cross section and v_{th} is the thermal velocity. From the above-mentioned trap concentration and thermal depth, the capture cross section σ can be determined from Eqs. (8) and (9). We found that σ could be written as

$$\sigma = \sigma_\infty \exp(-E_\sigma/kT). \tag{10}$$

The results are shown in Fig. 7. From this figure we determined $\sigma_\infty \sim 10^{-15}\ cm^2$ and $E_\sigma \cong (0.32 \pm 0.02)$ eV.

In Table IV, we summarized the results of noise measurements by comparing the trap parameters extracted from the noise spectroscopy with those of the trap $E2$.

The thermal depth is the only parameter of the trap that reasonably agrees with that of $E2$. The other parameters do not agree at all. This might suggest that the observed g-r noise is associated with an unknown defect produced by the electron irradiation. The concentration following from the g-r noise gives the value $7 \times 10^{-2}\ cm^{-1}$

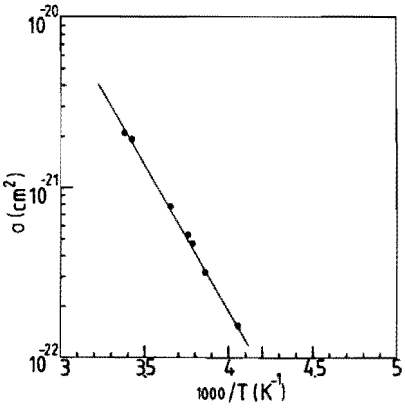

FIG. 7. Capture cross section obtained from the noise spectra as a function of inverse temperature: $\sigma_\infty \sim 10^{-15}$ cm^2; $E_\sigma \cong 0.32$ eV.

for the introduction rate. This rate is one order of magnitude lower than the rates of the other centers (see Table II).

The capture cross section at room temperature is about 2×10^{-21} cm^2, which is unusually small. Similar results were also obtained from the noise spectra for *DX* centers in $Al_{1-x}Ga_xAs$ epitaxial layers.[23] Such an extremely small cross section, which is definitely smaller than the geometric cross section of an atom and which is thermally activated, can normaly only be understood by the so-called multiphonon emission capture process due to a large lattice distortion around the defects.[24]

Before assigning the observed noise to an unknown center, it is worthwhile to examine other possibilities which could give rise to a small cross section when it is determined from the noise spectra. We see only one such possibility that the noise relaxation-time is enhanced when the g-r noise stems from the occupancy fluctuations of a trap level in the space-charge region near the surface or the interface. In such a space-charge region, the g-r noise relaxation time will be dependent on the distance to the surface. The full spectrum of g-r noise after integration over the whole space-charge region is a Lorenzian-like spectrum smeared out at high frequencies.[25] Like Kugler[25] we performed a numerical calculation for such a smeared-out Lorenzian spectrum assuming the traps to be *E*2 and *E*3. It should be mentioned here that there is one difference between Kugler's approach and ours. Taking Kleinpenning's remarks[26] into consideration, we took the calculated variances of carriers instead of simply assuming the variances to be equal to the total number of the traps. The spectra were indeed found to be smearing out at high frequencies with $f^{-(1.7\text{-}1.9)}$. However, both the characteristic relaxation time and the plateau levels were found to be too small to account for the experimental data.

TABLE IV. Comparison of the trap parameters obtained from the noise with those of *E*2.

Parameters	From g-r noise	*E*2
thermal depth $\Delta\epsilon$	$\sim$0.18 eV	0.15 eV
concentration	0.15×10^{15} cm^{-3}	4.7×10^{15} cm^{-3}
capture cross section:		
σ_∞	$\sim10^{-15}$ cm^2	$\sim10^{-13}$ cm^{2a}
E_σ	0.32 eV	$\sim0^a$

[a]See Ref. 9.

If we assign the observed g-r noise to an unknown center, then there remains the problem of why we do not observe g-r spectra from *E*1 and *E*2. The absence of *E*1 and *E*2 spectra could be due to their large capture cross sections. We applied the three-level noise theory[21] using the trap concentrations known from the Hall-effect and the known cross sections of *E*1 and *E*2.[9] After numerically solving the eigenvalues of the noise relaxation-time matrix, we estimated that the corner frequencies are in the frequency range 10^8–10^9 Hz and that the low-frequency plateaus are too low to be detected in our experiments.

2. 1/f noise

The first term on the right hand side of Eq. (3) describes the $1/f$ noise in our samples. Using the sheet concentration of free electrons determined from the Hall-effect, we found the $1/f$ noise parameter α to be in the range of $(2\text{–}4)\times10^{-4}$ at room temperature, for different individual samples. We found no change in α within a 15% accuracy at room temperature when we compared the noise of the same sample both before and after irradiation.

We have also measured the noise at low temperatures. Due to the strong depletion of free electrons in the samples of *r*10 with an electron dose of about 2×10^{15} cm^{-2}, the temperature range in which the contacts stayed ohmic became narrow, so that reliable noise measurements were impossible to perform. We obtained noise data only from the two lower dose samples *r*1 and *r*3. At high temperatures the thermally activated behavior of α[12] is almost unchanged. At lower temperatures, the horizontal part of α was unchanged for the 2×10^{14} cm^{-2} dose samples, but increased by about a factor 3 or 4 for *r*3 with a dosage about 6×10^{14} cm^{-2}.

One model for $1/f$ noise is based on the "local interference" effect.[5] Quantum interference causes the resistance of the sample to be sensitive to the spatial configuration of defects. When the defects move around in the sample that configuration changes in time, and with it the resistance. We now briefly discuss whether the local interference model with mobile defects could apply to our samples.

Bourgoin *et al.*[10] have investigated the intrinsic point defects in gallium arsenide material grown by different techniques, and they found that in general a total concentration of intrinsic point defects in epitaxial materials is in the range 10^{14}–10^{15} cm^{-3}, about 100 times lower than in bulk materials. For our MBE-grown gallium arsenide, a concentration of the isolated point defects is consistent with the above figures; it is roughly $\approx10^{14}$ cm^{-3}. There-

fore, the concentration of the isolated point defects produced by the low dose irradiation would be one or two magnitudes higher than that of the intrinsic point defects. Furthermore, the induced As interstitials are known to be rather mobile,[9,10] which provides an obvious candidate for moving defects in GaAs. However, we did not observe any significant increase of $1/f$ noise. This result seems to be consistent with the "local interference" model,[5] in view of the fact that only point defects lacking spatial association were created by the electron irradiation. But it should be also noted that such a result also suggests that the $1/f$ noise induced by the defect motion is mostly generated at the extended defects like dislocation, precipitates, etc. However, such a postulation is unlikely to be true in view of the homogeneous distribution of the $1/f$ noise. In particular, considering that at high temperatures the transport of charge carriers is mainly dominated by phonon scattering, the defect motion is therefore unlikely to be the dominant noise source in our samples. This conclusion is supported by our observation that at high T the temperature dependence of the noise does not change with irradiation dosage. On the other hand, the defect motion is thermally activated. Following the standard arguments for the construction of the noise spectra,[1] the temperature dependence of the noise power-spectral-density $S_\nu(T)$ and the frequeny exponent γ are related by

$$\gamma(\omega,T)=1-\frac{1}{\ln(\omega\tau_0)}\left|\frac{\partial \ln S_\nu(\omega,T)}{\partial \ln T}-1\right|, \qquad (11)$$

where $\omega=2\pi f$ is the angular frequency and τ_0 is the average time interval between jumps of defects. If we assume that defect motion is the $1/f$ noise source, then we would expect a change in $\gamma(\omega,T)$ as a function of temperature because of the observed temperature dependence of the $1/f$ noise in our samples.[12] We expect γ to change from 1.0 to 1.4 in the temperature range 77–300 K, when we take $\tau_0\sim 10^{-12}$ s and $\omega\sim 1$ kHz. However, we did not observe any change in the slope γ either before or after irradiation. All spectra had slopes of $-(1.0\pm 0.1)$.

Finally, our results provide direct evidence for disproval of the suggestion that $1/f$ noise might result from capture and release of charge carriers at one discrete level involving lattice relaxation.[27]

IV. CONCLUSIONS

We measured the Hall-effect and noise in electron irradiated epitaxial layers of n-GaAs grown by molecular beam epitaxy. The defects identified by Hall-effect measurements agree with the literature for the well-known electron traps $E1$ and $E2$.[9] The low-frequency noise in the irradiated samples shows $1/f$ noise, g-r noise, and thermal noise. The analysis of the g-r noise suggests that an unknown defect with a low introduction rate and extremely small capture cross section was also induced by the electron irradiation. The exact nature of this defect cannot be given at present. The $1/f$ noise parameter α and the slopes of the spectra are not influenced by the defects created by the electron irradiation. Therefore, defect motion $1/f$ noise is unlikely to be the dominant noise source in our samples.

ACKNOWLEDGMENTS

The authors wish to thank W. C. v. d. Vleuten for growing the epitaxial layers, P. A. M. Nouwens for the preparation of the perfect ohmic contacts, and M. L. Hom for performing the electron irradiation. This work is part of the research program of the "Stichting voor Fundamenteel Onderzoek der Materie (FOM)", which is financially supported by the "Nederlandse organisatie voor Wetenschappelijk Onderzoek (NWO)".

[1] P. Dutta, P. Dimon, and P. M. Horn, Phys. Rev. Lett. 43, 646 (1979).
[2] R. D. Black, P. J. Restle, and M. B. Weissman, Phys. Rev. Lett. 51, 1476 (1983).
[3] J. Pelz and J. Clarke, Phys. Rev. Lett. 55, 738 (1985).
[4] Sh. M. Kogan and K. E. Nagaev, Solid-State Commun. 49, 387 (1984).
[5] J. Pelz and J. Clarke, Phys. Rev. B 36, 4479 (1987).
[6] N. M. Zimmerman and W. W. Webb, Phys. Rev. Lett. 61, 889 (1988).
[7] S. Hershfield, Phys. Rev. B 37, 8557 (1988).
[8] L. K. J. Vandamme and S. Oosterhoff, J. Appl. Phys. 59, 3169 (1986).
[9] D. Pons and J. C. Bourgoin, J. Phys. C: Solid-State Phys. 18, 3839 (1985).
[10] J. C. Bourgoin and H. J. von Bardeleben, J. Appl. Phys. 64, R65 (1988).
[11] L. Ren and M. R. Leys, Physica B 172, 319 (1991).
[12] L. Ren and F. N. Hooge, Physica B 176, 209 (1992).
[13] L. H. Luthjens, M. L. Hom, and M. J. W. Vermeulen, Internal Report SC-82-01 (1982), Interfaculty Reactor Institute (IRI)-Delft University of Technology (in Dutch).
[14] D. C. Look, Appl. Phys. Lett. 51, 843 (1987).
[15] A. Chandra, C. E. C. Wood, D. W. Woodard, and L. F. Eastman, Solid-State Electron. 22, 645 (1979).
[16] T. R. Lepknowski, R. Y. Dejule, N. C. Tien, M. H. Kim, and G. E. Stillman, J. Appl. Phys. 61, 4808 (1987).
[17] G. E. Stillman and C. M. Wolfe, Thin Solid Films 31, 69 (1976).
[18] H. Brooks, Adv. Electron. Phys. 7, 158 (1955).
[19] F. N. Hooge, Phys. Lett. 29A, 139 (1969).
[20] F. N. Hooge and L. Ren (to be published).
[21] A. D. van Rheenen, G. Bosman, and C. M. van Vliet, Solid-State Electron. 28, 457 (1985).
[22] A. D. van Rheenen, G. Bosman, and R. J. J. Zijlstra, Solid-State Electron. 30, 259 (1987).
[23] F. Hoffman, R. J. J. Zijlstra, J. M. Bettencourt de Freitas, and J. C. M. Henning, Solid-State Electron. 34, 23 (1991).
[24] D. V. Lang, in *Deep Centres in Semiconductors, a State-of-the-Art Approach*, edited by S. T. Pantelides (Gordon and Breach, New York, 1986), Chap. 7.
[25] S. Kugler, J. Appl. Phys. 66, 2195 (1989).
[26] T. G. M. Kleinpenning, IEEE Trans. Electron. Dev. 37, 2084 (1990).
[27] N. B. Lukyanchikova, M. V. Petrichuk, N. P. Garbar, A. P. Saacik, and D. I. Kropman, Physica B 167, 201 (1990).

Part II.

ON GENERATION-RECOMBINATION NOISE

F.N. Hooge and L. Ren

Department of Electrical Engineering

Eindhoven University of Technology

Eindhoven, Netherlands

Abstract

We deal with the generation-recombination noise of a three-level system, consisting of a conduction band and two traps. This problem has long been solved, but the results were expressed in a complicated formalism.
We present here simple explicit relations which make it easy to interpret experimentally observed GR spectra.
We derive the conditions under which the spectrum is the sum of two Lorenzians, each of them characterizing one trap. We also give results for the cases where these conditions are not fulfilled.

(submitted to Physica B)

1. Introduction

The theory of GR noise is fully understood for a two-level model such as a conduction band and a single trap. The spectrum is then Lorenzian

$$S = A \frac{4\tau}{1 + \omega^2\tau^2} \quad , \tag{1}$$

where the relaxation time τ is related to the capture cross-section σ of the trap. The cross-section and its thermal activation energy are known for many traps. The low-frequency plateau $4A\tau$ is determined by A, which is a relation of the numbers (not the concentrations) of empty and occupied traps.

The problem becomes very complicated when we come to a three-level model, such as a conduction band with two kinds of traps. We may find one or two Lorenzians. When two Lorenzians are found, they may be the simple one-trap Lorenzians, but the two Lorenzians could also have relaxation times and plateaux that differ from those that would have been found if we had two different samples each with only one trap, and therefore with noise of only one Lorenzian. The problem was solved many years ago, in a classic paper by Fasset and van Vliet[1]. The results were presented as matrices, which makes it difficult to see how the cross-sections and concentrations of the traps could be determined from two observed Lorenzians.

We do not propose corrections to the published physical model or to the mathematical analysis. We are, however, looking for explicit relations for τ and A and for the conditions under which observed τ and A values are characteristic of the individual traps. We therefore consider the problem of an experimentalist who observes a Lorenzian in the noise of a sample that he knows well. He knows which traps are present and in what concentrations. His problem is whether A and τ from the observed spectrum agree with the concentration and cross-section of one of the known traps. If that is not the case, is it then correct to claim that a new trap has been discovered by noise spectroscopy ?

In the derivation of the variances in a two-level model use was made of Burgess' theorem. Since the applicability of Burgess' theorem in a three-level

model is open to doubt, we completely avoid the use of this theorem. In a subsequent publication we intend to discuss the differences between Fasset and Van Vliet's paper and ours. We shall then also discuss Burgess' theorem.

In this paper we derive explicit relations for the GR spectrum. The theoretical treatment is as short as possible. Its only purpose is to prove that the results and the approximations used are correct. The results are summarised in Fig. 3. We shall prove that it is perfectly safe to use Fig. 3 when interpreting observed spectra.

Fig. 1 shows the symbols we use for numbers of states and transition probabilities. The effective number of states in the conduction band is C, which is approximately C_p, the number of empty states. According to our notation, C_n is the number of occupied states. We write N instead of C_n since N is the normal symbol for the number of free electrons

$$N << C_p \cong C. \tag{2}$$

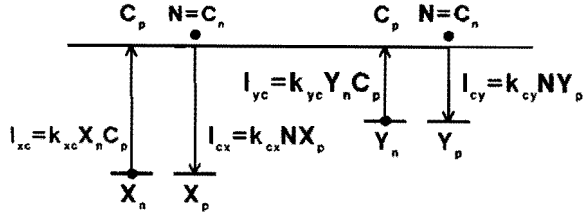

Fig. 1 The three-level model: conduction band with two traps X and Y.

2. Variances

The number of distinguishable permutations of X levels, of which X_n are occupied by electrons and X_p are empty, is given by

$$g = \frac{X!}{X_n!X_p!} . \tag{3}$$

Using Sterling's approximation,

$$\frac{d\ln g}{dX_n} = \ln \frac{X_p}{X_n} = \ln \frac{\bar{X}_p}{\bar{X}_n} - \left(\frac{1}{\bar{X}_n} + \frac{1}{\bar{X}_p}\right) \Delta X = \ln \frac{\bar{X}_p}{\bar{X}_n} - \frac{1}{x} \Delta X \tag{4}$$

where ΔX is defined by

$$\Delta X \equiv \Delta X_n = (X_n - \bar{X}_n) = - \Delta X_p = - (X_p - \bar{X}_p) \ . \tag{5}$$

Our whole treatment is based on the quantity x, introduced in (4) as

$$\frac{1}{x} \equiv \frac{1}{\bar{X}_n} + \frac{1}{\bar{X}_p} \ . \tag{6}$$

Using x we shall distinguish several regions of the concentrations in which different approximations of the exact solutions hold good. An attempt to arrive at such a distinction in concentration regions was made in previous publications by considering the Fermi level [2-5] or the Shockley-Reed recombination level [5]. Our x is related to Copeland's $F(\Theta)$ [6]. The first terms of an expansion of $d\ln g/dX_n$ in ΔX thus reads:

$$\frac{d\ln g}{d\Delta X} = \ln \frac{\bar{X}_p}{\bar{X}_n} - \frac{1}{x} \Delta X \tag{7}$$

A One level, X.

We consider a large system with many states.

There are X_i levels at energy E_i; X_{n_i} are occupied, X_{p_i} are empty. We follow the procedure for deriving the Fermi occupancy factor. We look for the distribution with maximum probability P, keeping the total number of electrons and the total energy constant :

$$\sum_i \Delta X_i = 0 \qquad \text{and} \qquad \sum_i E_i \Delta X_i = 0 \ . \tag{8}$$

Using Lagrange multipliers we find for the equilibrium distribution

$$\Delta \ln P = \sum_i \Delta \ln p_i = \sum_i \Delta (\ln g_i - \alpha X_{n_i} - \beta E_i X_{n_i})$$

$$= \sum_i \left(\frac{d \ln g_i}{d\Delta X_i} - \alpha - \beta E_i \right) \Delta X_i = 0 \ . \tag{9}$$

At each level i the expression between brackets must be zero, as the ΔX_i are uncorrelated.

The equilibrium concentration at level X_i with $\Delta X_i = 0$ then follows from :

$$\left(\frac{d \ln p_i}{d\Delta X_i} \right)_0 = \left(\frac{d \ln g_i}{d\Delta X_i} \right)_0 - \alpha - \beta E_i = 0 \tag{10}$$

$$\ln \frac{\bar{X}_p}{\bar{X}_n} = \alpha + \beta E_i \tag{11}$$

which leads to the Fermi factor. For the probability of small fluctuations ΔX_i we find

$$\left(\frac{d \ln p_i}{d\Delta X_i}\right)_{\Delta X_i} = \left(\frac{d \ln g_i}{d\Delta X_i}\right)_{\Delta X_i} - \alpha - \beta E_i = \left(\frac{d \ln g_i}{d\Delta X_i}\right)_0 - \frac{1}{x}\Delta X_i - \alpha - \beta E_i = -\frac{1}{x}\Delta X_i . \tag{12}$$

ΔX_i has a gaussian distribution as

$$\ln p(\Delta X_i) = \ln p(0) - \frac{1}{2x}(\Delta X_i)^2 \tag{13}$$

$$p(\Delta X_i) = p(0)\exp\left[-\frac{1}{2x}(\Delta X_i)^2\right] \tag{14}$$

The variance $\overline{(\Delta X_i)^2}$ equals x in this general case with no other condition than (8): the total number and the total energy are constant.

B Two levels, X and Y.

We consider this case under the condition that the number of electrons distributed over these two levels is constant:

$$\Delta X = -\Delta Y . \tag{15}$$

We have two equations analogous to (14) for $p(\Delta X)$ and $p(\Delta Y)$, from which it follows that

$$\ln P(\Delta X) = \ln p(\Delta X) + \ln p(\Delta Y) = \ln P(0) - \frac{1}{2}\left(\frac{1}{x} + \frac{1}{y}\right)(\Delta X)^2 . \tag{16}$$

ΔX has a gaussian distribution with variance:

$$\frac{1}{\overline{(\Delta X)^2}^{o}} = \frac{1}{x} + \frac{1}{y} . \tag{17}$$

We use the symbol $\overline{\qquad}^{o}$ to indicate averaging over situations in which the sum of the fluctuations is zero. $\overline{\qquad}^{o}$ means $\overline{\qquad}$ with $\Delta X + \Delta Y = 0$.

C Three levels, conduction band and traps X and Y.

The constant number of electrons to be distributed requires:

$$\Delta X + \Delta Y + \Delta N = 0. \tag{18}$$

We write $\ln P(\Delta X, \Delta Y, \Delta N)$ as:

$$\log P(\Delta X, \Delta Y, \Delta N) = \log P(0) - \frac{1}{2}\left[\frac{(\Delta X)^2}{x} + \frac{(\Delta Y)^2}{y} + \frac{(\Delta N)^2}{\bar{N}}\right] . \tag{19}$$

We develop the terms between brackets:

$$[\ldots] = \frac{(\Delta X)^2}{x} + \frac{(\Delta N + \Delta X)^2}{y} + \frac{(\Delta N)^2}{\bar{N}}$$

$$= \frac{(\Delta X)^2}{x} + \frac{\bar{N}+y}{\bar{N}y}\,(\Delta N + \frac{\bar{N}}{\bar{N}+y}\,\Delta X)^2 + \frac{1}{\bar{N}+y}\,(\Delta X)^2$$

$$= (\frac{1}{x} + \frac{1}{\bar{N}+y})(\Delta X)^2 + \frac{\bar{N}+y}{\bar{N}y}\,(\Delta N + \frac{\bar{N}}{\bar{N}+y}\,\Delta X)^2 \ . \qquad (20)$$

We first consider a constant value of ΔX and let ΔN take on all possible values.

We find an average value for the probability of this ΔX by taking:

$$\int_{-\infty}^{\infty} \ldots \, dN = \int_{-\infty}^{\infty} \ldots \, d(\Delta N + \frac{\bar{N}}{(\bar{N}+y)}\,\Delta X) \qquad (21)$$

with ΔX constant. The second term in (20) gives rise to a gaussian term in $(\Delta N + \frac{\bar{N}}{\bar{N}+y}\,\Delta X)$, which after integration yields a constant.

$P(\Delta X)$ with restriction (18), is therefore a gaussian curve with a variance determined by the first term of (20):

$$\frac{1}{\overline{(\Delta X)^2}^{\circ}} = \frac{1}{x} + \frac{1}{\bar{N}+y} \ . \qquad (22)$$

We find the variances of ΔY and ΔN by similar procedures. It will not cause confusion if from now on we write N instead of $\bar{N}$:

$$\frac{1}{\overline{(\Delta X)^2}^{\circ}} = \frac{1}{x} + \frac{1}{N+y} \quad , \quad \overline{(\Delta X)^2}^{\circ} = \frac{x(N+y)}{N+x+y} \qquad (23)$$

$$\frac{1}{\overline{(\Delta Y)^2}^{\circ}} = \frac{1}{y} + \frac{1}{N+x} \quad , \quad \overline{(\Delta Y)^2}^{\circ} = \frac{y(N+x)}{N+x+y} \qquad (24)$$

$$\frac{1}{\overline{(\Delta N)^2}^{\circ}} = \frac{1}{N} + \frac{1}{x+y} \quad , \quad \overline{(\Delta N)^2}^{\circ} = \frac{N(x+y)}{N+x+y} \ . \qquad (25)$$

As $-\Delta N = \Delta X + \Delta Y$, we have:

$$\overline{(\Delta N)^2}^{\circ} = \overline{(\Delta X)^2}^{\circ} + \overline{(\Delta Y)^2}^{\circ} + 2\,\overline{\Delta X\ \Delta Y}^{\circ} \qquad (26)$$

$$\overline{\Delta X\ \Delta Y}^{\circ} = \frac{-xy}{N+x+y} \ . \qquad (27)$$

For reasons of symmetry:

$$\overline{\Delta N \Delta X}^{\circ} = \frac{-Nx}{N+x+y} \qquad (28)$$

$$\overline{\Delta N \Delta Y}^{\circ} = \frac{-Ny}{N+x+y} \ . \qquad (29)$$

Since these relations follow from thermodynamic arguments, they will not depend on kinetic properties of the systems e.g. direct transitions between X and Y.

3. Time dependence

For the processes at the X centre we can write:

$$\frac{d\Delta X_n}{dt} = I_{cx} - I_{xc} = (I_{cx} - I_{xc})_{equil.} + \left[\frac{dI_{cx}}{dX_n} - \frac{dI_{xc}}{dX_n}\right]\Delta X_n = \frac{-\Delta X_n}{\tau} \qquad (30)$$

From the terms between brackets we obtain:

$$I_{cx}\left[\frac{\Delta X_p}{X_p} + \frac{\Delta N}{N} - \frac{\Delta X_n}{X_n}\right] = -\frac{\Delta X_n}{\tau} \cdot \qquad (31)$$

In view of (5) this is written as:

$$I_{cx}\left[(\frac{1}{N} + \frac{1}{x})\Delta X + \frac{1}{N}\Delta Y\right] = \frac{\Delta X}{\tau} \cdot \qquad (32)$$

By analogy:

$$I_{cy}\left[\frac{1}{N}\Delta X + (\frac{1}{N} + \frac{1}{y})\Delta Y\right] = \frac{\Delta Y}{\tau} \cdot \qquad (33)$$

If $Y = 0$, $\tau = T_x$ where $\frac{1}{T_x} = I_{cx}(\frac{1}{N} + \frac{1}{x})$ · (34)

If $X = 0$, $\tau = T_y$ where $\frac{1}{T_y} = I_{cy}(\frac{1}{N} + \frac{1}{y})$ · (35)

(32) and (33) become:

$$(\frac{1}{T_x} - \frac{1}{\tau})\Delta X + \xi\,\frac{1}{T_x}\Delta Y = 0 \qquad (36)$$

$$\eta\,\frac{1}{T_y}\Delta X + (\frac{1}{T_y} - \frac{1}{\tau})\Delta Y = 0 \qquad (37)$$

with

$$\xi = \frac{x}{N+x} \quad 0 < \xi < 1$$

$$\eta = \frac{y}{N+y} \quad 0 < \eta < 1 \,. \qquad (38)$$

There are two solutions for τ. We shall show that one approaches T_x when $\xi\eta \to 0$; the other then approaches T_y. Therefore, we call them τ_x and τ_y. To simplify the notation we introduce:

$$a = \frac{1}{\tau} \qquad a_x = \frac{1}{\tau_x} \qquad A_x = \frac{1}{T_x}$$

$$a_y = \frac{1}{\tau_y} \qquad A_y = \frac{1}{T_y} \quad . \tag{39}$$

In this way we obtain two equations on which our further analysis is based:

$$(A_x - a)\Delta X + \xi A_x \Delta Y = 0 \tag{40}$$

$$\eta A_y \Delta X + (A_y - a)\Delta Y = 0 \quad . \tag{41}$$

(40) and (41) give two solutions for a, which we will call a_x an a_y :

$$a^2 - a(A_x + A_y) + (1 - \xi\eta)A_x A_y = 0 \tag{42}$$

Two limit situations are immediately clear:

$$\text{if } \xi\eta = 0, \quad a_x = A_x \quad \text{and } a_y = A_y \tag{43}$$

$$\text{if } \xi\eta = 1, \quad a_x = 0 \quad \text{and } a_y = A_x + A_y$$

$$\text{or} \quad a_x = A_x + A_y \text{ and } a_y = 0 \quad . \tag{44}$$

The discriminant D of the quadratic equation (42) is:

$$D = (A_x - A_y)^2 + 4\,\xi\eta\, A_x A_y \tag{45}$$

D is nowhere zero as both terms at the right-hand side are positive in the range $0 < \xi\eta < 1$. The two branches, a_x and a_y, will nowhere intersect. The higher branch will be connected to $A_x + A_y$ at $\xi\eta = 1$. The lower branch will go to 0 at $\xi\eta = 1$. See fig. 2.

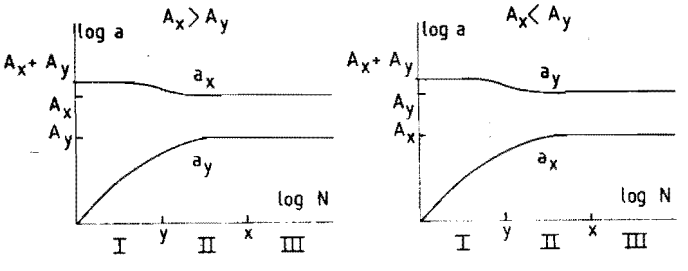

Fig. 2 The inverse frequencies as functions of N.

Nothing has been said thus far about which centre is called X and which Y. Here we choose the symbols X and Y on the basis of:

$$x >> y \ . \tag{46}$$

With this choice, $x >> y$, we could have $A_x > A_y$ but also $A_x < A_y$. For the case $A_x > A_y$ we find from (42):

$$a_x = \tfrac{1}{2}(A_x + A_y) + \tfrac{1}{2}\left[(A_x - A_y)^2 + 4\,\xi\eta\,A_xA_y\right]^{\frac{1}{2}} \tag{47}$$

$$a_y = \tfrac{1}{2}(A_x + A_y) - \tfrac{1}{2}\left[(A_x - A_y)^2 + 4\,\xi\eta\,A_xA_y\right]^{\frac{1}{2}} \ . \tag{48}$$

The exact solutions (47) and (48) run close to the linear approximations $A_x + \xi\eta\,A_y$ and $A_y - \xi\eta\,A_y$.

Substitution of (47) and (48) in (40) and (41) makes it possible to write ΔX as the sum of the two exponentials. Also, ΔY will be the sum of two exponentials, like ΔN. As we know the variances (23), (24) and (25), we find two Lorenzians for S_N. The problem is solved in principle.

For a straight-forward interpretation of experimentally observed spectra, however, we need much simpler explicit expressions, which we shall now work out using a few approximations. The various situations, each with its own approximate results, will be defined by the relative magnitudes of N, x and y. We define three regions in which different approximations hold good: I $N << y << x$, II $y << N << x$ and III $y << x << N$.

In the appendix we show how the approximate results are obtained. The solutions for the frequencies are given as a_x and a_y in fig. 2. We find there $a_x \cong A_x$ and $a_y \cong A_y$ in regions II and III. The spectra show the simple recombination times of the independent traps if $y << N$. This condition was also found by Van Rheenen, Bosman and Van Vliet [4]. In our notation their relation (42) reads:

$$1 << (1 + \frac{N}{x})(1 + \frac{N}{y}) \ , \tag{49}$$

which is satisfied in regions II and III.

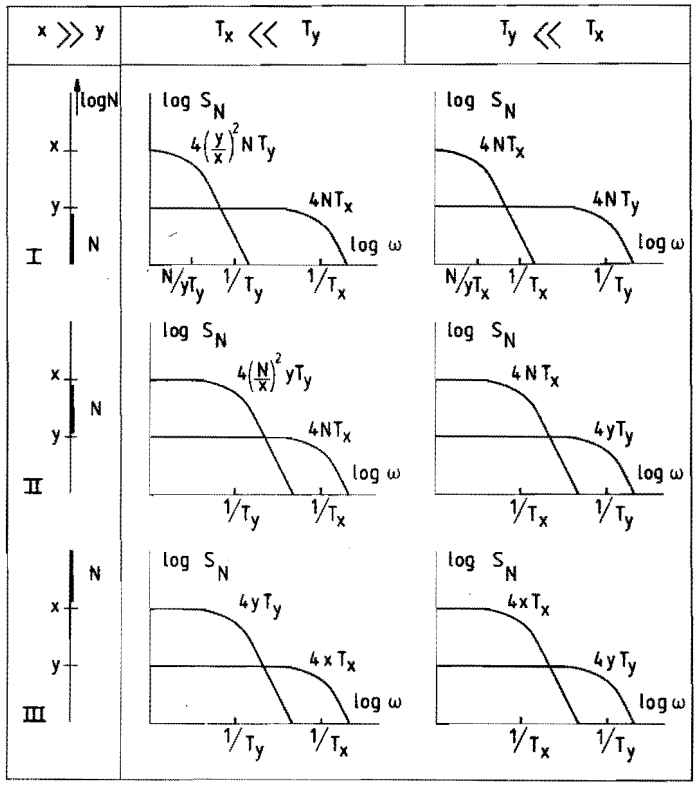

Fig. 3 Approximate solutions for the generation-recombination spectrum of the three-level model with traps X and Y.

Fig. 3 shows the Lorenzians. When $T_y \ll T_x$ there will always be two Lorenzians. When $T_x \ll T_y$, however, the low-frequency y-spectrum may be below the white plateau of the x-spectrum, so that only one Lorenzian is observed.

The spectra look like those of independent traps if the low-frequency plateaux equal $4xT_x$ and $4yT_y$. The appendix and Fig. 3 show that this is only the case in region III. Only in region III is a naive interpretation correct. We agree with Van Rheenen, Bosman and Van Vliet [4], who for this situation found their relation (46), which in our notation reads: $1/N \ll 1/x$ and $1/N \ll 1/y$. They also state that the Fermi level should be a few kT away from either of the traps. This is incorrect. There is no condition for the Fermi level.

Situations in which the observed white plateau corresponds to N, x or y will be easily recognized. There are, however, situations in which the plateau does not correspond to simply N, x or y. With a naive interpretation this will lead to strange activation energies and concentrations, suggesting the discovery of a new generation-recombination centre.

5. The interpretation of observed spectra

Here we summarize the results without paying attention to the mathematical treatment. The experimentalist who is interested in applying the results will find in this section all he needs for understanding fig. 3. We therefore repeat some definitions which are scattered over the text.

We assume that we know all equilibrium concentrations in the sample. N is the number -not the concentration- of the free electrons. X is the number of one kind of trap. The number of occupied traps is X_n; X_p is the number of empty traps. The second trap is Y with $Y_n + Y_p = Y$. Our final results are so simple because they are expressed in quantities x and y, defined by:

$$\frac{1}{x} = \frac{1}{X_n} + \frac{1}{X_p} \qquad \frac{1}{y} = \frac{1}{Y_n} + \frac{1}{Y_p} \,. \tag{6}$$

When X_n and X_p have different orders of magnitude, x is the smaller of the two.

There are no conditions for the donor or acceptor character of Y and X. All cases will have a charge neutrality equation for the fluctuations:

$$\Delta X + \Delta Y + \Delta N = 0 \,. \tag{18}$$

When x, y and N have different orders of magnitude the approximations given in Fig. 3 can safely be used. When this is not the case, we must use the exact relations (23) to (29) for the variances and (47) and (48) for the relaxation times $\tau_x = a_x^{-1}$ and $\tau_y = a_y^{-1}$.
In these relations and in Fig. 3 there appear the characteristic times T_x and T_y, which are the relaxation times of samples with X only or Y only, respectively. T_x and T_y are given by the relations (34) and (35). Fig. 3 shows the situations in which $\tau_x = T_x$ and $\tau_y = T_y$: N should be larger than y.

The denominator of the expressions (23-29) for the variance, N+x+y, may give rise to a well-known factor 2 in the case of a quite normal charge neutrality condition such as $N = D^+$, where D^+ is an empty donor: ($y << N = x = D^+ << D^o \cong D$).

Acknowledgements

We wish to thank Prof. J.P. Nougier of the Université des Sciences et Techniques du Languedoc at Montpellier for critical discussions.

This work is part of the research programme of the "Stichting voor Fundamenteel Onderzoek der Materie" (FOM), which is financially supported by the "Nederlandse Organisatie voor Wetenschappelijk Onderzoek" (NWO).

References

1. K.M. van Vliet and J.R. Fassett
   Chapter 7 in Fluctuation Phenomena in Solids
   R.E. Burgess Ed. Academic Press, New York (65)
2. H.J. Hoffmann and W. Sohn
   Physica Status Solidi A44, 237 (77)
3. H.J. Hoffmann and E. Huber
   Physica 111B, 249 (81)
4. A.D. van Rheenen, G. Bosman and C.M. van Vliet
   Solid State Electronics 28, 457 (85)
5. A.D. van Rheenen, G. Bosman and R.J.J. Zijlstra
   Solid State Electronics 30, 259 (87)
6. J.A. Copeland
   IEEE Transactions Electron Devices ED 18, 50 (71)

APPENDIX

In this appendix we derive the approximate solutions shown in fig. 3. Substitution of a_x in (40) or in (41) gives the ratio of ΔY_x and ΔX_x. The ratio of ΔX_y and ΔY_y is found by substitution of a_y in (40) or (41).

Then we obtain ΔN, expressed in ΔX_x and ΔY_y, which yields ΔN as a function of ΔX and ΔY. Using (23) to (29) we find approximations for the correlation function of N as the sum of two exponentials, one with τ_x, the other with τ_y, which in many cases can be approximated by T_x and T_y.

A Three approximations with $A_x >> A_y$

I $N << y << x$ $\qquad \xi \cong 1 - \frac{N}{x} \qquad \eta \cong 1 - \frac{N}{y}$

$$a_x \cong A_x + A_y - \left(\frac{N}{y} + \frac{N}{x}\right) A_y \rightarrow \Delta Y_x \cong \frac{A_y}{A_x} \Delta X_x$$

$$a_y \cong + \left(\frac{N}{y} + \frac{N}{x}\right) A_y \rightarrow \Delta X_y \cong - \left(1 - \frac{N}{x}\right) \Delta Y_y$$

$$\Delta X \cong \Delta X_x + \left(-1 + \frac{N}{x}\right) \Delta Y_y \rightarrow \Delta X_x \cong \Delta X + \Delta Y \cong - \Delta N$$

$$\Delta Y \cong \frac{A_y}{A_x} \Delta X_x + \Delta Y_y \rightarrow \Delta Y_y \cong - \frac{A_y}{A_x} \Delta X + \Delta Y$$

$$+ \qquad\qquad - \Delta N \cong \Delta X_x + \frac{N}{x} \Delta Y_y$$

$$\overbrace{\Delta N(0)\Delta(t)}^{N} \cong \left(\Delta N(0) \left[+ \Delta N(0) e^{-t/\tau_x} + \frac{N}{x} \left\{ \frac{A_y}{A_x} \Delta X(0) - \Delta Y(0) \right\} e^{-t/\tau_y} \right] \right)$$

$$\cong N e^{-t/\tau_x} + \frac{N}{x} N \left\{ \frac{y}{x} - \frac{A_y}{A_x} \right\} e^{-t/\tau_y}$$

with $\tau_x \cong T_x$ and $\tau_y \cong \frac{y}{N} T_y$

Low-frequency plateau of y-spectrum: $4\left(\frac{y}{x}\right)^2 NT_y - 4\left(\frac{y}{x}\right) NT_x$.

The second, negative, term can be neglected compared to the x-plateau $4NT_x$. If a low-frequency y-spectrum is observed it has a plateau of $4\left(\frac{y}{x}\right)^2 NT_y$. This requires $\left(\frac{y}{x}\right)^2 >> \frac{T_x}{T_y}$, which is possible but not necessary.

II $y << N << x$ $\qquad \xi \cong 1 - \frac{N}{x} \qquad \eta \cong \frac{y}{N}$

$$a_x \cong A_x + \frac{y}{N} A_y \quad \rightarrow \quad \Delta Y_x \cong \frac{A_y}{A_x} \cdot \frac{y}{N} \Delta X_x$$

$$a_y \cong A_y - \frac{y}{N} A_y \quad \rightarrow \quad \Delta X_y \cong - \left(1 - \frac{N}{x} + \frac{A_y}{A_x}\right) \Delta Y_y$$

$$\Delta X \cong \Delta X_x + \left(-1 + \frac{N}{x} - \frac{A_y}{A_x}\right) \Delta Y_y \quad \rightarrow \quad \Delta X_x \cong \Delta X + \Delta Y \cong - \Delta N$$

$$\Delta Y \cong \frac{A_y}{A_x} \cdot \frac{y}{N} \cdot \Delta X_x + \Delta Y_y \quad \rightarrow \quad \Delta Y_y \cong \Delta Y$$

$$+ \quad \text{---------------------------------}$$

$$- \Delta N \cong \Delta X_x + \left(\frac{N}{x} - \frac{A_y}{A_x}\right) \Delta Y_y$$

$$\overline{\Delta N(0) \Delta N(t)} \cong \left\langle \Delta N(0) \left[\Delta N(0) e^{-t/\tau_x} - \left\{ \frac{N}{x} - \frac{A_y}{A_x} \right\} \Delta Y(0) e^{-t/\tau_y} \right] \right\rangle$$

$$\cong N e^{-t/T_x} + \left\{ \frac{N}{x} - \frac{A_y}{A_x} \right\} \frac{Ny}{x} e^{-t/T_y}$$

Low-frequency plateau of y-spectrum: $4\left(\frac{N}{x}\right)^2 y T_y - 4 \frac{Ny}{x} T_x$.

The second, negative, term can be neglected compared to the x-plateau $4NT_x$.
If the low-frequency y-spectrum is observed it has a plateau of $4\left(\frac{N}{x}\right)^2 y T_y$.

III $y << x << N$ $\qquad \xi \cong \frac{x}{N}$ $\qquad \eta \cong \frac{y}{N}$

$$a_x \cong A_x + \frac{xy}{N^2} A_y \quad \rightarrow \quad \Delta Y_x \cong \frac{A_y}{A_x} \cdot \frac{y}{N} \Delta X_x$$

$$a_y \cong A_y - \frac{xy}{N^2} A_y \quad \rightarrow \quad \Delta X_y \cong - \frac{x}{N} \Delta Y_y$$

$$\Delta X \cong \Delta X_x - \frac{x}{N} \Delta Y_y \quad \rightarrow \quad \Delta X_x \cong \Delta X$$

$$\Delta Y \cong \frac{A_y}{A_x} \cdot \frac{y}{N} \Delta X_x + \Delta Y_y \quad \rightarrow \quad \Delta Y_y \cong \Delta Y$$

$$+ \quad \text{---------------------------------}$$

$$-\Delta N \cong \Delta X_x + \Delta Y_y$$

$$\overline{\Delta N(0) \Delta N(t)} \cong \left\langle \Delta N(0) \left[- \Delta X(0) e^{-t/\tau_x} - \Delta Y(0) e^{-t/\tau_y} \right] \right\rangle$$

$$\cong x e^{-t/T_x} + y e^{-t/T_y}$$

B Three approximations with $A_y >> A_x$

I $N << y << x$ $\qquad \xi \cong 1 - \frac{N}{x}$ $\qquad \eta \cong 1 - \frac{N}{y}$

$$a_x \cong + \left(\frac{N}{y} + \frac{N}{x}\right)A_x \quad \rightarrow \quad \Delta Y_x \cong - \left(1 - \frac{N}{y}\right)\Delta X_x$$

$$a_y \cong A_x + A_y - \left(\frac{N}{y} + \frac{N}{x}\right)A_x \quad \rightarrow \quad \Delta X_y \cong \frac{A_x}{A_y}\,\Delta Y_y$$

$$\Delta X \cong \Delta X_x + \frac{A_x}{A_y}\,\Delta Y_y \quad \rightarrow \quad \Delta X_x \cong \Delta X - \frac{A_x}{A_y}\,\Delta Y$$

$$\Delta Y \cong \left(-1 + \frac{N}{y}\right)\Delta X_x + \Delta Y_y \quad \rightarrow \quad \Delta Y_y \cong \Delta X + \Delta Y \cong - \Delta N$$

$$+ \qquad -\Delta N \cong \frac{N}{y}\,\Delta X_x + \Delta Y_y$$

$$\overline{\Delta N(0)\Delta N(t)} \cong \left\langle \Delta N(0)\left[-\frac{N}{y}\,\Delta X(0)e^{-t/\tau_x} + \Delta N(0)e^{-t/\tau_y}\right]\right\rangle$$

$$\cong \frac{N}{y} \cdot N e^{-t/\tau_x} + N e^{-t/\tau_y}$$

with $\tau_x \cong \frac{y}{N}\,T_x$ and $\tau_y = T_y$

II $y << N << x$ $\qquad \xi \cong 1 - \frac{N}{x}$ $\qquad \eta \cong \frac{y}{N}$

$$a_x \cong A_x - \frac{A_x}{A_y} \cdot \frac{y}{N}\,A_x \quad \rightarrow \quad \Delta Y_x \cong - \frac{y}{N}\,\Delta X_x$$

$$a_y \cong A_y + \frac{A_x}{A_y} \cdot \frac{y}{N}\,A_x \quad \rightarrow \quad \Delta X_y \cong \frac{A_x}{A_y}\,\Delta Y_y$$

$$\Delta X \cong \Delta X_x + \frac{A_x}{A_y}\,\Delta Y_y \quad \rightarrow \quad \Delta X_x \cong \Delta X$$

$$\Delta Y \cong - \frac{y}{N}\,\Delta X_x + \Delta Y_y \quad \rightarrow \quad \Delta Y_y \cong \Delta Y + \frac{y}{N}\,\Delta X$$

$$+ \qquad -\Delta N \cong \Delta X_x + \Delta Y_y$$

$$\overline{\Delta N(0)\Delta N(+)} \cong \left\langle \Delta N(0)\left[-\Delta X(0)e^{-t/\tau_x} - \left\{\frac{y}{N}\,\Delta X(0) + \Delta Y(0)\right\} e^{-t/\tau_y}\right]\right\rangle$$

$$\cong N e^{-t/T_x} + \left\{\frac{y}{N}\,N + \frac{yN}{x}\right\} e^{-t/T_y}$$

$$\cong N e^{-t/T_x} + y\, e^{-t/T_y}$$

III $y \ll x \ll N$ $\qquad \xi \cong \frac{x}{N}$ $\qquad \eta \cong \frac{y}{N}$

$$a_x \cong A_x + \frac{xy}{N^2} A_x \quad \rightarrow \quad \Delta Y_x \cong -\frac{y}{N} \Delta X_x$$

$$a_y \cong A_y - \frac{xy}{N^2} A_x \quad \rightarrow \quad \Delta X_y \cong \frac{A_x}{A_y} \cdot \frac{x}{N} \Delta Y_y$$

$$\Delta X \cong \Delta X_x + \frac{A_x}{A_y} \cdot \frac{x}{N} \Delta Y_y \quad \rightarrow \quad \Delta X_x \cong \Delta X$$

$$\Delta Y \cong -\frac{y}{N} \Delta X_x + \Delta Y_y \quad \rightarrow \quad \Delta Y_y \cong \Delta Y + \frac{y}{N} \Delta X$$

$$+ \qquad\qquad\qquad\qquad\qquad\qquad\qquad\qquad$$

$$-\Delta N \cong \Delta X_x + \Delta Y_y$$

$$\overline{\Delta N(0)\Delta N(t)} \cong \left\langle \Delta N(0) \left[-\Delta X(0) e^{-t/\tau_x} - \left\{ \frac{y}{N} \Delta X(0) + \Delta Y(0) \right\} e^{-t/\tau_y} \right] \right\rangle$$

$$\cong x\, e^{-t/T_x} + \left\{ \frac{xy}{N} + y \right\} e^{-t/T_y} \cong x\, e^{-t/T_x} + y\, e^{-t/T_y}$$

Chapter 5

Intrinsic and Extrinsic 1/f Noise Sources in Proton-irradiated n-GaAs Epitaxial Layers

L. Ren

Department of Electrical Engineering

Eindhoven University of Technology

5600 MB Eindhoven, The Netherlands

Abstract

The low-frequency resistance noise of proton-irradiated n-GaAs epitaxial layers was studied at temperatures from 77 to 300 K. Two types of 1/f noise were identified from the temperature dependence of the 1/f noise parameter α. One type of 1/f noise, which is dominating at high temperatures, seems to be of intrinsic origin related to the lattice phonon scattering. The other one dominating at lower temperatures, is then of extrinsic origin induced by the irradiation. The extrinsic type of 1/f noise is consistent with the picture of quantum "local-interference" effect and can reasonably be described by the Dutta-Dimon-Horn model [1].

(submitted to Journal of Applied Physics)

I. Introduction

Evidence in support of a relation between 1/f noise and lattice defects has been continuously accumulating [1-12]. In particular, in metal films the 1/f noise is commonly described by the so-called Dutta-Dimon-Horn (DDH) model [1], as arising from a distribution of thermally activated processes with typical activation energies centered at ~ 1 eV and a width of several tenths of eV. Other direct evidence pointing to defect hopping as the microscopic source of 1/f noise in metal films has also been put forward [13-15]. It was demonstrated that the quantum interference effects are responsible for the coupling of defect motion to the fluctuations in the electrical resistance [16-18]. In semiconductors, however, the 1/f noise is poorly understood [19]. For a long time, it has been demonstrated that an empirical relation[20] is successful in describing the 1/f noise in homogeneous samples and in semiconductor devices [21]. This relation relates the relative 1/f noise power density S_R/R^2 of the fluctuations in the resistance R to the total number of charge carriers N in the sample:

$$\frac{S_R}{R^2} = \frac{\alpha}{fN} \qquad (1)$$

α is often called the 1/f noise parameter. Relation (1) is more likely to suggest an intrinsic origin of the 1/f noise as caused by mobility fluctuations, since the total number of charge carriers N appears as the normalizing factor [22]. However, recent experimental results on the temperature dependence of α are difficult to understand [23], especially the 1/f noise in epitaxial GaAs, which was understood to be caused by mobility fluctuations [24]. The strong temperature dependence of α in epitaxial n-GaAs was found not able to be described by the DDH model [23]. In Si, the noise parameter α and its temperature dependence were found to depend on the manu-

facturing processes [25,26], which indicates that α is sensitive to crystal quality. But in a what way does α depend on the perfectness of crystal lattice is still an open question.

In order to obtain a better understanding of the quality dependence of α in semiconductors, we have studied the noise of epitaxial n-GaAs irradiated by 3 MeV electrons [27], where the induced point defects turned out to have little effect on α or on its temperature dependence. Here, we report on the noise in epitaxial n-GaAs bombarded by 3 MeV protons. In this way, the influence of some sort of clusters induced by the proton irradiation was examined. The results clearly show that there coexist two types of noise sources, which we call intrinsic and extrinsic 1/f noise sources.

II. Experimental Procedures

Epitaxial n-GaAs doped with Si was grown by a VARIAN MOD 3" molecular beam epitaxy (MBE) system. The structure of the samples used in this study was somewhat different from the previously-used bulk samples [27-29]. Two sandwitched $Al_xGa_{1-x}As$ (x=0.3) layers of 20 nm thick were used to confine the electron transport in the bulk region by forming the band-gap mismatched barriers at interfaces. The bulk n-GaAs doped with Si to a level of $2x10^{16}cm^{-3}$ was grown on a 2 mm thick semi-insulating GaAs substrate. The $Al_xGa_{1-x}As$ layers were doped with Si to a level of $1.3x10^{16}cm^{-3}$. The growth temperature was 600 °C. The thickness of the epitaxial layers was 3.2μm. Hall bar structures with six side contacts were prepared using conventional photolithography and wet-etching procedures. The width of the bars was 260μm. The length of the bars was 2400μm. Ohmic contacts to the epitaxial layer were formed by placing tin balls on the contact areas and annealing in a N_2/H_2 mixture at 400 °C for one minute on a strip heater.

The samples were irradiated with 3 MeV proton (H^+) beams produced by the 30 MeV AVF cyclotron of the Eindhoven University of Technology. The proton beam was homogenised by a diffuser and checked to be homogeneously distributed within a circle with a radius of about 4 cm. The current in a centre area with a radius of 4 mm was measured in order to calculate the irradiation intensity. This was carried out by a rotating vane in front of the sample. Scattered protons were measured at an angle of 90° by means of a surface barrier detector. The calibration was performed with the measured current in a Tocaday cup without the sample in the beam as well as with a small beam stop in front of the sample behind a ϕ 4 mm diaphragm. A thick graphite disk was used to protect the contact areas from irradiation, while the centre part of the samples was exposed to the incoming protons through a rectangular hole. Five different doses were used. Table I gives the sample code, irradiation intensity and the dose ϕ, which is the number of protons per cm^2.

Table I. Sample code, irradiation intensity, time and doses.

Sample	Irradiation intensity (H^+/cm^2s)	Irradiation time (s)	Dose ϕ (H^+/cm^2)
1	1.9×10^{11}	5	9.5×10^{11}
2	7.7×10^{11}	2.5	1.9×10^{12}
3	3.75×10^{11}	20	7.5×10^{12}
4	3.75×10^{11}	40	1.5×10^{13}
5	1.9×10^{11}	160	3.0×10^{13}

The depth distribution of the implanted ions can be well approximated by a Gaussian distribution, which is determined

by the projected range R_p and the straggling ΔR_p [30]. For the most common ion-substrate combinations, the range parameters have been tabulated, for example by Biersack [31]. By extrapolating his data, we could find the R_p and ΔR_p to be about 50μm and 1μm, respectively for 3 MeV protons in GaAs. Consequently, the protons were stopped deep in the substrate. The defect production in the epitaxial layer can be regarded to be homogeneous, in view of the thickness of our epitaxial layers and the distribution of the protons over the sample.

The experimental set-up for measuring noise is described in detail elsewhere [28]. A cryostat was used to perform the temperature dependence of noise and Hall effect measurements. The cryostat was cooled with liquid nitrogen. The temperature was measured by a copper-constantan thermocouple mounted on the sample holder close to the sample. The resistance R of the sample as a function of temperature and the thermal noise level 4kTR were also measured to check the real sample temperature. Both the voltage fluctuations along and perpendicular to the current path were measured to ensure that the noise contribution from contacts could be neglected.

III. Experimental results

A. Hall effect

The Hall effect was measured between 77 and 300 K with a current of 50 μA and a magnetic field of 0.5 T. Fig. 1 shows a plot of n, the concentration of the free charge carriers, as a function of inverse temperature, 1000/T. We assumed for the Hall factor r=1.0, independent of temperature. It is clear that the irradiation creates mainly acceptors since the concentration of the charge-carriers decreases with the increase of the dose, as indicated in Fig. 1. By using the charge neutrality equations [32], it was estimated that a deep level of about 0.1 eV could account for the temperature dependence

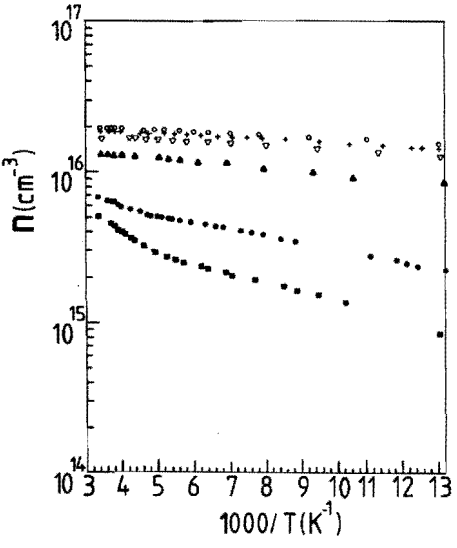

Fig. 1 Concentration of free charge carriers versus inverse temperature.

○: Before irradiation
+: irradiation dose $9.5 \times 10^{11} cm^{-2}$
▽: $1.9 \times 10^{12} cm^{-2}$
▲: $7.5 \times 10^{12} cm^{-2}$
●: $1.5 \times 10^{13} cm^{-2}$
■: $3.0 \times 10^{13} cm^{-2}$

of the free charge carriers at high temperatures from 300 to 200 K. This deep level could be the well-known electron trap E2 [33].

Fig. 2 shows the mobility μ as a function of temperature. For comparison, the lattice mobility calculated for the polar optical phonon scattering is also shown. For hydrogen in crystalline semiconductors, it is quite well known that the impurities and lattice defects are often passivated by the hydrogen through H bonding [34]. Mobility in the hydrogenated materials is, therefore, expected to be enhanced. Our results in Fig. 2, where mobility decreases with increasing irradiati-

on dose, are consistent with the fact that the protons were stopped in the substrate.

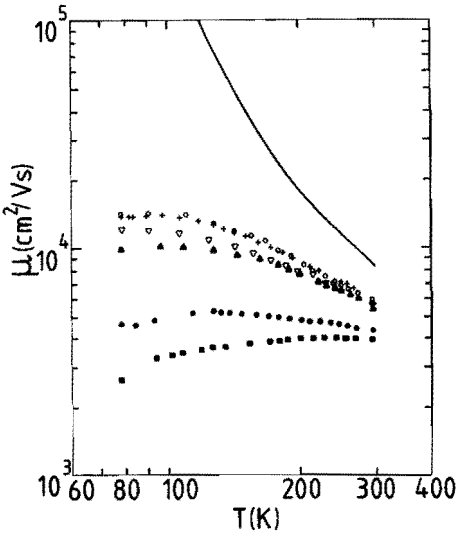

Fig. 2 Mobility versus temperature (symbols have the same meaning as in Fig. 1). The solid line shows the cal culated mobility caused by polar optical phonon scat tering.

B. Noise

Excess resistance noise has been measured both before and after H^+ irradiation. The noise was measured as a function of the irradiation dose and temperature between 77 and 300 K in a frequency range of 1 Hz to 20 kHz. Several bias voltages were applied in order to check whether the measured noise stemmed from resistivity fluctuations. The results always showed a quadratic dependence of the noise on the bias voltage.

Before irradiation, all noise spectra had a good 1/f shape at

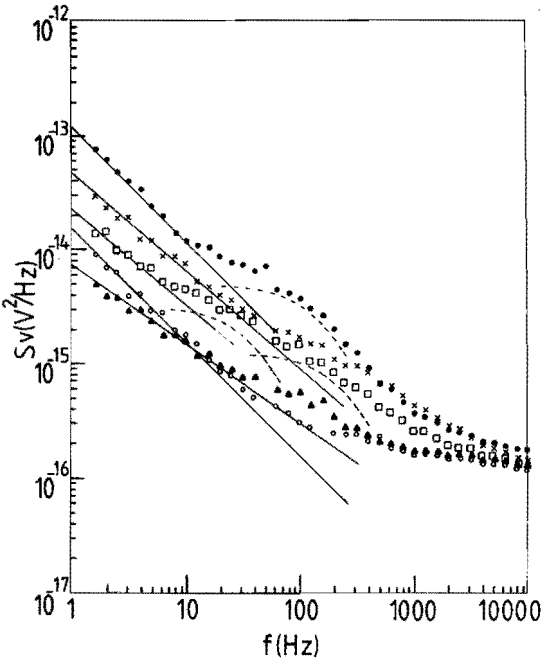

Fig. 3 Several noise spectra at different temperatures for sample 4. The solid lines are the best fits to the $1/f^{\gamma}$ spectra. The broken lines indicate the g-r components.
•: longitudinal noise at E = 9 V/cm and T = 295 K;
x: longitudinal noise at E = 5.2 V/cm and T = 214 K;
□: longitudinal noise at E = 3.6 V/cm and T = 205 K;
▲: transversal noise at E = 3.5 V/cm and T = 188 K;
○: longitudinal noise at E = 2.7 V/cm and T = 78 K.

all temperatures at which the noise data was taken. After irradiation, several changes in the noise spectra were observed. Below 150K, all samples showed good 1/f spectra at low frequencies. Above 150K, several distinct generation-recombination (g-r) humps growing with the irradiation doses were observed in addition to the 1/f noise. Here, it was difficult to fit such g-r humps by a single Lorentzian, while there were no such problems with the electron-irradiated samples [27]. Furthermore, in the temperature range where the g-r humps appeared, the 1/f noise deviated from slope -1.0 for the

samples with the two highest doses. Fig. 3 shows a number of spectra from sample 4 with a irradiation dose of $1.5 \times 10^{13} cm^{-2}$.

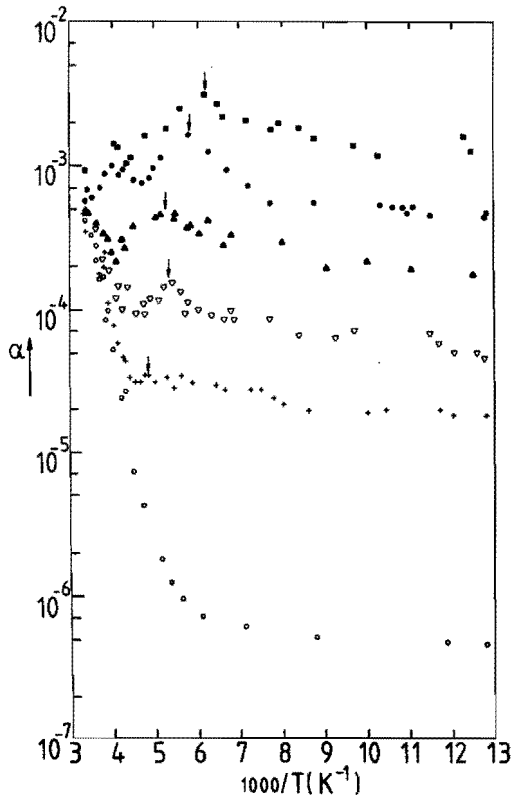

Fig. 4 α as a function of inverse temperature (symbols have the same meaning as in Fig. 1). Arrows indicate the noise peak (see text).

In Fig. 4, we present the 1/f noise parameter α as a function of inverse temperature. The α-values were evaluated at 1 Hz from NS_v/V^2, where N is the number of charge carriers as determined from the Hall effect, S_v is the voltage spectral power density and V is the bias voltage. The noise power density was found to be reproducible during several temperature cyclings.

Before irradiation, two branches with different temperature dependences of α [29] were found. After irradiation, the striking result is that at high temperatures where α is strongly temperature dependent, the 1/f noise is not affected by the proton irradiation. While at low temperatures, where α is weakly dependent on temperature, α increases with the irradiation doses. In contrast to the electron-irradiated samples [27], α of H^+ irradiated samples is very sensitive to the irradiation at low temperatures. Although there is less than 10% change in the mobility at 78 K in the sample 1, a change of almost two orders of magnitude in α was observed. In Fig. 5, we plot the α-values at 78K (representing the temperature-independent branch of α) and α-values at 300 K (representing the temperature dependent branch of α) versus the irradiation dose ϕ. Fig. 5 shows that α-values at 78 K are almost linearly

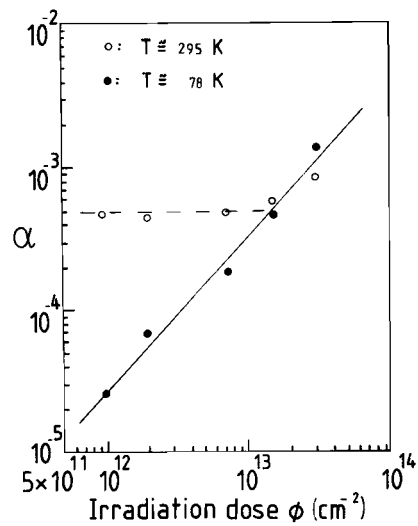

Fig. 5 α-values at 300 K and at 78 K as a function of the irradiation doses ϕ. The solid line is the best fit to the data at 78 K. The broken line represents dose-independent α-values at 300 K. Obviously, the relatively higher α-values at 300 K of the samples 4 and 5 are caused by the contribution from the extrinsic 1/f noise source.

proportional to ϕ while α-values at 300 K are almost independent of ϕ.

IV. Discussion

Considering the different behaviour of the 1/f noise under proton irradiation, the noise data in Fig. 4 clearly reveals that the two branches of the temperature dependence of α correspond to two different noise mechanisms: at the high temperatures, the 1/f noise seems to be dominated by an unknown source of an intrinsic origin, while at low temperatures the noise is obviously dominated by an extrinsic noise source induced by the irradiation. We observed that in almost all the samples, a peak in the 1/f noise power density showed up around 180 K. At the high temperature side of the peak, the α-values tended to coincide with the intrinsic values. The peaks, as indicated by the arrows in Fig. 4, were slightly moving to low temperature as the irradiation dose increased. This phenomenon reminded us of the DDH model. According to that model, the temperature dependence of the noise power density, S_v, simply represents the behaviour of the distribution function of activation energies, $D(E_o)$ [1] via

$$D(E_0) \sim \frac{\omega S_V(\omega, T)}{kT} \qquad (2)$$

Here $E_o = -kT\ln(\omega\tau_o)$, where T is the temperature, k is Boltzmann's constant, $\omega = 2\pi f$ is the angular frequency and τ_o is the attempt time of the activated processes.

Therefore, the peak energy E_p in $D(E_o)$ is related to the peak temperature in the noise power density, T_p, by

$$E_p \approx -kT_p\ln(\omega\tau_0) \qquad (3)$$

This implies that E_p was slightly reduced as the irradiation dose increased, which can be understood by attributing the

activated processes to some defect hoppings through the lattice. The higher the dose, the heavier the lattice damage, hence the easier the motion of the defect. If we take a typical value of 10^{-12}s for τ_o, a value of about 0.35eV can be estimated from eq. (3) from our noise data of sample 4.

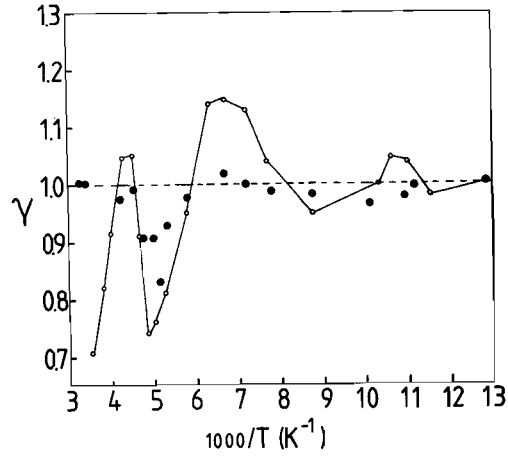

Fig. 6 The frequency exponent γ as a function of inverse temperature for sample 4. The solid dots are the experimental data points and the open circles connected by the solid lines, are the calculated results following from eq. (4).

Around the peaks there is a strong temperature dependence of the noise, which enables us to test the most characteristic feature of DDH model, the relation between $S_v(\omega,T)$ and the frequency exponent $\gamma = -(\partial \ln S_v/\partial \ln f)$ through the expression [1]

$$\gamma(T) = 1 - \frac{1}{\ln(\omega\tau_0)}\left[\frac{\partial \ln S_V(\omega,T)}{\partial \ln T} - 1\right] \qquad (4)$$

The directly measured values of γ , using the least square fit to the spectra S_v at the low frequencies where no obvious

"knees" or "bendings" appear, is plotted in Fig. 6 as a function of inverse temperature. In order to get rid of the temperature dependence of the concentration of the charge carriers, we used the temperature dependence of α instead of that of S_v versus T to calculate $\gamma(T)$ from eq. (4). The calculated values of γ from eq. 4 at different temperatures, using the spline fit to $\alpha(T)$ and $\tau_o=10^{-12}$s, are also shown in Fig. 6. Although there is a large scattering in the calculated γ, the general pattern of calculated $\gamma(T)$ is well matched to that of the experimental data, except near room temperature. The disagreement between the trend of calculated and experimental $\gamma(T)$ near room temperature could be due to the domination of the intrinsic noise source at high temperatures.

In the clean limit (defined as the inelastic scattering rate being greater that the elastic scattering rate), which is true for non-degenerate semiconductors at most of interest temperatures, the quantum "local-interference" effect is resulted from the "Born-approximation" [18]. It requires a close spatial correlation among the defects, within a few lattice constants [17]. Therefore, the comparisons to the noise data of n-GaAs irradiated by 3 MeV electrons [27] suggest that the extrinsic type 1/f noise in our H^+ irradiated n-GaAs samples is consistent with the "local-interference" model. A notable difference between the electron- and proton-irradiated samples is that the electron irradiation influence the conductivity more than α; while the influences of H^+-irradiation has just the opposite trend. This fact simply reflects the difference in the microstructure of the damage in the lattice. Since the mass of the electrons is much smaller than the masses of host atoms, the energy transmitted to the host atoms by collisions is very small [35], compared with the 3 MeV kinetic energy. It is just of the order of the threshold energy: the energy required to displace one atom to produce a vacancy and interstitial pair (~10 eV in GaAs). Thus, only simple intrinsic

point defects, randomly distributed in the lattice, are created by high-energy electron irradiation. Those point defects are then expected to act mainly as electron traps and charged scattering centres. Hence, with electron irradiation, we expect little effect on 1/f noise according to the "local-interference" model, where only moving defects with a close spatial correlation contribute to the 1/f noise generation [17]. On the other hand, the damage to the GaAs lattice caused by the high-energy protons is much more severe because the transmitted energy is large [35], many orders higher than the threshold energy. The displaced atoms themselves, can thus also displace other atoms, so that a cascade of displacements of atoms results. This leads to an accumulation of vacancies and interstitials, as well as other complex lattice defects, along the ion path. At low irradiation doses, isolated damaged regions are first created. With an increase of the dose, the size of a damaged region expands. At a very high dose, the damaged regions overlap until the entire irradiated region is converted to an amorphous phase. The correspondent critical dose is about $4x10^{17}cm^{-2}$ for 1 MeV protons implanted into GaAs, according to Pearton *et al.* [34]. Therefore, considering the doses of our irradiation ($9x10^{11}$ - 10^{14} cm^{-2}), the damages are like some sort of clusters, where the inner part of the clusters is composed of agglomerated vacancies and they are surrounded by point defects like the interstitials and the complexes of escaping vacancies with impurities, etc. Hence, more noise is expected based on the "local-interference" model. This conclusion is supported by the result in Fig. 5, where $\alpha \propto \phi$ simply implies that the moving defects are associated with the clusters since the number of clusters is expected to be directly proportional to the dose ϕ. However, for a quantitative analysis based on the quantum interference theories [17,18], the species of the mobile defects, their quantities and their spatial arrangements have to be indentified. Qualitatively, our experimental observations are quite good in

agreement with the quantum "local-interference" model.

An explanation is still missing for the intrinsic type of 1/f noise as identified in our samples. However, it may be interesting to speculate on physical mechanisms which could account for such a strong temperature-dependent α observed in our n-GaAs samples, and at the same time show a 1/f spectrum. From our measurements of the 1/f noise in Hall voltage [24], it suggests that the intrinsic noise source is related to the lattice phonon scattering. The present results also support this idea in view of that the lattice phonon scattering is little affected by the low-dose H^+ irradiation. For an assumption that the 1/f noise is caused by phonon energy fluctuations, Musha *et al.* [36] even demonstrated that the fluctuations in phonon number per mode is indeed a 1/f spectrum, by their light scattering experiment. However, as we shall point out, this cannot explain a strong temperature dependence in α under the thermal equilibrium condition, since from the empirical relation, eq.(1), one expects:

$$\alpha(T) \sim \frac{\langle(\Delta\mu_{phonon})^2\rangle}{\mu_{phonon}^2} \sim \frac{\langle(\Delta n_q)^2\rangle}{(n_q)^2} \qquad (5)$$

Where in thermal equilibrium, according to Bose-Einstein distribution, the average number n_q of the phonon mode q is

$$\langle n_q\rangle = \frac{1}{\exp(\frac{h\omega_q}{kT}) - 1} \qquad (6)$$

and the variance of phonon number fluctuations is

$$\langle(\Delta n_q)^2\rangle = \langle n_q\rangle(\langle n_q\rangle + 1) \qquad (7)$$

Therefore, no temperature dependence of α would be expected from eq. (5), since at normal temperature the average phonon number is much larger than unity. But, on the other hand, one could ask "Do phonon excitations really reach their thermal equilibrium state in a normal measuring time scale?" This

question has already been raised by Musha and Borbely [37].

V. Conclusion

We have performed noise measurement on the proton-irradiated n-GaAs epitaxial layers in a temperature range from 77 to 300 K. Two different types of 1/f noise sources were revealed from the temperature dependence of α. The one dominating at high temperatures and with a thermally activated α, was found to be independent of the irradiation doses. Therefore it is likely to have an intrinsic origin. The other one with a temperature independent α and important at low temperatures, was found to be very sensitive to the irradiation doses. We attributed it to an extrinsic origin. The noise kinetics of the extrinsic type of 1/f noise reasonably agree with the thermal activated model proposed by Dutta *et al.*[1]. Comparisons to the noise data of the electron-irradiated samples, suggest that the defect motion is the microscopic source for the observed irradiation-induced 1/f noise.

VI. Acknowledgements

The author is indebted to L.C. de Folter of the Physics Department for carrying out the irradiation. The author wishes to thank Prof.Dr. F.N. Hooge and Prof.Dr. M.J.A. de Voigt for their critical reading of the manuscript and Dr. M.R. Leijs for providing the samples. The author would also like to thank E. Goujou and F. Valckx for performing a large part of measurements. This work is part of the research programme of the "Stichting voor Fundamenteel Onderzoek der Materie"(FOM), which is financially supported by the "Nederlandse Organisatie voor Wetenschappelijke Onderzoek"(NWO).

References

[1] P. Dutta and P.M. Horn, Rev. Mod. Phys. 53(1981)497.

[2] M.B. Weissman, Rev. Mod. Phys. 60(1988)537.

[3] D.M. Fleetwood and N. Giordano, Phys. Rev. B 28(1983)3625.

[4] F.N.H. Robinson, Phys. Lett. 97A(1983)162.

[5] Sh.M. Kogan and K.E. Nagaev, Solid-St. Comm. 49(1984)387.

[6] J.H. Scofield and J.V. Mantese, Phys. Rev. B 32(1985)736.

[7] D.M. Fleetwood and N. Giordano, Phys. Rev. B 31(1985)1157.

[8] J. Pelz and J. Clarke, Phys. Rev. Lett. 55(1985)738.

[9] L.K.J. Vandamme and S. Oosterhoff, J. Appl. Phys. 59 (1986)3169.

[10] C.D. Keener and M.B. Weissman, Phys. Rev. B 44(1991)9178.

[11] K.S. Ralls and R.A. Buhrman, Phys. Rev. B 44(1991)5800.

[12] G.B. Alers and M.B. Weissman, Phys. Rev. B 44(1991)7192.

[13] N.M. Zimmerman and W.W. Webb, Phys. Rev. Lett. 61 (1988) 889.

[14] N.M. Zimmerman and W.W. Webb, Phys. Rev. Lett. 65 (1990) 1040.

[15] N.O. Birge and B. Golding, W.H. Haemmerle, Phys. Rev. B 42(1990)2735.

[16] S. Feng and P.A. Lee, A.D. Stone, Phys. Rev. Lett. 56 (1986)1960.

[17] J. Pelz and J. Clarke, Phys. Rev. B 36(1987)4479.

[18] S. Hershfield, Phys. Rev. B 37(1988)8557.

[19] F.N. Hooge, in *Proc. of the Int. on Noise in Physical Systems and 1/f Noise*, edited by T. Musha, S. Sato and M. Yamamoto, Kyoto, 1991(Ohmsa, Tokyo)p.7.

[20] F.N. Hooge, Phys. Lett. A 29(1969)139.

[21] F.N. Hooge, T.G.M. Kleinpenning and L.K.J. Vandamme, Rep. Prog. Phys. 44(1981)479.

[22] F.N. Hooge, Physica B 162(1990)344.

[23] L. Ren, in *Proc. of the Int. on Noise in Physical Systems and 1/f Noise*, edited by T. Musha, S. Sato and M. Yamamoto, Kyoto, 1991(Ohmsa, Tokyo)p. 45.

[24] L. Ren and J.S. Libris, Physica B **183**(1993)40.

[25] J. Luo, W.F. Love and S.C. Miller, J. Appl. Phys. **60** (1986)3196.

[26] R.H.M. Clevers, Physica B **154**(1989)214.

[27] L. Ren, P. Baucour, F.N. Hooge, L.H. Luthjens and M.R. Leijs, J. Appl. Phys. (in press).

[28] L. Ren and M.R. Leijs, Physica B **172**(1991)319.

[29] L. Ren and F.N. Hooge, Physica B **176**(1992)209.

[30] H. Ryssel and I. Ruge: *Ion Implantation*, John Wiley & Sons, Chichester-New York-Brisbane-Toronto-Singapore (1986).

[31] J.P. Biersack, Nucl. Inst. Meth. **182/183**(1981)199.

[32] D.C. Look, in *Semiconductors and Semimetals*, edited by R.K. Willardson and A.C. Beer, vol. **19**, p. 93, Academic Press, New York(1983).

[33] D. Pons and J.C. Bourgoin, J. Phys. C: Solid State Phys. **18**(1985)3839.

[34] J. Pearton, W. Corbett and M. Stavola, *Hydrogen in Crystalline Semiconductors*, Springer Series in Materials Science, vol. **16**, Springer-Verlag(1992).

[35] J.C. Bourgoin and M. Lannoo, *Point Defects in Semiconductors: Experimental Aspects*, Chap. **8**, Springer, Berlin (1983).

[36] T. Musha, G. Borbely and M. Shoji, Phys. Rev. Lett. **64** (1990)2394.

[37] T. Musha and G. Borbely, Jpn. J. Appl. Phys. **31**(1992) L370.

Chapter 6

1/f Noise in an $Al_xGa_{1-x}As$/GaAs Heterostructure between 77 and 300 K

L. Ren and M.R. Leys

Department of Electrical Engineering & Department of Physics

Eindhoven University of Technology

5600 MB Eindhoven, The Netherlands

ABSTRACT

Low-frequency (LF) noise was measured on an $Al_xGa_{1-x}As$/GaAs heterostructure in the temperature range from 77 to 300 K. Two types of excess noise, 1/f and an extremely broadened (EB) Lorentzian noise, were observed. Like van Die *et al.*, we attributed the observed EB-Lorentzian noise to the real-space transfer of the electrons from the two-dimensional electron gas (2DEG) to the n-$Al_xGa_{1-x}As$ layer and *vice versa*. A good agreement of α-values of the 1/f noise at high temperatures and their temperature dependences in the heterostructures with those of bulk n-GaAs indicate that the 1/f noise in the heterostructures has the same origin as in bulk n-GaAs.

(submitted to Physicsa B)

I. INTRODUCTION

Heterostructures are realised by growing a wide band-gap semiconductor on top of a small band-gap semiconductor. For the well-known system, Si-doped $Al_xGa_{1-x}As$ on undoped-GaAs, the electrons are accumulated and confined in a quantum well formed at the interface of GaAs to $Al_xGa_{1-x}As$ [1]. The transport of the electrons confined in the quantum well is quantized in the direction perpendicular to the interface. These electrons are often called a two-dimensional electron gas (2DEG). The mobility of the 2DEG electrons is very high as a result of the absence of charged impurity scattering in the conducting channel, because of the spatial separation of the electrons from their parent donors in the n-$Al_xGa_{1-x}As$ layer. Therefore, such a heterostructure provides an opportunity to study the 1/f noise, which is caused by lattice scattering only. Such a study is not possible with homogeneous samples of high purity GaAs because of the difficulties of making good Ohmic contacts.

Low-frequency noise in the $Al_xGa_{1-x}As$/GaAs heterostructures and in heterostructure field effect transistors has been studied intensively [2-12]. Most of the investigations show that generation-recombination (g-r) noise dominates over 1/f noise at low frequencies. The g-r noise is frequently attributed to trapping-detrapping of the charge carriers at the DX centres which are present in the n-$Al_xGa_{1-x}As$ layers [4-8]. Tacano *et al.* [10, 11] observed 1/f noise in $Al_xGa_{1-x}As$/GaAs heterostructures with SnAu contacts and in a device with a Van der Pauw shape. They found that at room temperature the 1/f noise parameter α, as defined by Hooge's empirical relation [13], was about 7.1×10^{-4} [11] and 1.7×10^{-3} [10] for the heterostructures. However, nothing was reported on the temperature dependence of the 1/f noise in those heterostructures. Therefore, the purpose of this paper is to compare the 1/f noise and

its temperature dependence measured on an $Al_xGa_{1-x}As/GaAs$ heterostructure with those obtained on homogeneous n-GaAs samples [14] in order to identify the 1/f noise sources in the heterostructures.

II. EXPERIMENTAL PROCEDURE

The heterostructures used in our experiments were grown by a VARIAN MOD 3" molecular beam epitaxy (MBE) system. The growing sequences of the multilayer structures were as follows: an undoped GaAs buffer layer of 4μm thick on top of the semi-insulating Cr-doped GaAs substrate; an undoped $Al_{0.3}Ga_{0.7}As$ spacer layer of 20nm thick; a $1.8x10^{18}cm^{-3}$ Si-doped $Al_{0.3}Ga_{0.7}As$ carrier supply layer of 40nm thick; then an undoped GaAs cap layer of 17nm. Fig. 1 shows the layer structure and the con-

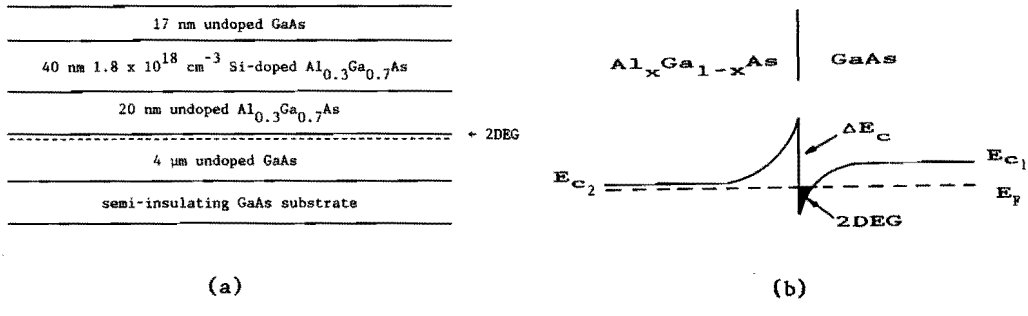

Fig. 1 (a) Layer structure of the sample;
(b) Conduction band diagram of an $Al_xGa_{1-x}As/GaAs$ heterostructure. The current flows parallel to the interface.

duction band diagram of the heterostructure. The growth temperatures was 630 °C. The GaAs growth rate was 1μm/hr. Hall bar structures with six side contacts were prepared using conventional photolithography and wet-etching procedures. The width of the bars was 260μm. The length of the bars was 2400μm. Ohmic contacts to the heterostructure were formed by pla-

cing tin balls on the contact areas and annealing in a N_2/H_2 mixture at 400 °C for one minute on a strip heater. The contacts show good Ohmic I-V characteristics in the whole temperature range.

The low-frequency noise was measured under several bias conditions and at temperatures between 77 and 300 K in a frequency range from 1 Hz up to 20 KHz. Both the longitudinal and transversal noise (defined as the noise measured along or perpendicular to the current) were measured in order to study the spatial distribution of the 1/f noise. The experimental set-up and the arrangement for the longitudinal and transversal noise measurement were the same as described in ref. [15].

III. EXPERIMENTAL RESULTS AND DISCUSSION

A. Hall effect measurements

In order to characterise the heterostructure, we made Hall effect and resistivity measurements on our standard Hall bars. The Hall effect was measured in its linear range both regarding the magnetic field and the current. Typical values for the magnetic field and current were 0.2 T and 50 μA, respectively. Fig. 2 and Fig. 3 show the sheet Hall electron concentration n_H and the Hall mobility μ_H versus the temperature. The calculated mobility due to only the polar optical phonon scattering is also shown in Fig. 3, for comparison. At reasonably low temperatures, the transport of charge carriers is dominated by the 2DEG. At high temperatures, the parallel conduction in the 2DEG and in the $Al_xGa_{1-x}As$ layer has to be considered. According to Petritz's parallel layer model [16], the experimental Hall concentration and the Hall mobility are determined by:

$$n_H = \frac{(n_{2D}\mu_{2D} + n_{AlGaAs}\mu_{AlGaAs})^2}{n_{2D}\mu_{2D}^2 + n_{AlGaAs}\mu_{AlGaAs}^2}, \qquad (1)$$

$$\mu_H = \frac{n_{2D}\mu_{2D}^2 + n_{AlGaAs}\mu_{AlGaAs}^2}{n_{2D}\mu_{2D} + n_{AlGaAs}\mu_{AlGaAs}}. \qquad (2)$$

Where the subscripts 2D and AlGaAs stand for the 2DEG and $Al_xGa_{1-x}As$, respectively.

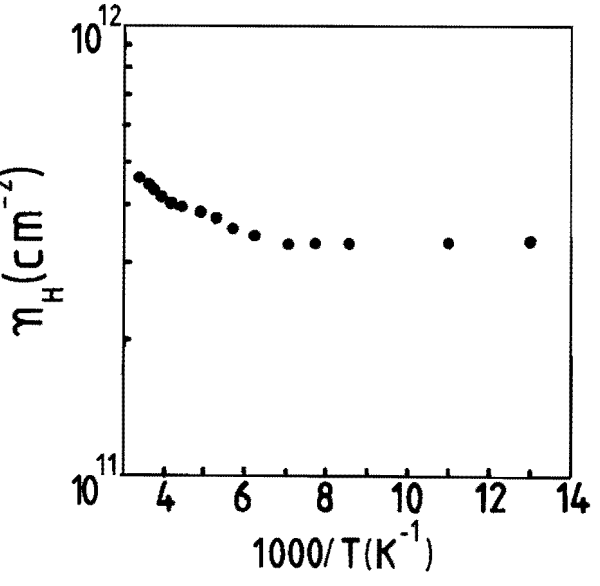

Fig. 2 Hall electron concentration as a function of inverse temperature.

The carrier concentration in the 2DEG, n_{2D}, is expected to be almost temperature independent since the charge carriers of 2DEG are separated from their parent donors and are usually degenerated. In the bulk $Al_xGa_{1-x}As$ layer with x>0.22, the concentration of the carriers is governed by the so-called DX centres[17] and n_{AlGaAs} decreases exponentially with 1/T as a result of the freeze-out of the charge-carriers to a deep donor level [18]. Considering a rather large self-compensation

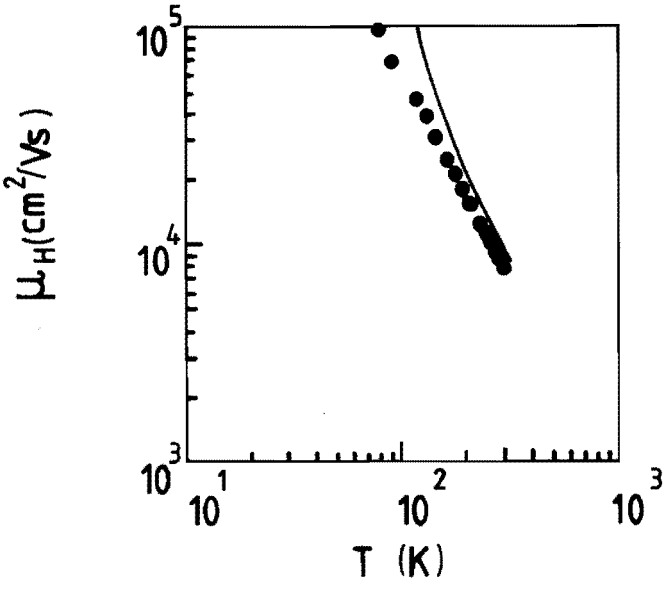

Fig. 3 Hall mobility as a function of temperature. The solid curve corresponds to polar optical phonon scattering.

of the Si dopant in III-V compounds, n_{AlGaAs} will decreases, according to [19], as

$$n_{AlGaAs} \propto \exp(-\frac{\Delta E_d}{kT}). \qquad (3)$$

Where ΔE_d is the thermal depth of the dominant deep donor level, k is the Boltzmann's constant and T is the temperature.

Therefore, we can attribute the horizontal part of n_H vs 1000/T in Fig. 2 to the electrons in the 2DEG. Hence n_{2D}=3.3x $10^{11}cm^{-2}$. In the highly doped $Al_xGa_{1-x}As$ ($1.8x10^{18}$ cm^{-3} for our sample), μ_{AlGaAs} is very low, about 1000 cm^2/Vs [20] and weakly dependent on temperature. With μ_{2D} much higher than μ_{AlGaAs}, the ratio

of $(n_{AlGaAs}\mu_{AlGaAs})/(n_{2D}\mu_{2D})$ is small compared to 1. Eq. (1) can be reduced to:

$$n_H = n_{2D} + 2n_{AlGaAs}(\mu_{AlGaAs}/\mu_{2D}) . \qquad (4)$$

We can estimate the thermal depth of the dominant DX centre in the $Al_xGa_{1-x}As$ from eq. (4) if the temperature dependence of the mobility ratio is weaker than that of n_{AlGaAs}. Combining eqs. (3) and (4), we found a thermal depth of about 60 meV. Considering that the thermal depth of the DX centre in the Si-doped $Al_xGa_{1-x}As$ is found to vary almost linearly from 0 to about 160 meV with x from 0.22 to 0.45 [17], we can estimate a thermal depth of $\Delta E_d \approx 55$ meV for the DX centre when x=0.3. Therefore, the value of about 60 meV (as estimated from the Hall effect) is in good agreement with that of the DX centre.

B. Noise measurements

Two types of the excess noise, 1/f noise and an extremely broadened (EB) Lorentzian noise, were identified from the noise spectra. For both types of the noise, the noise power densities were found to be quadratically dependent on the bias voltage, indicating resistivity fluctuations. The ratio between the longitudinal and transversal noise power density was found to be in good agreement with the theoretical value of about 0.12 for our sample configuration [15]. This indicated that both types of noise were homogeneously distributed in the conducting channel. Fig. 4 shows a number of the noise spectra measured at different temperatures. The noise spectra presented in Fig. 4(a) are the longitudinal noise. The other noise spectra concern the transversal noise. Between 77 and about 120 K, only 1/f and thermal noise were observed, as indicated in Fig.4(a). Above 140 K, the extremely broadened Lorentzian noise was moving in during the temperature scan, as indicated by its high-frequency branch of $S_V \propto f^{-2}$ in Fig. 4(b). The EB Lorentzian spectrum became so broad that its middle frequency part was actually developed into a kind of $1/f^{\gamma}$ noise

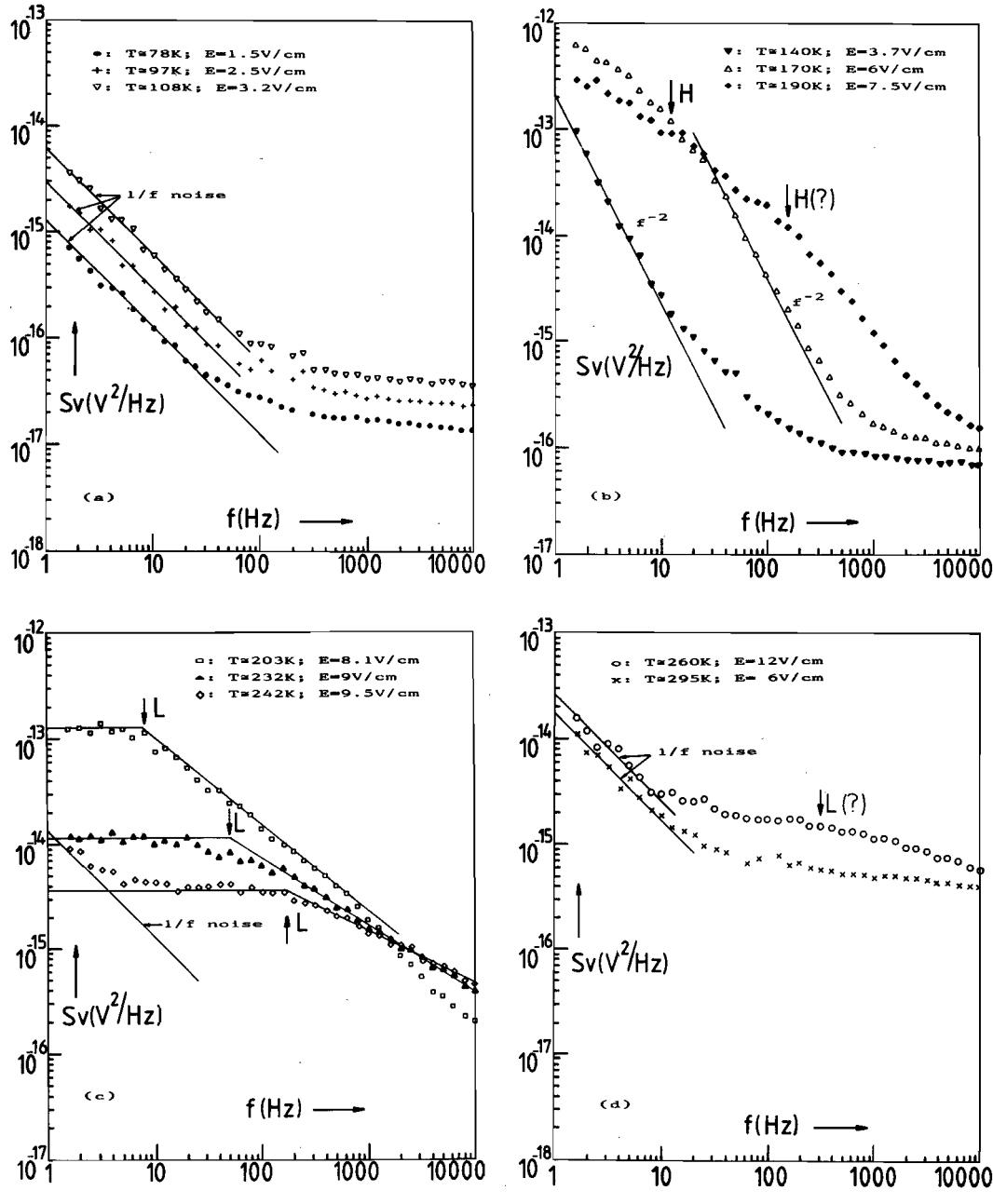

Fig. 4 Several noise spectra at different temperatures.
(a) 77K≤T≤120 K; (b) 140K≤T≤200K; (c) 200K≤T<250K;
(d) 250K<T≤300K.
Arrows indicate the corner frequencies (L stands for the lower corner frequency and H for the higher corner frequency).

spectrum with γ between 0.5 and 0.85. Around 200 K, the low-frequency plateaus of the EB Lorentzian spectrum showed up, as is shown in Fig. 4(c). Between 250 and 300 K, the EB Lorentzian noise was faded to higher frequencies and the 1/f noise became dominant again, as is shown in Fig. 4(d).

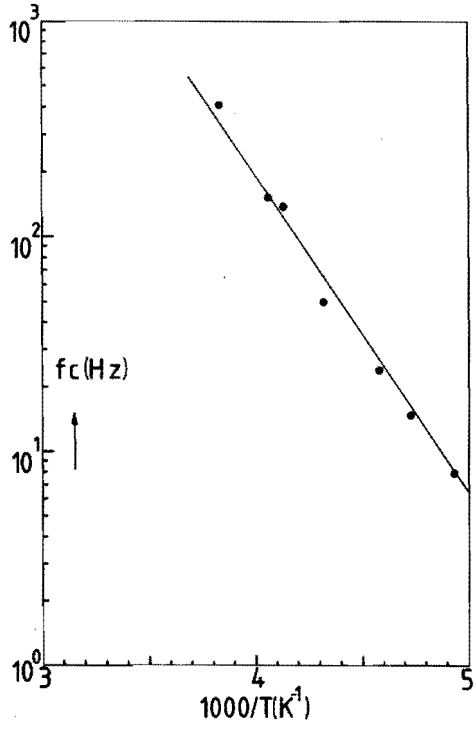

Fig. 5 The lower corner frequency as a function of inverse temperature. The solid line is the least square fit.

There are two corner frequencies, which characterise the EB Lorentzian spectrum. The low corner frequency, we called, is the frequency where the two branches $S_v \propto f^0$ and $S_v \propto f^{-\gamma}$ intersect and the high corner frequency is the frequency where the two branches $S_v \propto f^{-\gamma}$ and $S_v \propto f^{-2}$ intersect. With different biases, it was found that neither the corner frequencies nor the shape of

the EB Lorentzian spectrum depend on the electrical field. In Fig. 5, we plotted the lower corner frequencies of the EB Lorentzian noise versus 1000/T. The plot reveals that the EB Lorentzian noise has thermally activated corner frequencies, which can be written as:

$$f_c = f_0 \exp(-E/kT) \qquad (5)$$

From Fig. 5, an activation energy of about 350 meV can be determined for the lower corner frequencies. Obviously, the broadening of the Lorentzian noise was due to a distribution in the activation energy E [21]. By extrapolating the data of Fig. 5 to infinite temperature ($1000/T \rightarrow 0$), f_o was found to be about 5x10^{9}Hz. Using this value and the spectra shown in Fig. 4(b), an activation of about 260 meV can be determined from eq. (5) for the high corner frequencies of the EB Lorentzian noise. Therefore, a range of activation energies from 260 to 350 meV of the corner frequency would account for the broadening of our observed EB Lorentzian noise. Such an EB Lorentzian noise has also been reported by van Die *et al.* [9] for an InGaAs/GaAs pseudomorphic heterostructure field effect transistor in the same temperature range. They attributed their EB Lorentzian noise to the thermally activated real-space transfer of the charge carriers over the interface barrier. By assuming a Gaussian distribution of the barrier height with a standard deviation of about 35 meV, they have successfully modelled the observed EB-Lorentzian noise. The width of distribution in the barrier height at AlGaAs/InGaAs interface was consistent with the consequence of the fluctuations in the alloy composition. For our $Al_{0.3}Ga_{0.7}Ga$/GaAs heterostructures, the conduction band discontinuity can be estimated with the 65:35 rule [22] as ΔE_c=245 meV, which is somewhat lower than the activation energy obtained from the EB-Lorentzian noise (~305 meV).

However, in view of a similar energy distribution in the bar-

rier height (the half width of about 45 meV) found for our samples as compared to those found by van Die *et al.* [9] and the large error in the activation energies as determined from the EB Lorentzian noise, it is not unreasonable to attribute our EB Lorentzian noise also to the real-space transfer of electrons at the AlGaAs/GaAs interface.

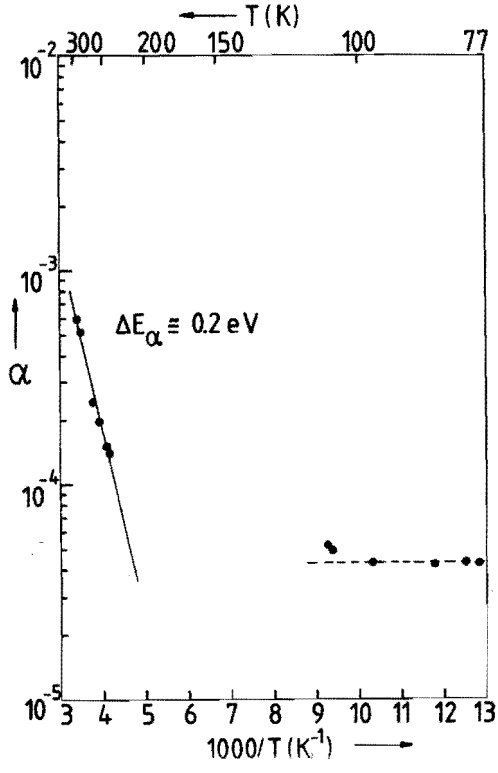

Fig. 6 α as a function of inverse temperature. No 1/f noise could be observed between 120 and 240 K because of the domination of the EB-Lorentzian noise. The solid and broken lines indicate two different temperature dependences of α.

For the 1/f noise, the parameter α was evaluated at different temperatures from the measured noise spectra, via the empirical relation

$$\frac{S_V}{V^2} = \frac{\alpha}{n_H f A}. \qquad (6)$$

Where S_V is the noise spectral density, V is the applied voltage, f is the frequency, n_H is the total sheet carrier concentration determined from the Hall effect and A is the area involved in the noise generation.

Fig.6 shows the α-values as a function of inverse temperature. For the parallel conduction in the two layers, n-$Al_xGa_{1-x}As$ and 2DEG, the conductivity is determined by:

$$\sigma = q n_H \mu_H = q(n_{2D}\mu_{2D} + n_{AlGaAs}\mu_{AlGaAs}), \qquad (7)$$

where q is the elemental charge of electron.

If we assume that the 1/f noise both in the n-$Al_xGa_{1-x}As$ layer and in the 2DEG are caused by mobility fluctuations and that they are uncorrelated, we obtain

$$\frac{S_\sigma}{\sigma^2} = \left(\frac{n_{2D}\mu_{2D}}{n_{2D}\mu_{2D} + n_{AlGaAs}\mu_{AlGaAs}}\right)^2 \left(\frac{S_{\mu_{2D}}}{\mu_{2D}^2}\right) + \left(\frac{n_{AlGaAs}\mu_{AlGaAs}}{n_{2D}\mu_{2D} + n_{AlGaAs}\mu_{AlGaAs}}\right)^2 \left(\frac{S_{\mu_{AlGaAs}}}{\mu_{AlGaAs}^2}\right) \qquad (8)$$

When we substitute n_H from eq. (1) into eq. (6), eq. (8) will give

$$\alpha = \left(\frac{n_{2D}\mu_{2D}^2}{n_{2D}\mu_{2D}^2 + n_{AlGaAs}\mu_{AlGaAs}^2}\right)\alpha_{2D} + \left(\frac{n_{AlGaAs}\mu_{AlGaAs}^2}{n_{2D}\mu_{2D}^2 + n_{AlGaAs}\mu_{AlGaAs}^2}\right)\alpha_{AlGaAs}, \qquad (9)$$

Eq. (9) shows that the 1/f noise mainly stems from the 2DEG at low temperatures, where the ratio $n_{AlGaAs}\mu_{AlGaAs}^2/n_{2D}\mu_{2D}^2$ is much smaller than 1. At T = 300 K, if we take $\mu_{AlGaAs} \approx 1000$ cm²/Vs, $\mu_{2D} \approx 8000$ cm²/Vs and if n_{2D} is of the order of n_{AlGaAs}, we could conclude that the 1/f noise at 300 K is also dominated by the

noise from the 2DEG provided that $\alpha_{2D} \sim \alpha_{AlGaAs}$.

The data shown in Fig. 6 agrees quite well with the common characteristics of the temperature dependence of α in epitaxial n-GaAs [14]: two branches at high and at low temperatures with different temperature dependences. Therefore, this fact is a justification for our assumption that the 1/f noise in the heterostructures is due to mobility fluctuations. From Fig. 6, an activation energy of about 0.2 eV, could be determined for the thermally activated branch of α. This value is comparable to a value of about 0.13 eV found for α_{latt} in epitaxial n-GaAs [14].

In Fig. 7, we present the α-values of our heterostructures versus the Hall mobility at temperatures of 300 K and 77 K in a plot for bulk n-GaAs[13] made previously. The α-values for heterostructures from ref. [6,9,11] and the α-values [23] for a bulk n-GaAs with a dope level of 2×10^{16} cm^{-3} are also included. The α-values of the heterostructures at 300 K are in quite good agreement with those of the bulk n-GaAs. This, together with the similar temperature dependence, is an indication that the 1/f noise in the heterostructure is of the same nature as in bulk n-GaAs. At 77 K, the α-values of the heterostructures are higher than those of the bulk n-GaAs. Nevertheless, the increase of the α-values of the heterostructures is consistent with the assumption [13] that charged-impurity scattering does not generate 1/f noise since there is less impurity scattering in the 2DEG compared to the bulk samples with a same dope level.

In ref. [23] we showed that for the temperature-independent branch of α, its value was proportional to the damage caused by proton-irradiation. Therefore, the α-values at the low temperatures are expected to be sensitive to the quality of the crystal lattice. The conduction in the heterostructures by

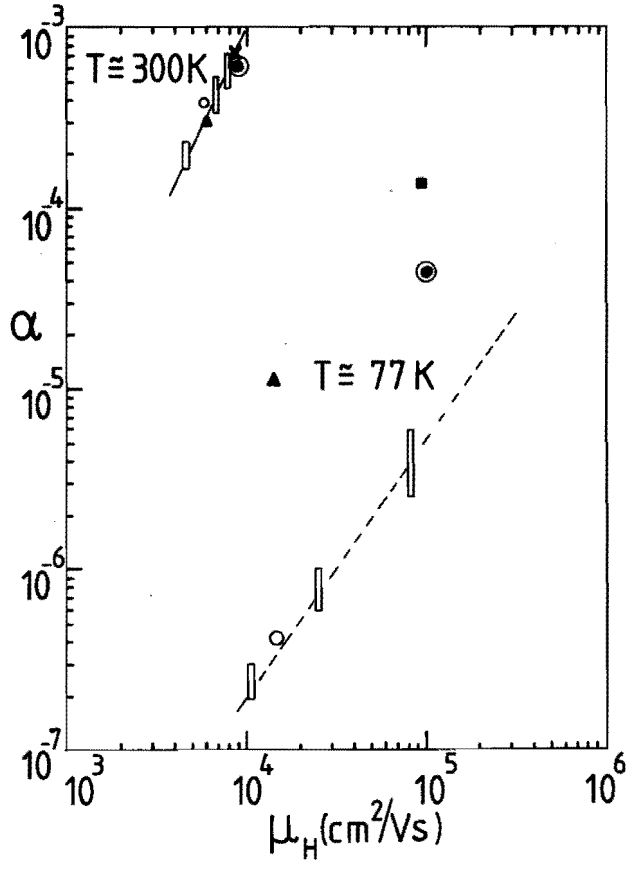

Fig. 7 α vs μ_H. The open bars [13] and the open circles [21] are our data for bulk n-GaAs. The solid symbols are the data for the heterostructures: ● from this work; ▲ from ref. [9]; ■ from ref. [6]; ✖ from ref. [11]. The solid and broken lines are the best fit lines with $\alpha \propto \mu_H^{2.0}$ and $\alpha \propto \mu_H^{1.5}$ [13], respectively.

the 2DEG is close to the interface, which has a less perfect crystal lattice compared with the inner part, so that its α-values are expected to be higher than far away from an interface.

IV. CONCLUSION

The low-frequency noise in an $Al_xGa_{1-x}As/GaAs$ heterostructure has been investigated in the temperature range from 77 to 300 K. Between 140 and 240 K, an extremely broadened Lorentzian (EB Lorentzian) noise was observed dominating over the other types of noise. Below 120 K and above 240 K, 1/f noise was observed as the dominant excess noise. The corner frequency of the EB Lorentzian noise has a typical thermally activated behaviour and does not depend on the electrical field. From the experimental data, a range of about 260 - 350 meV for the activation energy was determined. Following van Die *et al.*[9], we assigned the observed EB Lorentzian noise to the real-space transfer of electrons from the 2DEG to the $n\text{-}Al_xGa_{1-x}As$ layer and *vice versa*. Using the parallel layer model and under the assumption of mobility fluctuations, it has been shown that the 1/f noise at all temperatures stemmed from the 2DEG. The good agreement between the measured temperature dependence of α in the heterostructures and that of bulk n-GaAs justified our doing so. The relatively higher α-values in the heterostructures at low temperatures may be caused by the crystal-quality-dependent 1/f noise source since the conduction in the heterostructures is close to the interface, where the lattice quality is less perfect compared to the bulk of the crystal.

ACKNOWLEDGEMENTS

The authors wish to thank Dr. A. van Die and Prof.Dr. J.I. Dijkhuis for providing the manuscript of their future publica-

tion. The authors thank W. van der Vleuten for growing the samples.

This work is part of the research program of the "Stichting voor Fundamenteel Onderzoek der Materie (FOM)", which is financially supported by the "Nederlandse organisatie voor Wetenschappelijk Onderzoek (NWO)".

REFERENCES

[1] T. Ando, J. Phys. Soc. Jpn. 51, 3893(1982).

[2] L. Loreck, H. Dambkes, K. Heime, K. Ploog and G. Weimann, IEEE Electron Dev. Lett. EDL-5, 9(1984).

[3] H. Wolf, L. Bliek, G. Weimann and W. Schlapp, Semicon. Sci. Technol. 3, 1184(1988).

[4] J.R. Kirtley, T.N. Theis, P.M. Mooney and S.L. Wright, J. Appl. Phys. 63, 1541(1988).

[5] S. Kugler, J. Appl. Phys. 66, 219(1989).

[6] F. Hofman, R.J.J. Zijlstra and J.M. Bettencourt de Freitas, J. Appl. Phys. 67, 2482(1990).

[7] F. Hofman, Ph. D. dissertation, University of Utrecht (1990).

[8] S. Tehrani, A.D. van Rheenen, M.M. Hoogstra, J.A. Curless and M.S. Peffley, IEEE Trans. Electron Dev. 39, 1070 (1992).

[9] A. van Die and J.I. Dijkhuis, submitted to J. Appl. Phys.

[10] M. Tacano, Y. Sugiyama and T. Taguchi, IEEE Electron Dev. Lett. EDL-8, 22(1987).

[11] M. Tacano, Y. Sugiyama and H. Soga, Sold-St. Electron. 32, 49(1989).

[12] J.M. Peransin, P. Vignaud, D. Rigaud and L.K.J. Vandamme, IEEE Trans. Electron. Dev. **37**, 2250(1990).

[13] F.N. Hooge, Phys. Lett. **A29**, 139(1969).

[14] L. Ren and F.N. Hooge, Physica **B176**, 209(1992).

[15] L. Ren and M.R. Leijs, Physica **B172**, 319(1991).

[16] R.L. Petritz, Phys. Rev. **110**, 1254(1958).

[17] P.M. Mooney, J. Appl. Phys. **67**, R1(1990).

[18] N. Chand, T. Henderson, J. Klem, W.T. Masselink and R. Fisher, Phys. Rev. **B30**, 4481(1984).

[19] R.A. Smith, *Semiconductors*, Chap. **4**, Cambrige Univ. Press, Cambridge, 1978.

[20] S. Hiyamizu, K. Nanbu, T. Mimura, T. Fuji and H. Hashimoto, Jpn. J. Appl. Phys. **20**, L378(1981).

[21] P. Dutta and P.M. Horn, Rev. Mod. Phys. **53**, 497(1981).

[22] D. Fritzsche, Solid-St. Electron. **30**, 1183(1987).

[23] L. Ren, submitted to J. Appl. Phys.

Chapter 7

CONCLUSIONS

This thesis deals with an investigation into the origin of 1/f noise in epitaxial GaAs. The problem of 1/f noise magnitude depending on crystal-quality has been addressed. Thanks to the high performance of modern crystal-grown techniques, like MBE, MOCVD, etc. which made such a study possible. Both the 1/f noise and its temperature dependence in MBE-grown n-GaAs have been studied. In particular, attention has been paid to the effects on 1/f noise after introducing lattice defects in a controlled way by means of high-energy electron irradiation or proton irradiation. The main results obtained in this thesis are:

(1) 1/f noise in n-GaAs epitaxial layers is a bulk effect and is well-described by Hooge's empirical relation with a characteristic parameter α.

(2) 1/f noise in epitaxial n-GaAs is due to mobility fluctuations.

(3) the parameter α of epitaxial n-GaAs shows a thermally activated behaviour at high temperatures (above about 150 K) and a plateau at low temperatures. In the whole temperature range from 300K to 77 K, the 1/f noise reduction factor $(\mu/\mu_{latt})^2$ is valid for the doping dependent α-values in epitaxial n-GaAs.

(4) The two branches of $\alpha(T)$ correspond to two different noise

mechanisms. The thermally activated branch of $\alpha(T)$ has an intrinsic origin and seems to be related to the lattice phonon scattering. The other branch, the plateau, has obviously an extrinsic origin, dependent on the density of lattice defects. The quantum "local-interference" effect is very likely the mechanism of the extrinsic type of 1/f noise.

SUGGESTIONS FOR FUTURE WORK

(1) Considering conclusion (4) for the intrinsic 1/f noise, it sounds strange to attribute it to the lattice-phonon scattering because it would be difficult to imagine that the α of the lattice-phonon scattering is thermally activated, since at thermal equilibrium we expect:

$$\alpha(T) \propto \frac{\langle(\Delta n)^2\rangle}{n^2} = 1+\frac{1}{n} \approx 1, \qquad (1)$$

according to Bose-Einstein statistics. Here n is the number of phonons in a mode. However, in the frame of Musha's work, I could see a possibility that the α of lattice-phonon scattering can be thermally activated. According to Musha *et al.*, the phonon 1/f spectrum could result from some slow relaxation in the phonon energies, which is out of thermal equilibrium. This suggestion is supported by their light scattering experiment on water, where a fluctuation in the fraction phonon number of a mode, $\langle(\Delta n)^2\rangle/n^2$, was found much bigger than 1. Therefore, we could speculate that through some "modulation" effects by temperature a thermal activated behaviour of α could be possible. To test my speculation, here I propose two experiments: (i) directly measuring the temperature dependence of the 1/f fluctuations in the number of a phonon mode by a light scattering experiment; (ii) measuring the temperature dependence of 1/f noise far out of thermal equilibrium, for example measuring noise both during the

rising and decreasing of temperature. Perhaps some kind of "hysteresis loop" might then be observed.

(2) There still remains the intriguing question whether the extrinsic type of 1/f noise, as identified in our n-GaAs epitaxial samples, is also a type of mobility fluctuation. One way to check it is to study the validity of the noise reduction factor $(\mu/\mu_{latt})^2$ in the samples with different doping levels but with the same irradiation damage. This has been done with several samples. Fig. 1 shows our preliminary results, which seem to support the model of mobility fluctuations. However, the data in Fig. 1 also can be approximated by a relation steeper than quadratic. Further measurements are needed to establish a clear relation between α_{77K} and μ_H.

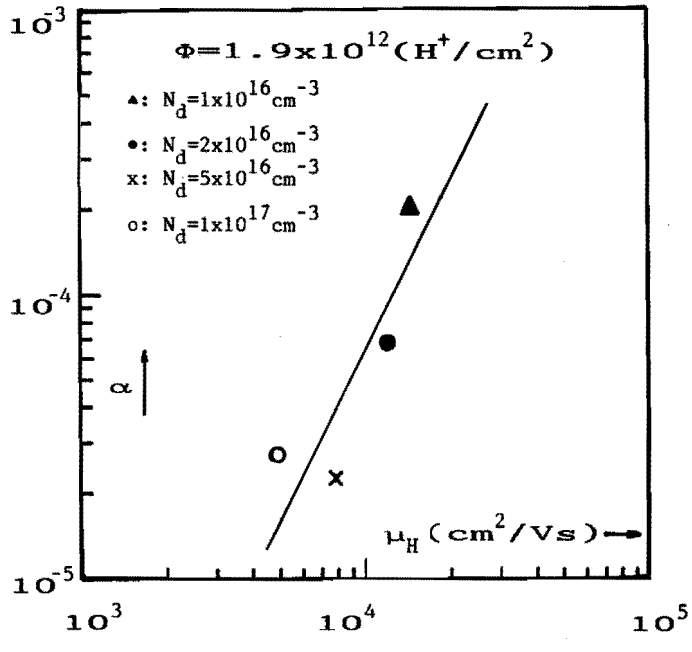

Fig. 1 α of the extrinsic 1/f noise versus μ_H at T=77K. The solid line indicates a quadratic dependence.

Summary

It is well known that almost any conductor through which current is flowing, exhibits voltage fluctuations with a power spectral density inversely proportional to the frequency. Although this so-called 1/f noise has been intensively explored, there is still no general agreement on its origin. However, it has been demonstrated that an empirical relation, established some 20 years ago, is successful in describing the 1/f noise in homogeneous materials of semiconductors and metals. This relation

$$\frac{S_R}{R^2} = \frac{\alpha}{fN} \qquad (1)$$

relates the relative 1/f noise power-density S_R/R^2 of the fluctuations in the resistance R to the total number of free charge-carriers N in the sample. α is called the 1/f noise parameter and is often used to compare the noise level in different samples. Eq. (1) does not imply anything about the noise mechanism. $\alpha \sim 10^{-4}$-10^{-3} are often reported for metals. For semiconductors, α scatters in a wide range of 10^{-7}-10^{-2}. However, in the samples made by advanced I.C. technology, α tends to be low, about 10^{-6} or 10^{-7}. This raised the question: is this due to the small dimensions of these samples or to the perfection of the crystal lattice? Experimental evidence suggests the latter reason. But how α could be dependent on the perfection of crystal lattice is still an open question.

To answer these questions mentioned above, we set up to attack the problem of α-values dependent on crystal quality by an experimental approach. Starting with well-defined high-quality

samples of GaAs and other III-V compounds grown by MBE and by MOCVD, the 1/f noise and its temperature dependence were investigated. We found that the α-values at room temperature were between $1x10^{-4}$ and $8x10^{-4}$ for n-GaAs, 2DEG n-GaAs and n-$In_xGa_{1-x}As$ (not reported in this thesis) independent of the growing techniques. The α-values at 300 K for these materials were also found to be independent of or weakly dependent on the doping, the growth temperature (between 600 and 700 °C), III/V ratios and the dislocation density in the substrate (not reported in this thesis). Different doping and temperature were used to change the relative contributions of the lattice scattering and impurity scattering. The experimental results were in good agreement with the 1/f noise reduction factor $(\mu/\mu_{latt})^2$ proposed by Hooge and Vandamme by assuming that impurity scattering does not contribute to the generation of 1/f noise. In n-GaAs, a strong and systematic temperature dependence of α was found. It shows two branches with different temperature dependence of α: thermally activated α at high temperatures and weakly temperature dependent α at the lower temperatures. The temperature dependence of α could not be explained by the Dutta-Dimon-Horn model. By measuring the 1/f noise in Hall-voltage both at 300 K and 77K, the 1/f noise in n-GaAs was found to be caused by mobility fluctuations.

After having deliberately induced lattice defects by irradiation, we studied the noise behaviour of the n-GaAs epitaxial layers grown by MBE. In the (3 MeV) electron-irradiated n-GaAs, two common electron traps E1 and E2 were identified from the Hall-effect measurements. Using the noise spectroscopy, another deep level at ~ [Ec - 0.18] eV with an extremely small capture cross-section was also identified. The 1/f noise turned out to be slightly affected by the electron irradiation. Hence, the point lattice-defects induced by the irradiation were shown to have no significant influence on α or on its temperature dependence. They only induce generation-

recombination noise. Furthermore, we have investigated the 1/f noise in MBE-grown n-GaAs bombarded with 3 MeV protons (H^+), where some kinds of clusters of lattice-defects were created. Two different types of 1/f noise were identified from the temperature dependence of α. The thermally activated branch of $\alpha(T)$ dominating at high temperatures, seems to have an intrinsic origin related to the lattice phonon scattering, while the temperature independent part of $\alpha(T)$ obviously has an extrinsic origin, dependent on the defects created by the H^+ bombardment. The Dutta-Dimon-Horn model reasonably well explained the extrinsic type of 1/f noise, which implies that the defect motion was the noise source. Considering that the α-values for the extrinsic type of 1/f noise were found proportional to the irradiation dose and in turn the number of clusters, it revealed that the moving defects were within the clusters. Our experimental data were consistent with the quantum "local-interference" model for the extrinsic type of 1/f noise induced by the irradiation.

Low-frequency noise in an $Al_xGa_{1-x}As/GaAs$ heterostructure was investigated in the temperature range 77-300 K and in the frequency range of 1 Hz-20 kHz. Two types of excess noise, 1/f and an extremely broadened (EB) Lorentzian noise, were observed to be dominant at different temperature ranges. The corner frequencies of the observed EB-Lorentzian show thermally activation with activation energies in the range between 260-350 meV. We attributed the EB-Lorentzian noise to the real-space transfer of the 2DEG electrons to the $n\text{-}Al_xGa_{1-x}As$ layer and *vice versa*. The α-values of the 1/f noise in the heterostructures and its temperature dependence were found to be comparable with those of bulk n-GaAs. This fact shows that the 1/f noise in the heterostructures has a same origin as the 1/f noise in the bulk n-GaAs.

Samenvatting

Het is een bekend feit, dat in bijna iedere geleider, waar een stroom doorheen loopt, spanningsfluctuaties optreden met een spectrale dichtheid die omgekeerd evenredig is met de frequentie. Hoewel deze zogenaamde 1/f ruis zeer uitvoerig bestudeerd is, is er nog steeds geen overeenstemming over de oorsprong hiervan. Wel is aangetoond dat een 20-jaar oude empirische relatie deze ruis succesvol beschrijft in homogene halfgeleiders en metalen. Deze relatie

$$\frac{S_R}{R^2} = \frac{\alpha}{fN} \qquad (1)$$

legt een verband tussen de relatieve ruisdichtheid S_R/R^2 van de fluctuaties in de weerstand R en het totale aantal vrije ladingsdragers N in het preparaat. α wordt de ruisparameter genoemd en wordt vaak gebruik voor de vergelijking van de grootte van de ruis in verschillende preparaten. Vergelijking (1) zegt niets over het ruismechanisme. In metalen worden vaak α-waarden tussen 10^{-4} en 10^{-3} gevonden. In halfgeleiders liggen de α-waarden verspreid over een wijd gebied van 10^{-7} tot 10^{-2}. Maar in het algemeen is α laag (10^{-6} - 10^{-7}) in preparaten die met moderne I-C technologie gemaakt zijn. Dit roept de vraag op, of dit komt door de kleine afmetingen van de preparaten of door de perfectie van het kristalrooster. Experimentele resultaten suggereren het laatste. Maar waarom α dan van de roosterperfectie afhangt, is nog steeds een open vraag.

Om deze vragen over het verband tussen α en roosterperfectie te beantwoorden kozen we de experimentele weg. We onderzochten de

1/f ruis en zijn temperatuur afhankelijkheid aan goed gedefinieerde, vrijwel perfecte preparaten van GaAs en andere III-V verbindingen, gegroeid door MBE en MOCVD. We vonden kamertemperatuur α waarden tussen 1 x 10^{-4} en 8 x 10^{-4} in n-GaAs, 2DEG n-GaAs en (niet beschreven in dit proefschrift) n-$In_xGa_{1-x}As$. Deze α waarden zijn onafhankelijk van de gebruikte groeitechniek. Bij 300 K zijn ze geheel of vrijwel onafhankelijk van de dope concentratie, de groeitemperatuur (600 - 700 °C), de verhouding van de aantallen III en V atomen en (niet beschreven in dit proefschrift) de dislocatiedichtheid in het substraat. De relatieve bijdragen van de roosterstrooiing en de strooiingen aan onzuiverheden werden gevarieerd door verschillende dope concentraties en meettemperaturen te kiezen. De experimentele resultaten stemden goed overeen met de factor $(\mu/\mu_{latt})^2$. Deze reductiefactor voor de 1/f ruis is door Hooge en Vandamme voorgesteld, aannemende dat de strooiing aan onzuiverheden geen 1/f ruis genereert. We vonden een grote, systematische temperatuurafhankelijkheid voor α in n-GaAs. De grafiek van logα tegen 1/T vertoont twee takken: een thermisch geactiveerde α bij hoge temperatuur en een zwak temperatuurafhankelijke bij lage temperatuur. Deze temperatuurafhankelijkheid kan niet verklaard worden met het Dutta-Dimon-Horn model. Dat de 1/f ruis in n-GaAs beweeglijkheidsfluctuaties zijn, volgt ook uit metingen van de ruis in de Hall spanning bij 300 K en bij 77 K.

We bestudeerden ook de ruis in onze epitaxiale lagen, nadat we opzettelijk roosterfouten gemaakt hadden door bestraling. In met 3MeV-electronen bestraalde preparaten vonden we door Hall effect metingen de bekende E1 en E2 traps. Uit de ruisspectra leidden we af dat er nog een diep niveau op - 0,18 eV gemaakt was met een uitzonderlijk kleine invangstdoorsnede. De 1/f ruis veranderde nauwelijks door de electronenbestraling. De gecreëerde puntfouten hadden dus nauwelijks invloed op de α of op de temperatuur afhankelijkheid. Er werd alleen generatie-recombinatie ruis geïntroduceerd.

Daarnaast is de ruis bestudeerd van preparaten die met 3MeV-protonen (H^+) bestraald waren. Hierbij werden clusters van roosterfouten gecreëerd. Uit de temperatuur afhankelijkheid van α concludeeerden we dat er twee soorten 1/f ruis bestaan. De thermisch geactiveerde tak bij hoge temperatuur blijkt overeen te komen met een intrinsieke ruis die samenhangt met de strooiing aan phononen van de roostertrillingen. De temperatuur-onafhankelijke tak bij lage temperatuur is daarentegen extrinsiek en hangt af van de roosterfouten tengevolge van het protonenbombardement. Het Dutta-Dimon-Horn model geeft een redelijke verklaring voor deze extrinsieke ruis, hetgeen betekent dat het bewegen van de fouten de ruisbron is. Uit het feit dat de α-waarden van de extrinsieke ruis evenredig zijn aan de stralingsdosis, en dus ook aan het aantal clusters, volgt dat de fouten binnen een cluster bewegen. Deze experimentele resultaten passen in het quantum "local interference model".

De laagfrequente ruis van een $Al_xGa_{1-x}As/GaAs$ heterostructur werd onderzocht in het temperatuurgebied 77 K tot 300 K en het frequentiebereik 1 Hz tot 20 kHz. We vonden twee soorten excess ruis: 1/f ruis en extreem verbrede Lorentz ruis, zogenaamde EB ruis. Welke soort overheerst hangt van de temperatuur af. De knikfrequentie van de EB ruis hangt van de temperatuur af met een activeringsenergie die ligt tussen 260 meV en 350 meV. We schrijven de EB ruis toe aan transport van de 2DEG electronen naar de $Al_xGa_{1-x}As$ laag en vice versa. De α waarden en de temperatuurafhankelijkheid in de heterostructuren zijn vergelijkbaar met die van bulk n-GaAs. Dit wijst er op dat de ruis in de heterostructuren en in bulk GaAs dezelfde oorsprong heeft.

Acknowledgements

First of all, I would like to thank all the people who have directly or indirectly contributed to the completion of this thesis. Especially, my thesis advisor, Prof.Dr. F.N. Hooge deserves credit for his good guidance. Discussions with Prof.Dr. T.G.M. Kleinpenning and Dr. L.K.J. Vandamme are highly acknowledged.

I wish to thank Ing. W.M.M.M. van de Eijnden for his technical support (including his advice which enabled me to repair my old television), J.A.E.M. Couwenberg for his technical support and taking care of all drawings. I shall never forget my former colleagues Rob J. Fronen and Stefan W.P. van Sterkenburg for their jokes during the Noise Conference at Budapest in 1989. Thanks are going to Dr. M.R. Leijs, L.C. de Folter (Physics Department) and Dr. L.H. Luthjens (I.R.I. of Delft University of Technology) for the nice cooperation I had with them. For the nice cooperation, I would also like to mention Dr. Ruud van de Berg and Arie de Vos (the Laboratory of Physiology and Physiological Physics of Leiden University). It was pity that we had to stop the measurements on noise in a mercury capillary due to several technical difficulties.

I am deeply grateful to Mrs. Els R. Gerritsen for her kind care and support during my stay in the Netherlands.

Curriculum Vitae

The author of this thesis was born on 12 March 1964 at Xi'an, Shaanxi Province, China. In 1981, he finished his middle-school education at Xi'an. At the same year, he began his university education at Xi'an Jiaotong University and finished it in 1985 with the Bachelor's degree with specialisation of Medical Electronics. Then, he went to the graduate school of Xi'an Jiaotong University. In June 1988, he was awarded the Master of Science degree with specialisation of Electronic Materials. From June 1988 to May 1989, he worked at the Department of Electronics of Xi'an Jiaotong University as a research assistant on multifunctional ceramics. Since June 1989, he has been with the "Stichting voor Fundamenteel Onderzoek der Materie (FOM)" as an "Onderzoeker in Opleiding" working for his Ph. D. at the Department of Electrical Engineering, Eindhoven University of Technology, the Netherlands.

Stellingen

behorende bij het proefschrift van

Lin Ren

I

1/f noise in epitaxial GaAs is due to mobility fluctuations.
--- *Chapters 2 and 3 of this Thesis*

II

The impurity scattering at isolated point scatterers does not generate 1/f noise.
--- *Chapters 2 and 4 of this Thesis*

III

The two branches of the 1/f noise parameter α found in epitaxial n-GaAs correspond to two different noise mechanisms. This fact warns us that when one tries to model 1/f noise in devices, one has to know first which noise mechanism is dominating.
--- *Chapter 5 of this Thesis*

IV

The method of using the Arrhenius-plot of the generation-recombination noise, $\log(\tau T^2)$ versus $1/T$, to extract the thermal depth of the trap is not well justified in the literature. This method is only valid if

(i) the capture cross section is temperature independent;
(ii) the number of trapped electrons is much smaller than that of free charge carriers and of the traps.

V

The 1/f noise of electrons in 2D and 3D structures has the same origin.

--- *Chapter 6 of this Thesis*

VI

Random telegraph signal noise can be observed only in small electronic devices with a small number of free charge carriers.
--- T.G.M. Kleinpenning, *Physica B 164(1990)331.*

VII

The claim by Weissman that mobility fluctuations cannot persist for times longer than that a carrier remains in the sample is not correct. The point is that the time an individual carrier spends in the sample is irrelevant for the calculation of the average mobility fluctuations of the carriers.
--- M.B. Weissman, *Rev. Mod. Phys. 60(1988)537.*

VIII

Buddhism is one of the most peaceful religions in the world. During the gulf-war in 1991 both president Bush (Christian) and President Saddam (Moslem) claimed that God was on his side, but neither of them would ask whether he was on God's side. However, for a Buddhist, such ideas would not even come to his mind.

IX

Linear acceleration 1/f noise does not exist.
--- C.M. Van Vliet, *Solid-St. Electronics 34(1991)1.*
--- L.K.J. Vandamme, *10th Int. Conf. on Noise in Physical System 491(1989).*

X

In global affairs, like peace, human rights, environment, etc., the United Nations should play a more important role than it does now. However, to function successfully, the United Nations should be neutral and the influence of the superpowers should be restricted.